

PHYSICAL AND CHEMICAL ASPECTS OF GRANITE  
WEATHERING IN NORTH CENTRAL NEW BRUNSWICK

PHYSICAL AND CHEMICAL ASPECTS OF GRANITE  
WEATHERING IN NORTH CENTRAL NEW BRUNSWICK

By

RICHARD BLAIR NEEDHAM

A Thesis

Submitted to the Department of Geology  
in Partial Fulfillment of the Requirements  
for the Degree  
Bachelor of Arts

McMaster University

May, 1979

BACHELOR OF ARTS (1979)  
(Geology with Geography)

McMASTER UNIVERSITY  
Hamilton, Ontario

TITLE:           Physical and chemical aspects of granite  
                  weathering in north central New Brunswick

AUTHOR:           Richard Blair Needham

SUPERVISOR:     Dr. James R. Kramer

NUMBER OF PAGES:   i-xi; 1-201

## ACKNOWLEDGEMENTS

The author wishes to thank the Geological Survey of Canada for allowing the collection of field data and samples during the 1978 field season, as well as providing geochemical analyses of the majority of the samples. The supply of maps and air photos was also much appreciated. I am deeply grateful to Mr. C. Gauthier for the suggestion of the topic and his advice in the field and in the writing of this thesis.

Thanks go to my supervisor, Dr. J.R. Kramer, for his advice throughout the year and especially for his critical review of the manuscript.

The author wishes to thank Mr. L.J. Zwicker for the preparation of thin sections, Mr. J. Whorwood for the preparation of photomicrographs. Mr. O. Mudroch must also be thanked for his assistance in the chemical analysis of the rocks and for his help in the identification of minerals in X-ray diffraction analyses.

A special thanks to my parents for putting up with me during the writing of this thesis and the little person in my life for her persistent encouragement.

Helen Elliott was able to quickly and accurately decipher my scribble in the typing of the manuscript. This was not a minor feat and her efforts were much appreciated.



Finally, I would like to thank my fellow comrades of Room 124 for their discussion and humour throughout the year.

## TABLE OF CONTENTS

	Page
CHAPTER I	
INTRODUCTION	1
1.1 Introduction - purpose of study	1
1.2 Location	2
1.3 Accessibility	4
1.4 Local topography, vegetation and climate	4
1.5 General geology of area and previous work	5
CHAPTER II	
FIELD STUDIES	12
2.1 Introduction	12
2.2 Geologic features and processes influencing chemical weathering	14
A. Big Bald Mountain	16
Microfractures	22
Solution features	25
Rock type	29
Other processes	29
2.2.2 Summary and discussion	31
B. Pierce Mountain	34
2.3 Methods of sampling	40
A. Big Bald Mountain	40
B. Pierce Mountain	42
2.4 Sample location	43
2.4.1 Introduction	43
2.4.2 Stratigraphic position	45
2.5 Sample description	48
A. Big Bald Mountain	48
B. Pierce Mountain	50

	Page
CHAPTER III      LABORATORY ANALYSES	54
3.1 Analytical methods	54
3.1.1 Introduction	54
3.1.2 Grain size analysis	54
3.1.3 Major element analysis	56
3.1.4 X-ray diffraction	58
3.1.5 Thin section preparation	59
3.2 Petrography	60
3.2.1 Introduction	60
3.2.2 Modal analysis	62
3.2.3 Normative analysis	65
3.2.4 Textures	74
3.2.5 Summary of petrography	91
3.2.6 Discussion	93
3.3	94
3.3.1 Grain size analysis	94
3.3.2 Histograms	94
A. Big Bald Mountain	95
B. Pierce Mountain	99
3.3.3 Cumulative probability plot	101
3.3.4 Rosin law probability plot	111
3.3.5 Discussion	116
3.4 X-ray diffraction	118
CHAPTER IV      CHEMICAL WEATHERING	125
4.1 Introduction to concepts of chemical weathering	125
4.2 Weathering index	132
4.3 Applications of weathering index	139
4.3.1 Weathering index vs. depth	139
4.3.2 The relative mobility of cations in weathering profile	143
4.4 Summary	168

		Page
CHAPTER V	CONCLUSIONS	169
REFERENCES		174
APPENDIX 1	MAJOR ELEMENT ANALYSES	183
APPENDIX 2	CATION PERCENTAGES	186
APPENDIX 3	MESONORM ANALYSIS	189
APPENDIX 4	WEATHERED VS. "FRESH" CATION % RATIOS	193

## LIST OF FIGURES

Figure		Page
1	General location map	3
2	Detailed geologic maps	9
3	Horizontal jointing	16
4	Sheeting parallel to topography	16
5	Convex smooth granite form	17
6	Dome form exposed on ridge	17
7	Same as Fig. 6; different orientation	18
8	Dome feature (developed with steep vertical side)	20
9	Tor compartmentation	20
10	Joint distribution rose diagram	21
11	Tor and dome (features developed in close)	24
12	Dome structure microfractures	24
13	Core stone developed on exfoliated granite	26
14	Interconnected "solution" basin forms	28
15	Rillen produced in granite	28
16	Block-like fracturing of boundary	29
17	Quartz vein within the regolith grus	34
18	Clay pocket (developed in weathering profile)	37
19	Deep iron pan (developed in colluvium)	39
20	Distinct colour variation	39
21	Sample location	44
22	Schematic model of deposits	46, 47

Figure		Page
23	Pierce Mountain model	48,49,50
24	Q:A:P diagram of modal analyses	63
25	Q:Ab:Or mesonorm ternary diagram for Big Bald Mt.	66
26	Q:Ab:Or mesonorm ternary plot for Pierce Mt.	67
27	Mesonorm Q:A:P ternary plot for Big Bald Mountain	68
28	Mesonorm Q:A:P ternary plot for Pierce Mountain	69
29	K:Na:Ca diagram for Big Bald Mountain	71
30	K:Na:Ca diagram for Pierce Mountain (Barth, 1959)	72
31	Effect of exfoliation on mineral grains	77
32	Typical interlocking aggregates of quartz grains	77
33	Difference in alteration between unaltered clear quartz and perthite	78
34	Thin section photomicrograph cross nicols sample 5a	78
35	Porphyritic texture	79
36	Typical hydromorphic granular texture of granite	85
37	Cataclastic texture of weathered granite	85
38	Highly altered granite forming sericite and quartz	86
39	Big Bald Mountain grain size histograms	97
40	Pierce Mountain grain size histograms	98
41	A. Big Bald Mountain cumulative probability plots	102- 104
	B. Pierce Mountain cumulative probability plots	105- 106

Figure		Page
42	A. Rosin's probability plot for Big Bald Mountain	112-113
	B. Rosin's probability plot for Pierce Mountain	114-115
43	Depth <u>vs.</u> weathering index	141-142
44	Cation % <u>vs.</u> weathering index for	
	A. Big Bald Mountain	148-151
	B. Pierce Mountain	160-163
45	$[\text{Cation \%}/\text{Al}]_{\text{parent}} / [\text{Cation \%}/\text{Al}]_{\text{weathered}}$ <u>vs.</u> weathering index for	
	A. Big Bald Mountain	152-155
	B. Pierce Mountain	163-167

## LIST OF TABLES

Table		Page
1	Analytical error	57
2	Modal analyses	61
3	Inman probability statistics	110
4	X-ray diffraction analyses	120-124
5	Weathering index values	133-135



## CHAPTER 1

### INTRODUCTION

#### Introduction

The purpose of this study is to describe the forms produced and processes involved in the weathering of granite in North Central New Brunswick. This is accomplished by the analysis of physical, geochemical and petrographic evidence gathered in the field and laboratory.

The field work was done in the summer of 1978 while working for the Geological Survey of Canada under the supervision of C. Gauthier. The study of the granite was of interest because of:

(1) The development of unusual granite forms and "deep" accumulation of angular grus in the vicinity of Big Bald Mountain.

(2) The development and exposure of a deep (4 m) weathering profile along the south branch of the Nepisiguit River.

The presence of these granite weathering profiles and forms are of special significance to the glacial history

of the area because their presence may suggest that the area has not been glaciated.

### Location

The two areas are located in the granitic batholith complex of central New Brunswick (see Figure 1).

The Big Bald Mountain area is located at the headwaters of the South Sevogle River. It and associated ridges act as the drainage divide between the South Sevogle and the Nepisiguit river basins. The study area is bounded by the latitudes  $47^{\circ}12'00''$  -  $47^{\circ}10'09''$  and longitudes  $63^{\circ}25'49''$  -  $63^{\circ}23'00''$ . The area can be found on the National Topographic System map 210/1 west.

The second site of this study is located approximately 5 km south of Popple Depot along the south branch of the Nepisiguit River. The section is cut into the eastern slope of a ridge which is locally called Pierce Mountain. The co-ordinates for the site are  $47^{\circ}18'18''$ - $66^{\circ}30'40''$ . The National Topographic System Co-ordinate map where the site can be found is 210/7 east. The Pierce Mountain site is 13.5 km, N27°W of Big Bald Mountain.

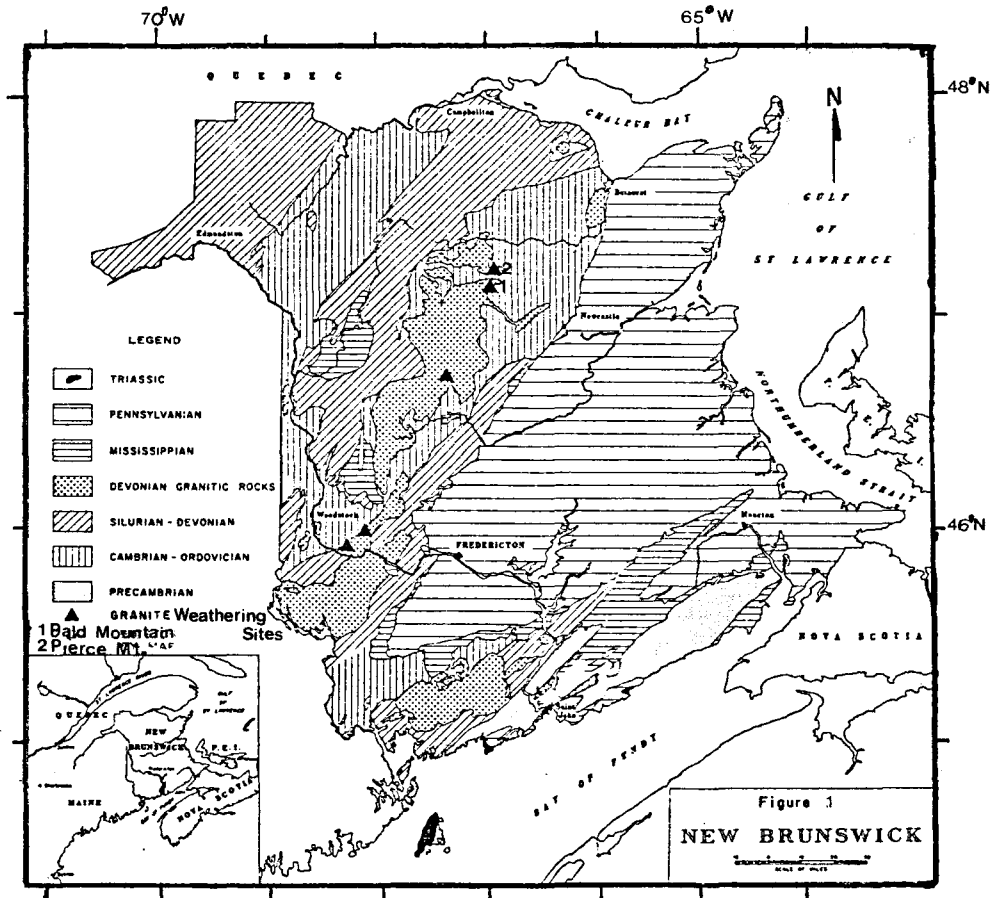


Figure 1. Location of sites in the granite belt of south and central New Brunswick.

Site 1 is Big Bald Mountain site  
 Site 2 is Pierce Mountain site

(Modified map from Hamilton, 1968)

### Accessibility

The Big Bald Mountain area is accessible from the Heath Steele-Newcastle highway (N.E. access route) or from the town of Sevogle (S.E. access route) by haulage roads initially, then by overgrown dirt roads.

The Mount Pierce area has good accessibility via haulage roads which are opening the area to logging operations from the Bathurst-Heath Steele haulage road.

### Local Topography, Vegetation and Climate

The Big Bald Mountain area has topographic relief of 600 ft. The ridges have generally a smooth profile except for the occurrence of tors or inselburgs near or at the top of the ridges. The valley plain is incised by creeks originating from springs at the base of the mountain.

Shallow small bogs occasionally occur in the valleys. The undulating hills in the valley east of the ridge, which trends N-S, were thought to be bedrock from air photo interpretation, but were found to be an accumulation of deep (minimum 1.5 m) granite grus.

The area is sparsely vegetated due to the occurrence of a forest fire in the past. This allowed easy access to

rock outcrop in the otherwise heavily forested area. Vegetation is limited to sparse spruce or pine, low lying bushes and lichen on frequently exposed bedrock.

The Pierce Mountain site extends for approximately 50 m and cuts into the slope a maximum depth of 4-5 m. The area is heavily vegetated with spruce and pine.

The area has a maritime climate. The mean annual precipitation is 37 inches which includes 100 inches of snowfall. The mean winter temperature is  $-11^{\circ}\text{C}$  and the mean summer temperature is  $18^{\circ}\text{C}$ . The mean maximum and minimum temperatures are  $33^{\circ}\text{C}$  and  $-35^{\circ}\text{C}$ , respectively. The dominant winter wind directions are W. and N. and in the summer are S.W. and S. Climate is of special significance in the study of chemical weathering.

### Geology of Area

Big Bald Mountain and Mount Pierce areas are part of a series of granite batholiths which trend N.E.-S.W. The area is part of the Miramichi Highlands of Central New Brunswick (see Figure 1 for position of the two areas studied in relation to the major granitic belt).

The granitic rocks consistently intrude Ordovician (Tetagouche Group) rocks and Silurian Devonian (sedimentary

and volcanic) rocks. Contact metamorphic aureoles in the host rock have been noted by Helmstaedt (1970), Skinner (1974), Anderson (1968), and Martin (1966). Chill margins or migmatic granite have also been noted along the host-intrusion boundary. Generally, the often massive granite does not exhibit the extensive deformation shown in pre-Lower Devonian host rocks. The extensive structural deformation of these host rocks is thought to be partially the result of the Acadian orogeny (Anderson, 1970).

Tupper and Hart (1961) carried out K-Ar dating at Big Bald Mountain and Popple Depot obtaining ages of  $365 \pm 15$  m.y. and  $395 \pm 15$  m.y., respectively.

Unconformably overlying the rocks discussed above, are nearly flat lying Carboniferous sedimentary rocks.

The granitic belt rocks include quartz monzonite, true granites, biotite granites and granodiorites. Also gneissic granites and granodiorites have been seen. The granites are commonly uniform, massive, medium to coarse grained, occasionally porphyritic, pink to gray-white rocks. Modal analyses of the rocks in this study, by Greiner (1970) and Skinner (1974) identify the major minerals to be quartz, orthoclase, perthite, plagioclase ( $An_5$ - $An_{30}$ ), microcline, and to a lesser extent, biotite/muscovite. Minor minerals reported include magnetite, sericite, zircon, chlorite and

hornblende . Textural variations in granites studied along the granitic belt include porphyritic, cataclastic, allotriomorphic granular and the typical hypidiomorphic granular "granitic" texture (Skinner, 1953, 1954, 1974; Greiner, 1970; Rose et al., 1962; Anderson, 1968, 1970; Shaw, 1935).

On the local scale the Bald Mountain area is "deplier" of a major batholith (see Figure 2). The "deplier" seems to have been rotationally faulted down with the S.E. boundary being the hinge of the N.W. trending fault.

A volcanic dyke is unconformably adjacent to the granite on the N.E. margin of the stock.

The Pierce Mountain site occurs in the central portion of an east-west elongated granite stock. The stock is commonly enveloped by a metamorphic aureole.

Both granite stocks/batholiths intrude argillaceous sedimentary rocks, tuffs and volcanic flows of the Tetagouche Group. The main granite stocks/batholiths are most likely joined at depth.

The weathering of the granitic intrusions mentioned earlier have been noted at several sites by other workers. They report varying degrees of disintegration and weathering of the granites. Anderson (1968) reported deeply weathered granite the Milleville, Woodstock map sheets in York County, N.B. His description of the weathered granite had the

following similarities with the present study:

(1) He describes the granite grains as coarse, angular granules and concludes that they had not been subject to abrasion due to transportation. Also the lack of cross-bedding or any sedimentary structures was noted in the accumulation of grus.

(2) In the Temperance Vale area he reports weathered granite sections (greater than 20 ft) in quarries where jointing and residual veins of aplite are still preserved (similar to Pierce Mountain site).

(3) He notes a gradational contact between the weathered and fresh bedrock.

(4) Feldspar minerals altered to kaolin and anomalously the biotite appears fresh in hand specimen.

(5) He describes the preferential accumulation of weathered granite on the lee side of valleys with respect to glacial flow (i.e. accumulation on eastern slopes).

In his memoir of the map areas in York County, Anderson proposed that the rock weathering cycle may be of the Carboniferous period due to the unroofing of the granite batholiths at that time. He believes this is shown by:

(1) A large number of granite fragments in Carboniferous sediments.

(2) The negative argument that not enough time has elapsed since the last glaciation (late Wisconsin) to allow the



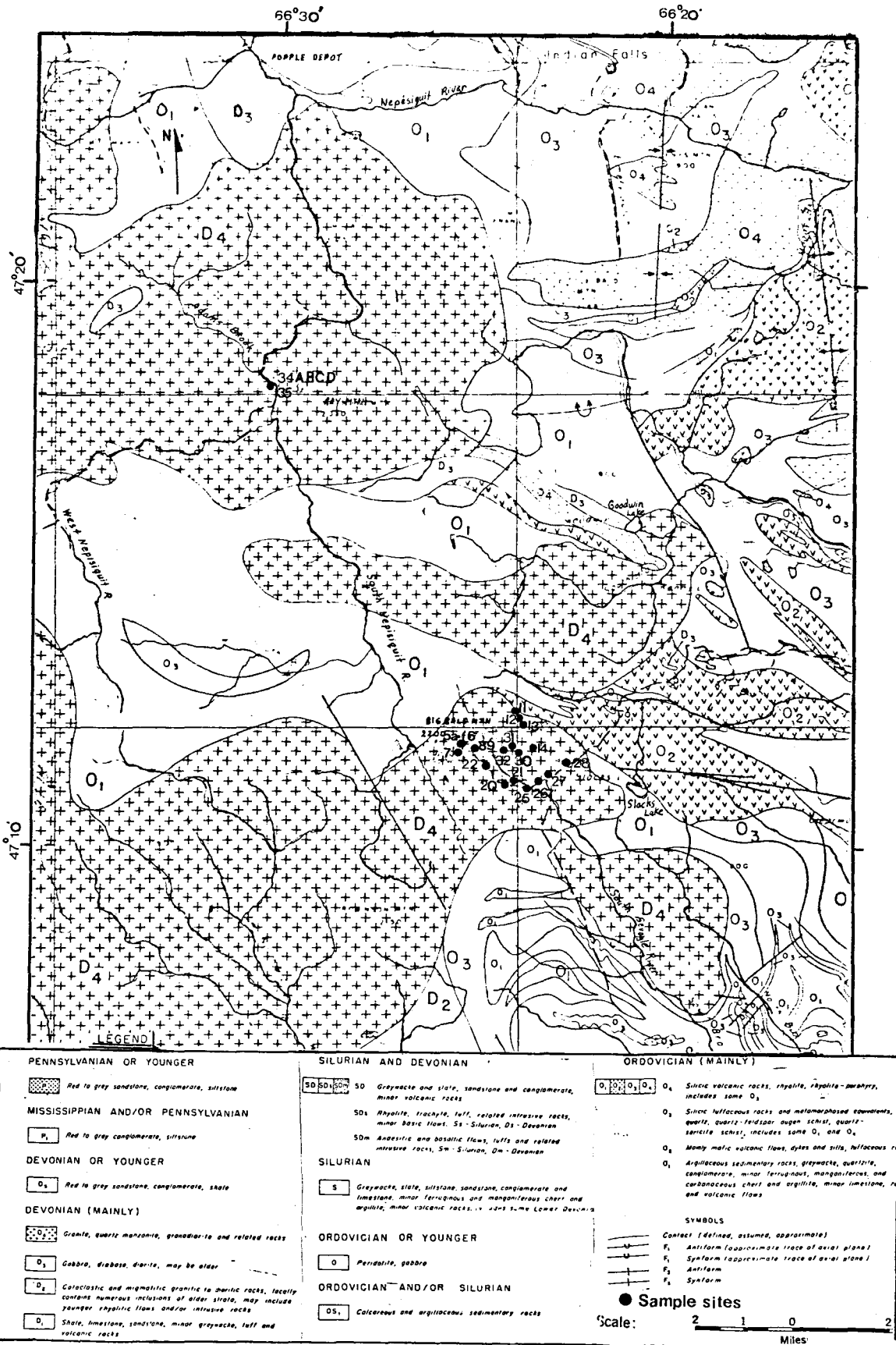


Figure 2. Detailed geologic map of study areas. Sample sites are located with solid dots.

(Modified map; from Davies, J.L., 1972).

weathering of granite to depths seen under the given climate of the post-glacial period.

An alternative is that the weathering profile has developed in a single period and has been preserved by burial until recent times. This possibility could be supported by the occurrence of weathered material grading down into the fresh granite in the Nepisiguit River stock near Rough Waters (Alcock, 1935). This weathering profile is then capped by Pennsylvanian sandstone.

Hamilton (1968) performed major element analyses and grain size analyses of three weathered granite exposures (including Temperance Vale site described by Anderson), to determine the use of the residual minerals. Grain size analyses show that the majority of the grains are medium sand size (i.e. 1.5  $\phi$  or larger). He also notes the friable character of the quartz-feldspar grains. The extent of the granite regolith reserves is thought by Hamilton to be large.

Wolfe (1961) offers an explanation contrary to the conventional weathering profile development implied by other investigators. He suggests that the granite alterations in the Popple Depot area are caused by hydrothermal solutions brought in contemporaneously with the granite intrusion and uses the following observations to support

his hypothesis:

- (1) The rock does not show penetrative deformation.
- (2) There is an increase in the alteration of the rock to the S. and S.W. of Popple Depot (i.e. toward the Pierce Mountain area).
- (3) There is a relatively strong alteration of the Portage Brook intrusion (differentiated diorite host rock).

From the above description of the geology of the area there is potential for the natural climatic weathering of the granites to have been aided by metasomatic solutions and by tectonic activity. The massive non-deformed nature and wide areal and latitudinal extent of most of the altered batholiths described tend to imply that these mechanisms are of local extent and have not played a major role in the alteration of the granites. The present study sites therefore are not unique with respect to the occurrence of weathered granite within the granitic belt.

## CHAPTER II

### FIELD STUDIES

#### 2.1 Introduction

Granite weathering can be thought of as a combination of physical and chemical weathering. The usually abrasion resistant granite disintegrates, resulting in the advancement of chemical decomposition of susceptible granite minerals. The enhancement of chemical weathering with all its controlling factors (such as pH, ground water salinity, alkalinity, etc.) is thought to be a combination of the following:

(1) exposure of a greater quantity of grains to potential chemical decomposition processes; (2) exposure of a larger grain surface area potentially allowing a greater proportion of the individual grain surface areas to become influenced by chemical weathering; (3) greater permeability of the rock allowing a greater volume of migrating ground water to enter the granite structure and therefore allowing the above two factors to become important.

The above suggests the coarser rocks should be more susceptible to disintegration. Any physical process or structure in the rock aiding in its disintegration will tend to complicate predictions on the rate or extent of rock weathering based only on textures, and mineral variations, or chemical thermodynamic mineral equilibrium.

The interrelationship of these two controlling processes (i.e. chemical and physical weathering) is apparent by the landforms and derived sediments produced. Thus the description and analyses of the products of weathering should be of enlightenment in determining the relative importance of physical, and/or chemical weathering in the study area.

Only after defining the physical features and possible process involved can we describe the variations in the weathering profile which are represented by the samples taken.

The two areas of study shall be discussed separately because:

- (1) The Big Bald Mountain study involves the determination of the spatial relationships between the bedrock and derived sediments;
- (2) The Pierce Mountain study involves the stratigraphic variations of an "in situ" weathering profile involving granite of slightly different composition

(see Chapter IV Petrography) taken from a different granite stock than Big Bald Mountain;

- (3) There are also apparent differences in the stage or mode of decomposition/alteration of the granites from the two areas.

## 2.2 Geologic features and processes influencing chemical weathering

### (A) Big Bald Mountain

A hierarchy of joint features has developed in the Big Bald Mountain area, each of which is significant in the weathering of the granite. As discussed previously, the late stage emplacement of the granite batholith including the Big Bald Mountain area is shown by cross cutting relationships and a boundary shear zone. Thus it would be called a late kinematic granite which is characterized by the well developed sheeting/jointing observed (Oen, 1965). Sheeting is thought to develop as a result of stress release. The sources of stress in the Big Bald Mountain area may include:

- (1) Lateral stress stored in the rock during the late stage of crustal upheaval. This is a possible mechanism since the area has been faulted and was

emplaced approximately 30 m.y. before the intrusion of the nearby Pierce Mountain stock (Tupper and Hart, 1961);

- (2) The effects of emplacement and density differences between the granite and country rock (Oen, 1965). This is also a possibility since the granite intruded less dense metasedimentary rocks;
- (3) The overlying load of country rock before the granite batholith was exposed to the surface.

Sheeting structures are evident on the top of Big Bald Mountain and in the small incised stream valleys. The sheeting structures develop approximately parallel to topographic slope. Figures 3, 4 and 5 depict the progression of sheeting forms developed with an increasing topographic gradient. Figure 3 shows the sheeting as very regular, almost "bedding like", horizontal planes. Note the preferential chemical weathering that takes place along these zones of weakness. The photo also shows the limited thickness of grus overlying the exfoliated bedrock. This feature appears to be anomalous if one considers that the undulating hills to the east of the stream valley have a minimum of 4-5 feet of grus accumulation. Figure 4 sheeting structures suggest that the accumulation of debris on this surface would be difficult due to washing of grus when the bedrock is exposed.

Figure 3. Horizontal jointing developed in the valley to the east of Big Bald Mountain. Note the bedding-like weathering profile produced and the system of two vertical joint surfaces. Also note the lack of grus outcrop of the bedrock.

Figure 4. Sheeting parallel to topographic slope. Note the accumulation of grus debris would be prevented by rainwater wash.



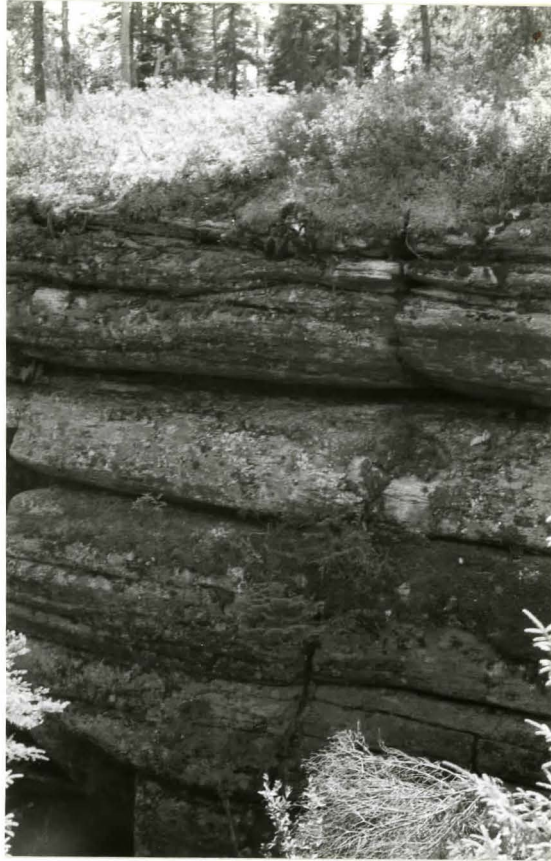


Figure 5. Convex smooth granite outcrop on the west side of Big Bald Mountain. Sheeting structures are no longer evident because the bedrock gradient is too high to retain the exfoliated granite. Glaciation may have had modifying effect on this face in the past.

Figure 6. Dome form exposed on ridge near Bald Mountain. Undercutting of form is thought to represent preferential solution along a jointing surface once covered with mantle grus. Modification may have resulted when the form was exposed to surface weathering (ex frost action). Also note the flat face developed at the base of the dome parallel to a vertical jointing surface.

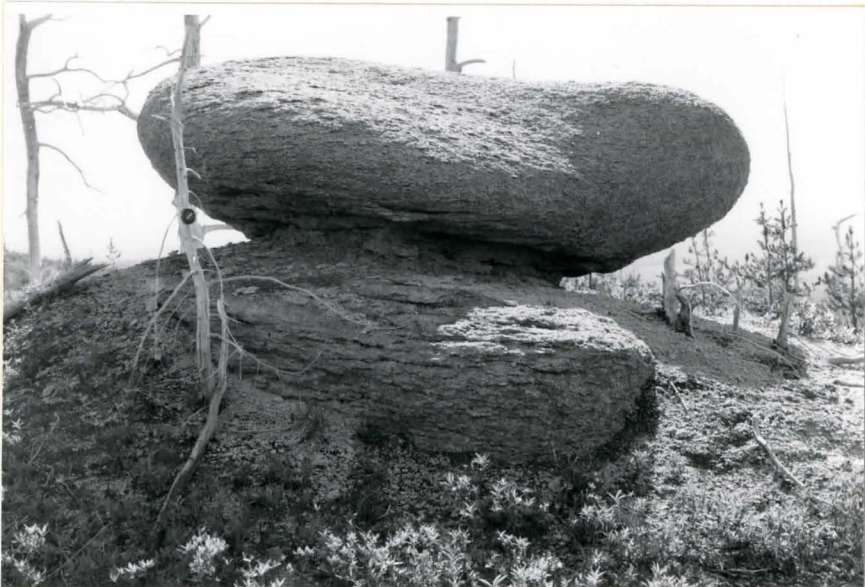




Figure 7. Figure 6 form viewed from a different orientation. Note the difference in the amount of undercutting and the accumulation of grus.

Figure 5 illustrates the smooth non-foliated face developed when topographic slope is too high to hold the sheeting structures. White (1945) believed that sheeting structures need not be required to explain these convex forms, but the disintegration of granite grains may be another cause. He thought that kaolinization along microfractures may also result in a smooth dome profile.

Sheeting however is the major influence in the Big Bald Mountain area. Residual tor development also is strongly influenced by sheeting structures and preferential weathering along these planes. Figure 6 shows the peculiar shapes developed on the summit of the ridges to the east of Big Bald Mountain (e.g. Site 30).

It seems unlikely that these forms developed if only exposed to the atmosphere. In Figure 6 note the sharp vertical face at the base of the outcrop representing the vertical joint system. Figure 7 represents the same outcrop at a different orientation. Note the difference in intensity of undercutting.

### Vertical joints

The development of vertical joints is shown by the preferred orientation of the vertical to sub-vertical inselburg faces, preferential elongation of microscale

solution basins and preferential weathering associated with sheeting. Figure 8 shows the relationship between landform profile and orientation of vertical joint faces. Note the preferred accumulation of grus on the "east" side of the photo which was taken parallel to the  $50^\circ$  joint orientation. There is a distinct lack of grus on the "west" side associated with the sharp rock face. The undercutting of this form may be occurring presently in the subsurface along a weathering front parallel to a horizontal joint plane.

Tors are characterized by the occurrence of two sets of near vertical joints which tend to compartment the outcrop into blocks (see Figure 9). Note the sharp junction between the near surface flat bedrock (erosional surface) and the massive tor.

The measurement of the vertical joints reveal two major near perpendicular trends at  $50^\circ$ - $230^\circ$  and  $140^\circ$ - $320^\circ$  as shown in the rose diagram (see Figure 10). This trend was found developed in tors on the ridge and in the incised bedrock in the valley (Figure 3).

The expansion and deepening of joints is related to the drainage of water along these joint faces. The maximum separation between jointed tors measured was 2.5 m, the minimum was 13 cm. The depth of solution along joints was variable, partially due to the accumulation of grus in the

Figure 8. Dome feature developed with steep vertical joint related face and grus debris apron on opposite side. Note the scaly texture of the granite surface thought to be related to microfractures in the rock. The photo is oriented parallel to the 50° joint surface.

Figure 9. Tor compartmentation due to vertical jointing. Note the sharp boundary between the tor and bedrock exposed at surface or near surface. Also note the solution features on the side and top of the tor. These are known as taffoni and basins, respectively.



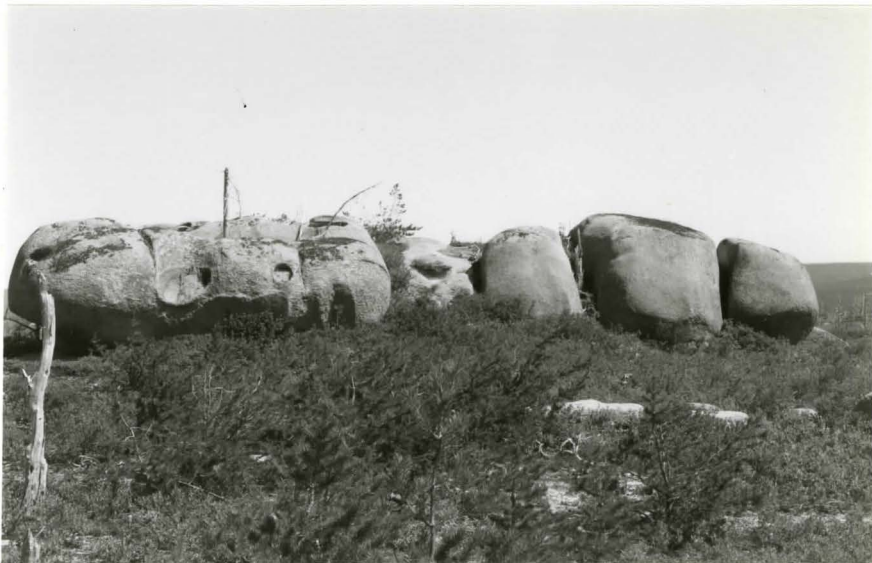
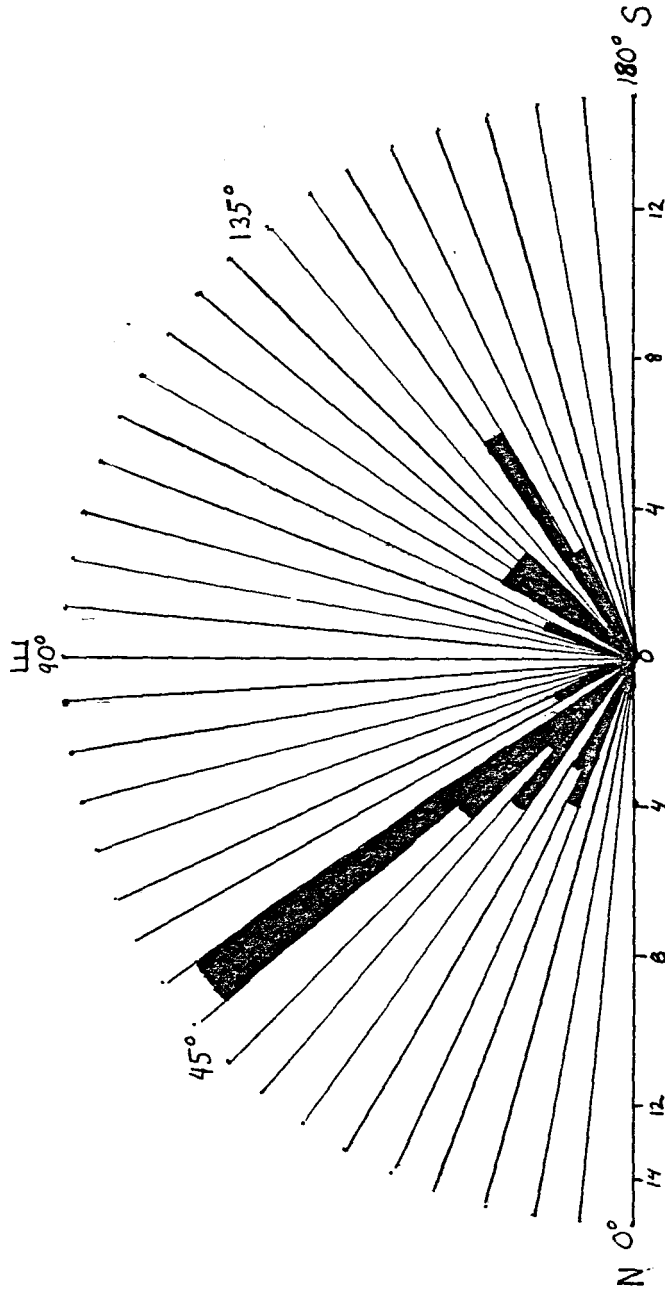




Figure 10. Vertical-Subvertical Joint Distribution



*1/2 cm per measurement made.*

joints. The maximum height of the tor parallel to these joint surfaces was 2.9 m.

### Microfractures

Microfractures or potential joints are defined as highly discontinuous faces or zones of weaknesses in the rock (Chapman, 1958).

These features are associated with the scaly nature of the dome structures seen in Figures 6, 7 and 8. Iron oxide stain encrust some of these fractured dome features. The grain relief is usually very high on these spherical tending forms allowing the grains to be easily plucked off by hand. Tors usually do not develop this system of microfractures. Oen (1965) and Thomas (1976) believe that the spherical weathering results from the unwrapping of layers of partially rotten rock-producing grus. The process is thought to be initiated by the combination of rock weathering and tensional collapse along freshly opened potential joints when the spherical form is exposed to the atmosphere.

Another possible method of producing potential joints is the oxidation of biotite in the granite. This would result in the expansion of the biotite possibly fracturing surrounding minerals. Several authors have recently advocated

the importance of biotite grossification (i.e. formation of microfractures allowing greater permeability in the granite making the rock more susceptible to chemical weathering) (Bustin and Mathews, 1979; Isherwood and Street, 1976).

It is believed, however, that areas where these conditions have been studied, the granite has been hydrothermally altered to make the biotite more susceptible to chemical attack.

Isherwood and Street (1976) state that one of the underlying conditions of biotite grossification is the intensity of chemical weathering is not great enough to alter the angular K-feldspar and quartz fragments present in the grus.

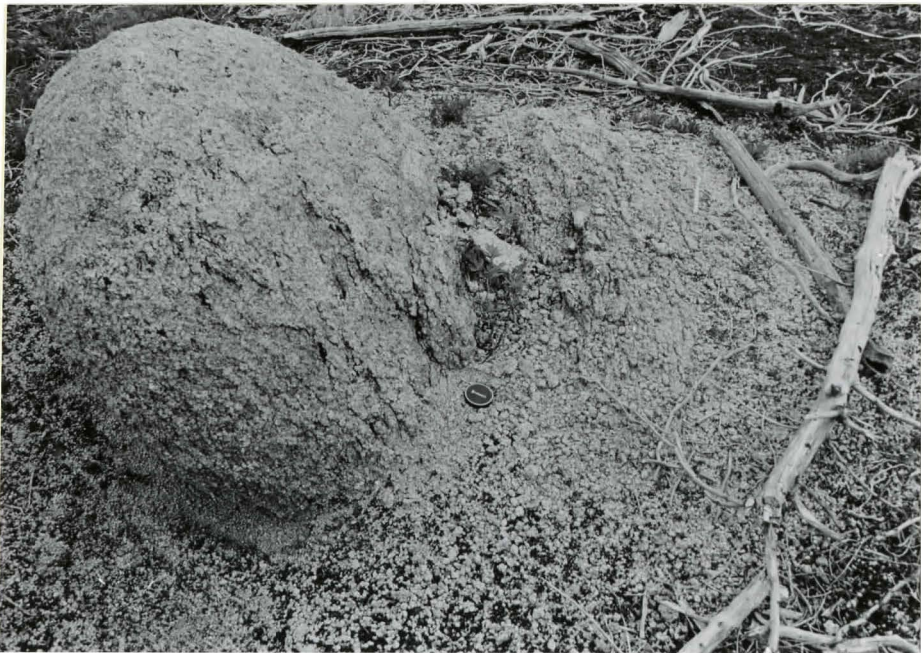
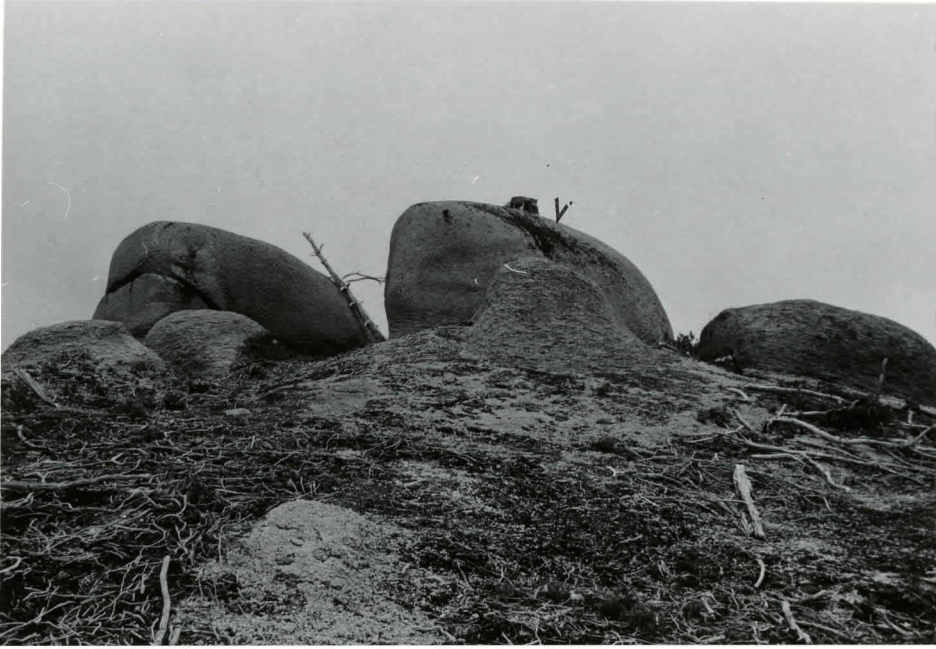
It is believed from hand specimen inspection, that a similar deposit may result due to the preferential weathering of Ca plagioclase in the granite. This would allow the residual K-feldspar and quartz to fall out of the rock matrix.

The potential joint theory may be used to explain the occurrence of spherical domes and tors in close proximity to each other, as seen in Figure 11. Note the difference in surface relief between the scaly dome in the foreground and the relatively smooth compartmented tor in the background of the photo. Figure 12 is a close-up photo of the dome feature.

The form appears to be deeply rotted shown by small scale fractures, high grain relief and grus apron surrounding

Figure 11. Tor and dome features developed in close proximity to each other. Note the difference in texture between the two forms. Also note the granules of residual quartz on the surface in the foreground. Sample site 14 is a grus sample taken between the tors.

Figure 12. Close-up photo of dome structure seen in Figure 11. Note the high surface grain relief and the presence of fractures in the form, both of which combine to give a scaly appearance.



form. The surface grus appears to be intensely leached shown by the dominance of only residual quartz. Thus initial difference in intensity of microfracture which were accentuated upon exposure to atmospheric weathering, could account for the difference in form. Another possibility is that the relict forms were not formed at the same time, thus representing different stages in the weathering process.

These forms must initially develop subaerially; as suggested by the occurrence of a dome on the exfoliated sloping surface illustrated in Figure 13. This corestone appears to be a relict of a former granite surface which has been washed or exfoliated downslope.

From the previous forms and deposits it is reasonable to conclude that the system of joints developed plays an important or even dominant role in the weathering of the Big Bald Mountain granite. However equally true, the presence of chemical weathering along jointing planes has had a modifying effect on the forms and structures produced.

#### Solution features

Other evidence of chemical "solution" of the granite includes the development of small scale solution basins in the bedrock. These forms were found on the top of ridges

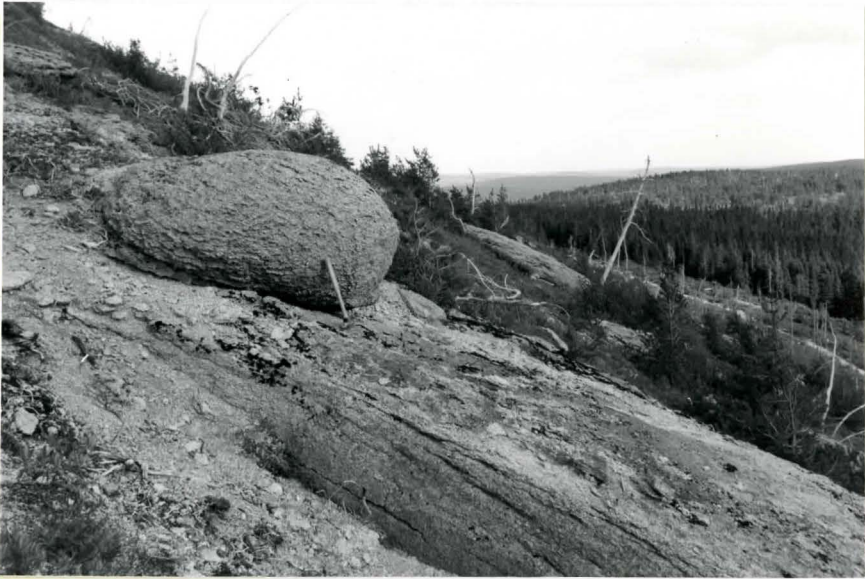


Figure 13. Core stone developed on exfoliated granite defining the presence of a former mantle on the slope which has been lost due to exfoliation and/or surface wash.

and also near the bottom of the ridges on exposed bedrock. Figure 9 illustrates the development of "arm chair" basins called taffoni on the side of a tor. They appear to be oriented parallel to vertical joints.

These features are developed on outcrops without scaly microfractures, thus producing a smooth but irregular surface relief. The diameter of these basin forms range from 0.21 cm to 1.30 m. Average size taken from 30 measurements was 63 cm. Basin forms also are often elongated, approximately parallel to the joint system. The depth of the features varied from 4-48 cm, averaging 21 cm. Figure 14 illustrates the irregular surface developed and typical undercutting nature of the sides of the basins. Note the interconnecting nature of the basins developing a step-like drainage network. The undercutting of the basin forms result in a small scale arch; this is developed when the growth of two basins interferes with each other. For this to occur the mechanism of weathering (solution) must be acting from the base upwards as would be expected.

Rillen solution patterns are also developed in the steep slope of the western face of Big Bald Mountain, as shown in Figure 15. These features are parallel to the 150° vertical joint system. Note the accumulation of grus and spalls at the base of the cliff. The occurrence of these forms are thought to be the result of subsurface preferential



Figure 14. Interconnected "solution" basin forms in the granite. Note the undercutting of the basin form from the base producing a lip to the basin form. The interference of two basins result in the small scale granite arch seen. The forms are developed on top of a large tor.

Figure 15. Rillen produced in granite due to "solution" along preferred planes of weakness on the steep western face of Big Bald Mountain. Note the accumulation of grus and spalls at the base of the cliff.



accumulation of moisture in zones of weakness in the bedrock. Upon exposure to the surface these forms are deepened due to growth of lichen in the basins. The lichen produce organic acids which corrode the feldspars. The presence of these forms thus define a former basal surface of weathering (Thomas, 1976). Thomas (1976) noted similar features in boulders of Rough Tor in England.

#### Rock type

The importance of rock type in the development of granite landforms is shown in Figure 16, which shows the blocky appearance of the rock along the batholith boundary shear zone. Samples 11a and 11c were taken from here. Note the lack of grus surrounding the outcrop which is common in previous illustrations. This rock is porphyritic and fine grain which may account for the differences in weathering.

#### Other processes

The occurrence of a forest fire in the Big Bald Mountain area may account for some of the scaly textures developed in the granite; however the form of spalls produced by fire do not correspond with fractures seen at Big Bald

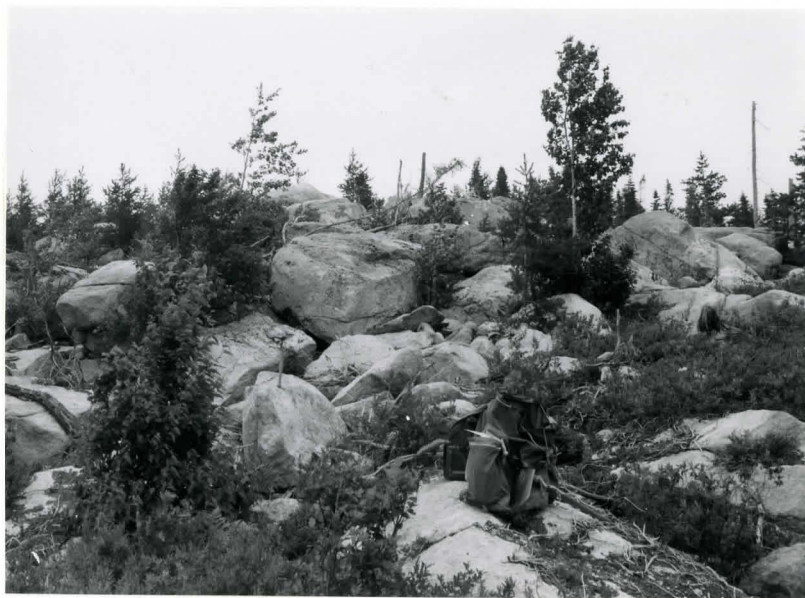


Figure 16. Block-like fracturing of boundary shear zone granitoid. Note the difference in weathering, the lack of exfoliation and grus accumulation typical of previous illustrations. This rock is porphyritic and fine grain which may account for its difference in weathering form.

Mountain (Blackwelder, 1927). It is believed that the effect of fire was therefore only to accentuate the weathering system previously developed.

### 2.2.2 Summary and Discussion

From the field evidence gathered, it appears that the jointing hierarchy developed in response to tectonic or on the microscale, mineral alteration (i.e. kaolinization; White, 1945) and/or biotite grussification (Isherwood and Street, 1976) seem to be the dominant processes involved in the weathering of the Big Bald Mountain granite. The effect of chemical "solution" is of minor importance, as evidenced by the relative freshness of the non-leached grus found in the incised plane to the east of Big Bald Mountain. The preferential accumulation of grus illustrated in several of the previous figures (eg 8) may be related to several processes:

(1) The preferential accumulation of debris on the eastern side because of the different moisture conditions typical of the northern hemisphere. This allows greater susceptibility of minerals to grussification. Note that the dominant wind pattern is from the west which would tend to dry western faces reducing the effect of chemical weathering.

(2) The presence of glaciation has a two-fold effect:

(i) changing storm pattern and climatic regime;

(ii) the modification of debris by erosion on stoss side and deposition on lee side of obstacles.

Freininger (1971) notes that the distribution of weathered granite is discontinuous in areas covered by Pleistocene ice sheets as seems to be the case in New Brunswick.

Chalmers (1898), who worked extensively in New Brunswick, considered the presence of deep regoliths to be remnants of formerly extensive mantles preferentially removed by glaciation. The presence of tors has often been quoted to be indicative of non-glaciated terrains; however, more and more evidence suggests this is not true, especially in light of Sugden and Johns' (1976) theory of the non-erosive power of cold based ice, which may well be present here in the highlands of New Brunswick. Possibly in conjunction with the above, Jahn (1976) suggests that if the tors were present subaerially they would suffer only minor resculpturing.

Thus the development of tors and dome features may be of preglacial origin, but they may have been modified during glacial or periglacial climate conditions. For example, the acidity of waters increases with colder temperature due

to greater  $P_{CO_2}$  in the water leading to the greater effect of chemical weathering. The solution features previously discussed may have developed in such a climatic environment.

The solifluction of debris in periglacial conditions and/or partial erosion by glacial ice may account for the accumulation of debris to the east of the ridge. Very limited abrasion of material would have occurred under such conditions. This is supported by McEwen et al. (1959) who determined that the texture of grus transported by a stream limited distances did not change significantly.

Thus the glacial modification of an already weathered granite profile is supported by:

- (1) The accumulation of debris on the lee side of obstructions with respect to the general eastwardly movement of ice in the region;
- (2) The solution forms found on the summit tors and inter-ridge valleys;
- (3) It provides a mechanism to aid in the erosion of grus from the ridges required since the evidence suggests that a mantle of derived sediments was once present;
- (4) The presence of very minor and small erratics in the deep grus and the non-bedded character of grus accumulations in the incised plain;
- (5) The presence of the smooth steep convex slopes on

the western margin of Big Bald Mountain may be the result of stoss side erosion aided by subsequent sheeting action.

Thus, the weathering deposit location is not only dependent on the jointing system developed and preferential chemical solution, but also by the modification resulting from glacial and periglacial conditions.

(B) Pierce Mountain

Geologic features and processes influencing  
chemical weathering

The Pierce Mountain site represents "in situ" development of deep granite grus and clay pockets. The development is known to be "in situ" because of the presence of a residual quartz vein in the grus (Figure 17). Note that the top portion of the vein has been shifted showing that colluviation processes are active at the site. This level is above the areas where clay pockets develop. Having established that the major portion of the deposit has not been transported, allows the description of the features seen in terms of a true weathering profile.



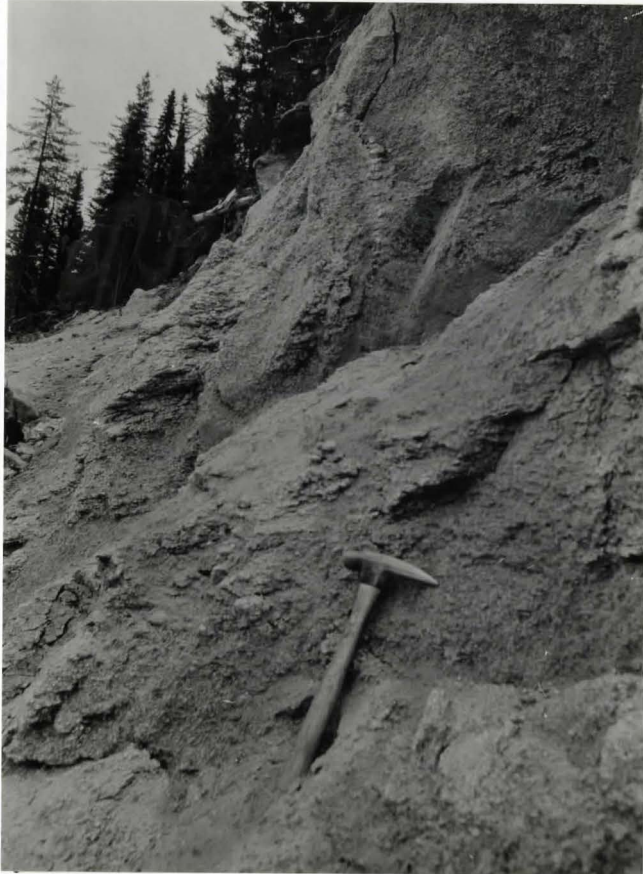


Figure 17. Quartz vein within the regolith-grus determines the deposit is "in situ". At the base, the vein is straight but in the upper portion the vein is offset in a stepwise manner indicating that colluviation processes are present. Note the sheeting structures are very thinly "bedded" and parallel to former valley slope.

One of the major assumptions in studies of weathering is that the source or parent rock was homogeneous in composition. This may not be the case at this site as the intense alteration makes identification difficult. The variations in colour in the outcrop is suggestive of different mineral assemblages. There was a distinct break between the pink granitoid gneiss and the white biotite granite host. Colour variations within the gneiss-regolith included light green powdery rock and deep pink K-feldspar rock discussed previously. These zones may have been the result of metasomatic or hydrothermal alteration. This is a possibility when one considers that this stock was emplaced 30 m.y. after the Big Bald Mountain batholith (Tuttle and Bowen, 1961). Thus volatiles may be concentrated in this late stage crystallizing magma.

The differentiation between hydrothermal and metasomatic alteration with vertical surficial weathering is difficult since they are not mutually exclusive processes. They often form the same products (Konta, 1969).

Evidence for metasomatic alteration includes:

(1) The irregular variations in intensity of weathering in the gneiss;

(2) The presence of clay pockets as seen in Figure 18. There was a joint surface along which ground waters are



Figure 18. Clay pocket developed in the weathering profile. Note that the grus above and below the deposit appear to be the same. Ground water flows parallel to the left boundary of the deposit possibly indicating some relation between the two. Note the fine lamellae in the upper portion of the clay pocket represents a black precipitate that parallels former exfoliation (sheeting).

percolating. This was a common feature. Note the drastic difference in texture between the grus and the clay pockets. The same grus lies above and below the pocket, indicating that depth variations shall not be of great importance at this site.

(3) The presence of black deposits along former sheeting planes in the clays may be related to humic acid percolation. Also iron oxide veins frequently run subvertically through these fine grain alteration products.

(4) The position of the site itself in a valley side allows for a good source of subsurface ground water seepage.

(5) The deep iron oxide B horizon developed in the colluvium above the deposit (Figure 19). This suggests the migration of water through the profile. Note the accumulation of organic material above the B horizon iron pan. This may be a source of acid water aiding in the alteration of the granite.

(6) Biotite in the host rock appears to be a brownish-yellow colour unlike the Big Bald Mountain granite where the biotite was black and shiny. An iron oxide stain frequently envelops the grains. Egger et al. (1964) showed that the hydrothermal alteration may only weaken the rock due to this type of biotite oxidation.

The intrusion of the granite, produced similar

Figure 19. Deep iron pan developed in the colluvium above the deposit. Note the corestones in the lower left portion of photo.

Figure 20. Distinct colour variations in the deposit seen in the upper portion of photo. Note that jointing is still distinguishable in this highly grussified deposit. Also note the variability in the colour of the grus within the deposit possibly indicating different rock type or horizontal migration of metasomatic or hydrothermal water.





microfractures and vertical joint patterns and sheeting as seen at Big Bald Mountain. The microfractures were commonly only 1 cm apart. Sheeting also tended to parallel the former valley slope. Figure 20 illustrates the two sets of vertical jointing in the highly friable but still lithified bedrock. Often bedrock features are still seen in the grus accumulation above.

### 2.3 Method of sampling

The purpose of the method of sampling was to obtain samples representative of variations in weathering landforms and derived sediments previously outlined in section 2.2. The laboratory studies on the samples were designed to test the hypothesis made from field evidence. Thus a sample was usually taken to define differences in the weathering profile seen by colour, texture, form or areal variations.

#### (A) Big Bald Mountain

The sampling procedure for the ridges of the Big Bald Mountain usually involved finding variations in the exfoliated bedrock with depth (a diamond drill core was obtained at the summit of Big Bald Mountain), or variations between the tors

and associated grus deposits. This was done for three ridges. Soil profile was very limited on the ridges, generally less than 1.5 feet. Examples of the distinctive surface leached accumulations which were composed of fine silt and quartz granules were taken. Some examples of bedrock-"soil" interface clay and silt were taken to determine the type of clay present. Soil samples were taken down the ridge to find if there were any variations with location or topographic setting. At the bottom of the ridge a small weathering profile was present over the exfoliated bedrock-regolith. Samples were taken representing the complete soil profile. The presence of a falls slightly to the north of the site gave a sample of the "fresh" bedrock, to complete the profile (Samples 20A,B,C,D and 21). On the incised plane 3 or 4 samples were taken of the deep grus accumulation which had a "deep" (1') iron pan above what appeared to be well sorted deposit of granules. This was unlike the other soil profiles developed, in that it lacked plates of exfoliated bedrock and silty matrix common to most of the previous samples. The presence of a few granules of volcanic rock made interpretation of the origin of the grus difficult (sample 27). A till was found over this grus identified by poor sorting and presence of erratics, a little further to the NE along the road (sample 28a,b).



Thus a representative cross section of the weathering products of the Big Bald Mountain was obtained.

(B) Pierce Mountain

A different style of sampling was used due to the excellent exposure of a deep weathering profile. Samples were taken to represent the change in texture, colour or degree of lithification within the profile with depth (e.g. samples Aa-Ag). Individual intensely altered pockets of green silt-clay were especially described and sampled (e.g. Ba and Db) at different positions in the section. Note that they were not continuous but were isolated within the generally deeply altered silty grus. Samples were usually taken above and below these clay pockets to see if there were any vertical changes with depth (e.g. samples Bb, Bc, Da, Dc). The boundary between grussified and lithified bedrock was gradational and irregular, thus vertical changes between different sections would be difficult to correlate. A sample of the partially lithified bedrock-grus boundary was obtained (e.g. samples Ag, C, Dc), which was commonly defined by a ledge in the profile. Finally a sample of the white biotite granite in the freshest condition obtainable was taken at the bottom of the section.

Total section was approximately 15 feet. Thus although a sample was not taken every "x" feet all the noticeable variations in rock weathering were sampled.

## 2.4 Sample location

### 2.4.1 Introduction

The location of the sites of all samples and the number of samples taken at each site, indicated by subscripts, are shown in Figure 21 with respect to topography. Note that the several samples taken at Pierce Mountain are located at Site 34. Figure 2 shows the location of each site in relation to the regional geology. The topographic position of a site is very important with respect to the chemical weathering processes active at the site.

### 2.4.2 Stratigraphic position

Figure 22A shows the stratigraphic relationship between a hypothetical profile at Big Bald Mountain based on Site 20 and Figure 22B, the Pierce Mountain (Section Aa-Ag, and 35).

The Big Bald Mountain section includes a summary



schematic of all deposits seen and their relative position in relation to each other. It includes:

- (a) A horizon;
- (b) B horizon;
- (c) Grus;
- (d) C horizon;
- (e) D horizon exfoliated, striated rock regolith;
- (f) Jointed bedrock.

Note for a given site the depth and even the presence of a horizon is variable depending on topography, drainage and amount of erosion of the weathering profile and/or the type of weathering deposits. A description of deposits follows (Figure 23).

Pierce Mountain stratigraphy is illustrated in Figure 23B. The vertical position is approximate since the sediment position in the profile was variable depending on local colluviation processes, ground water drainage, etc.

#### Sediment description

Figure 23 summarizes the position and basic characteristics of the deposits for both sites.

The following is a general description of the different deposits/bedrock found at Big Bald Mountain (refer to Figures 22A and 23A).

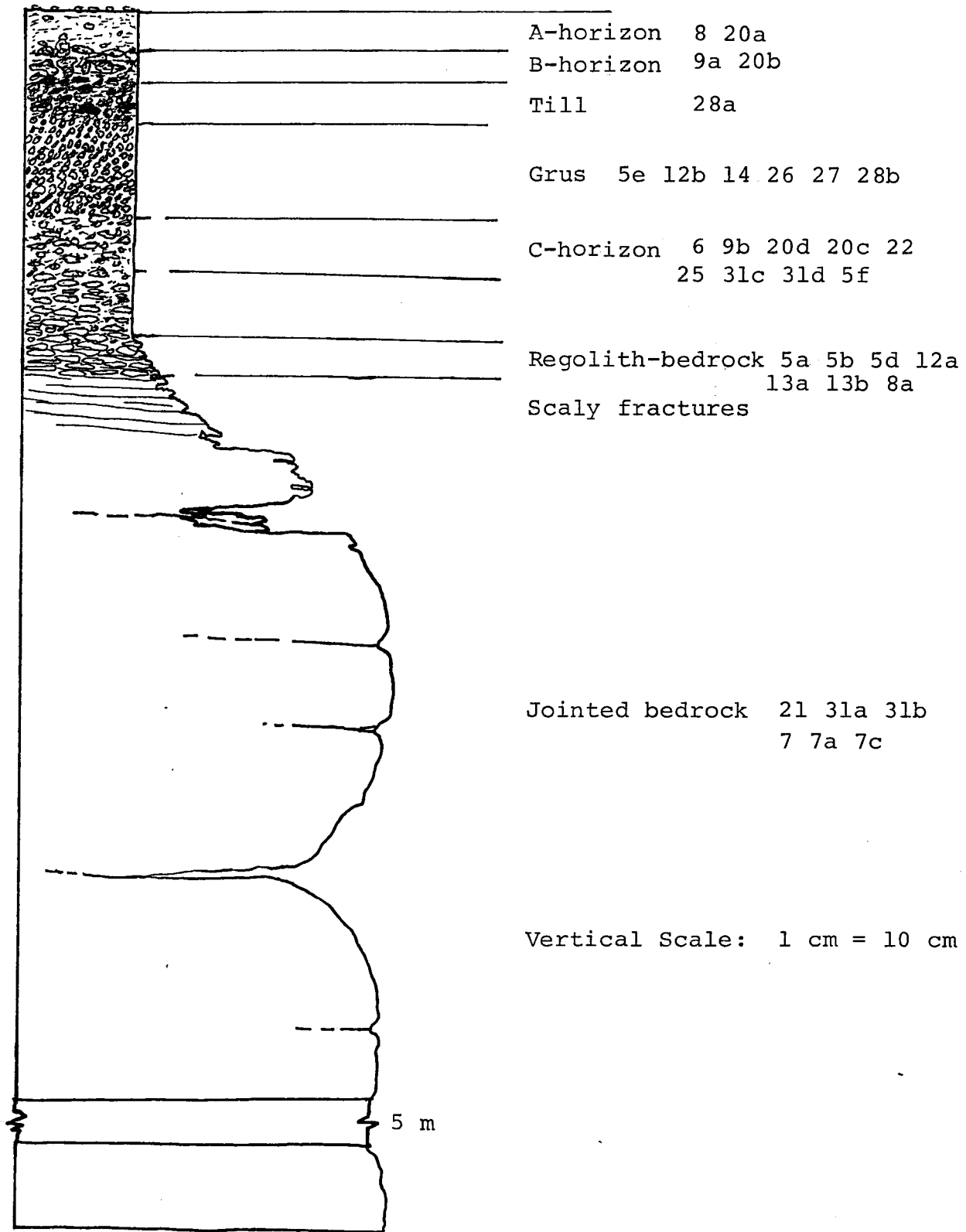
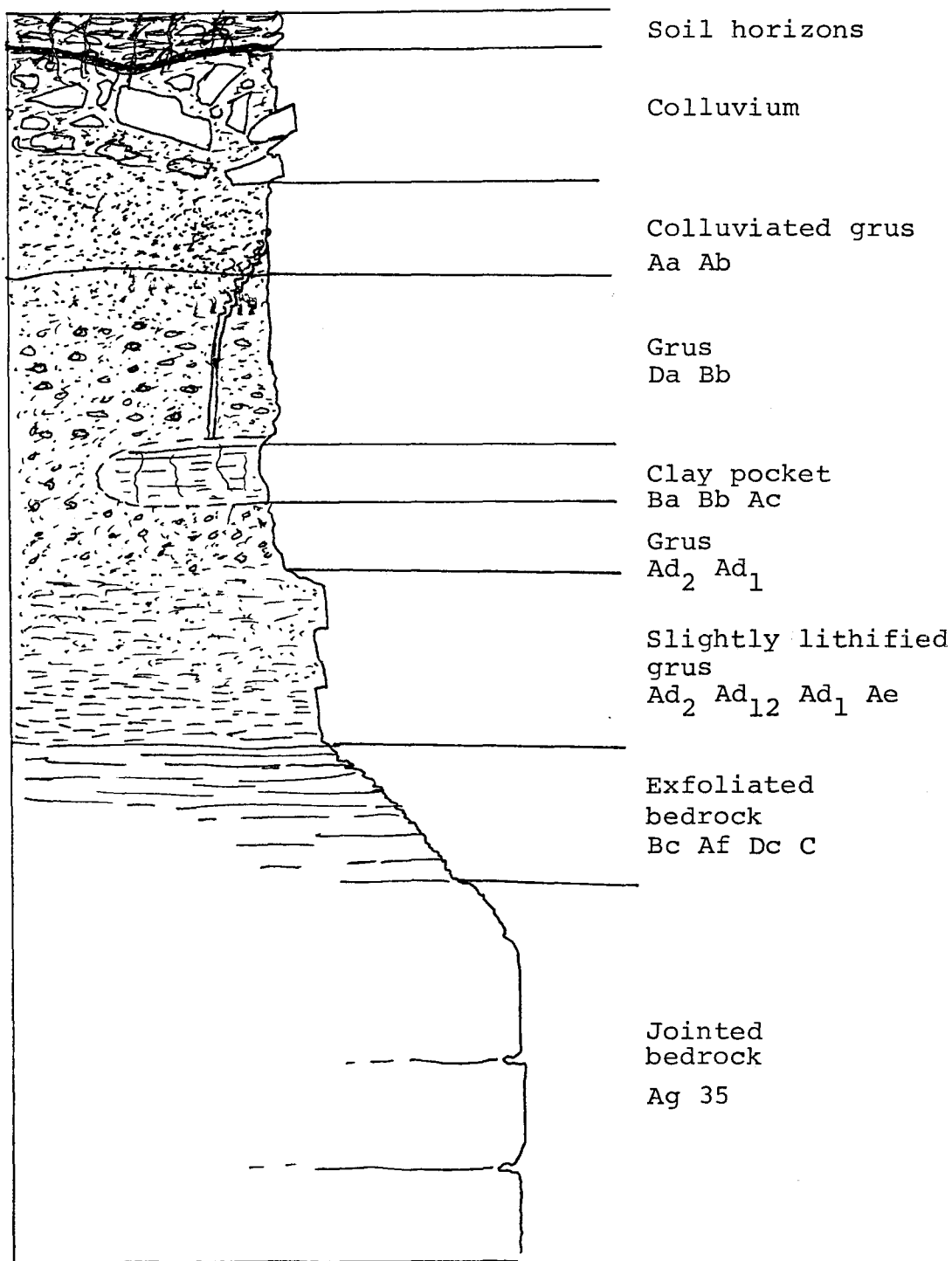


Figure 22A. Schematic model for the weathering deposits at Big Bald Mountain.



Vertical Scale: 1 cm = 30 cm

Figure 22B. Pierce Mountain model stratigraphy of weathering profile

## A. Big Bald Mountain

Sample	Symbol	Composition	Stratigraphy
5a	▲	Weathered bedrock, exfoliated	Top surface
5b	▲	Weathered bedrock, exfoliated	18 cm from top on the edge
5d	▲	Weathered bedrock, exfoliated	90 cm from top along joint
5e	■	Surface accumulation	1.58 metres from top
5f	□	Soil-clay bedrock interface	
6b	□	Soil-clay bedrock interface	10 cm from surface-soil thin
7	▲	Bedrock	Non exfoliated surface on west
7a	▲	Bedrock	Side sample
7c	▲	Highly weathered bedrock	Surface sample
8	○	Soil, residual, quartz	Thin soil layer chiefly quartz, <i>surface</i>
8a	▲		
9a	●	B horizon	15 cm to 30 cm
9b	□	C horizon	30 cm to 45 cm. Bedrock = 94 cm
12a	○	Weathered bedrock	Knocked off scaly exfoliated bedrock
12b	●	Soil debris grus south side	Surface
13a	▲	Bedrock	Top of outcrop
13b	▲	Bedrock	Middle of outcrop
14	■	Soil debris and grus	B horizon, <i>20cm</i>
20a	○	A horizon	Leached quartz residual, <i>surface</i>
20b	●	B horizon	FeO <sub>2</sub> stain - cemented, <i>10cm</i>
20c	□	C horizon.	Till? Fragmented exfoliated silt matrix

Figure 23/continued

Sample	Symbol	Composition	Stratigraphy
20d	□	C horizon	Regolith, exfoliated, no matrix
21	△	Bedrock, exfoliated, rock edge	2.4 m from top, water falls
22	□	C horizon	Weathered, not affected by soil processes
25	□	C horizon	45 cm from surface
26	■	grus transported	60 cm from surface. Feldspar quartz and K-feldspar with respect to river sand
27	■	Grus lacking silt	Intensive accumulation of granules, 1.2 m hole
28a		Till	Granite debris, rich silty - 0-21
28b	■	Grus	60 cm granules dominant
30b	■	Debris accumulation	Top 30 cm different in oxidation parallel to slope
31a	▲	Bedrock	Smooth weathered
31b	▲	Bedrock exfoliated	Near base of undercut
31c	□	Soil, granules of rock	45 cm to 75 cm matrix silty sand
31d	▲	Bedrock-regolith	75 cm
32b	■	Grus accumulation	Apron of grus



Figure 23B Sample Descriptions

B. Pierce Mountain

Sample	Symbol	Position	Composition
Aa	△	45-90 cm top soil below iron pan	Below soil layer, silty accumulation granules
Ab	△	90 cm-1.35 m of soil	Poorly sorted silty sand with granules
Ac	○	1.35 m from surface	Clay pocket, extremely weathered bedrock, powdery sand, generally white with lime green or pink stain
Ad <sub>1</sub>	△	Weathered bedrock	Green regolith, gradual contact with sample Ac
Ad <sub>2</sub>	△	Bedrock	Pink regolith
Ae	△	Regolith 1.35 m	Just above rock regolith contact
Af	□	Rock	Just below contact
Ag	■	Rock	Start of white weathered granite
Ba	○	90 cm	Clay pocket, green clay
Bb	△	60 cm	Pink granitic sandy silt
Bc	□	120 cm	Bedrock taken below green clay still lithified - hard
C	□	Rock	Pink feldspar bedrock above white granitic ledge.
Da	△	90 cm to 1.5 m	Poorly sorted granulitic silty sand with rock fragments and a black vein
Db	○	1.5-2.70 m	Granulitic green clay, lithified base
Dc	□	2.70 m	Powdery - lithified rock, greenish
35	■	4 m	Fresh bedrock, base of section

A horizon: This includes the surface leached accumulations of residual quartz on the summit and thicker soil leached zones in the valley plain. Essentially this deposit consists of white silty matrix with residual quartz grains and weathered white feldspar crystals. Some humus (roots) in the mixture results in the light grey-brown colour.

B horizon: Iron pans are frequently developed in soil profiles where the soil is of some depth (0.6 m). The iron oxide cements the granules of quartz and feldspar. The hardness varies from site to site. The rock fragment granules tend to break along quartz feldspar boundaries in the rock.

Grus: Developed especially in valley plain and as debris accumulation or aprons of granule-size sediment form at the base of tors. It usually consists of granule size to sand size angular granite and quartz or pink K-feldspar grains. Platy rock fragments are not present or rare. Sorting seen in the undulating hill and in the valley plain deposits is evident by the general lack of silt in the matrix. This suggests that the deposit has been fluviially washed, but no structures were seen in the deposit to a depth of 1.5 m. There is a distinct difference between this deposit and exfoliated plates typical of Section 20, C horizon.

C horizon: This is a poorly sorted yellow-brown to brownish-grey sediment. It usually consists of irregular non-oriented fragments - exfoliated plates of granite rock in a matrix dominated by K-feldspar and quartz grains. A relatively small percentage of fine silty sand was found dispersed through the deposit.

Exfoliated bedrock has similar composition to the source but often has iron stain coating the grains, as seen on some of the more scaly surface dome features.

Bedrock: The bedrock is a medium to coarse grain pink "biotite" granite.

Samples taken from the Pierce Mountain site can be categorized as clay, grus, regolith-bedrock and bedrock (Figures 22B, 23B).

Clays: These are found usually in distinct pockets, often light green and pink colours derived from the original bedrock stain the dominant white deposit. No granules are found in the silty fine sand sediment. Black precipitate tends to follow former exfoliated joints. Contact between grus and clay is usually distinct.

Grus: Relatively poorly sorted silty sand with granules of friable rock fragments in the matrix. The deposit is non-compacted, pink or light green sediment. If

undisturbed the sediment retains bedrock features such as exfoliation and quartz veins, etc.

Regolith Bedrock: The contact with the above is gradational as shown by the change to highly exfoliated bedrock which is easily broken with the hands. Biotite is noticeably dispersed through the matrix of pink feldspar and light green powdery rock.

Bedrock: There is a sharp contact with the above deposit. The rock is a white biotite granite.

## CHAPTER III

### LABORATORY ANALYSIS

It was the purpose of this section to determine if the evidence found in the field is supported by laboratory analyses. Techniques used include petrography, grain size analysis, X-ray diffraction and major element analysis.

#### 3.1 Analytical Methods

##### 3.1.1 Introduction

Several methods were used to determine variation in the chemical and physical properties of the altered bedrock grus and soil produced from the granite parent rocks. These included grain size analysis, major element analysis by optical emission analysis (G.S.C.) and X-ray fluorescence analyses and X-ray diffraction analysis.

##### 3.1.2 Grain size analysis

Grain size analysis were made on 19 samples in total, 11 from Big Bald Mountain site and the remainder from Pierce Mountain site. Samples were taken from A, B, C and D soil horizons, grus and silt-clay pockets. The samples were dried and checked for organic content. To separate the grain size fractions for each of the samples, Canadian Standard 8" sieves were used. One half phi interval sieves

were used for sieve sizes ranging from  $-3.00 \phi$  to  $2.0 \phi$ . For the finer fraction,  $1/4 \phi$  intervals were used up to  $3.5 \phi$ . The coarser and finer fractions were sieved separately in a Ro-tap machine each for 10 minutes. Up to 100 g of sample were separated so as to obtain a large enough fine fraction for further analyses. Each size fraction was measured by an analytical balance then stored in envelopes for future reference. Some error may have resulted due to the fracturing of rock fragments in the sieves.

The fine fraction was then allowed to settle in a graduated cylinder for 8 hours in water at a constant temperature of  $20^{\circ}\text{C}$ . The volume of distilled water in the column varied with the weight of sample used according to the method outlined by Black et al. (1965, p.550). According to Black et al. (1965) this would settle all but the  $2 \mu\text{m}$  clay fraction which would still be in suspension. After the allotted settling time the suspended sediment was separated from the heavier fraction using a pipette. Some error may have resulted at this stage by siphoning too much of the water column. The suspended sediment from the pipette was then filtered by vacuum leaving the clay on the GAF filter paper until the sample was dry. This method would result in an oriented clay sample. The filter paper and clay were later mounted on a glass slide for X-ray diffraction analysis.

### 3.1.3 Major element analysis

Whole rock analyses for 19 samples were obtained by using a Philips Model 1450 AHP automatic sequential X-ray fluorescence spectrometer. Sample preparation involved:

- (1) The crushing of sample to a fine powder using a rock crushing machine, jaw crusher, Bico pulverizer and finally a tungsten carbide pulverizer;
- (2) The mixing of 3.000 g of flux ( $\text{Li}_2\text{B}_4\text{O}_7$  and  $\text{LiBO}_2$ ) with 0.5000 g of rock powder;
- (3) This mixture was then melted to make a glass pellet which was then analysed in the XRF spectrometer. Loss on ignition measurements were made for each sample.

Another set of 34 samples were analysed by the Geological Survey of Canada by optical emission analyses. The exact method used is not known. Appendix 1 is a tabulation of the results from both analyses.

The accuracy of the two methods of analyses was determined by taking the ratio of each oxide per cent values times 100 and subtracting the result from 100. Thus a value of zero would indicate that the analyses were the same, and any deviation from 0 would indicate the laboratory variability of the two methods (measured in percent). Table 1 illustrates this collation.

Table 1. Comparison of major element method accuracy

$$\left(100 - \frac{\text{XRF}}{\text{Op. Em.}}\right)$$

Sample	SiO <sub>2</sub>	Al <sub>2</sub> O <sub>3</sub>	TiO <sub>2</sub>	Fe <sub>2</sub> O <sub>3</sub>	MnO	MgO	CaO	Na <sub>2</sub> O	K <sub>2</sub> O	P <sub>2</sub> O <sub>5</sub>	H <sub>2</sub> O+
(A) 5e	0.62	-0.82	-14.29	1.43	-50.0	7.69	-100	-4.35	-4.14	0	38.3
(B) Ad <sub>1</sub>	0.43	-1.17	-9.09	-50	-300	-62.50	-120	13.67	6.02		-7.2
Avg. error	0.53	-1.00	-11.69	variable	-175	variable	-110	variable	variable		variable

Note that positive values (%) represent either an overestimation of the oxide by the optical emission method or an underestimation of the oxide by X-ray fluorescence. For negative values the opposite is true.



From Table 1 it can be seen that for the major oxides (i.e.  $\text{SiO}_2, \text{Al}_2\text{O}_3$ ) the accuracy is within  $\pm 1.00\%$ . However accuracy is more variable for  $\text{TiO}_2, \text{Na}_2\text{O}, \text{K}_2\text{O}$  but values are within  $\pm 15\%$ . Highly variable ratios or ratios showing no trend (i.e. one value positive, the other negative) were found for  $\text{MnO}, \text{CaO}$  and  $\text{Fe}_2\text{O}_3, \text{MgO}$ , respectively.

If the above trend is true for all the analyses, then the comparison of the geochemical analyses from the two methods may be erroneous resulting in scatter of data points, especially for oxides with low total oxide percent values.

Mesonorm analyses for granitoid rocks were calculated using a computer program initially derived from Barth (1959). The data output was in terms of cation percentage which were used in later geochemical analyses. An exception to the above occurs in the calculation of petrogenetic Ab-An-Qtz or Or diagrams where oxide weight per cent values were used.

#### 3.1.4 X-ray diffraction

Cu  $K\alpha$  radiation with a Ni filter was used at 30 KV and 16 amps. Each prepared sample was scanned at a rate of  $2^\circ 2\theta$  per minute from  $5^\circ$  to a maximum of  $50^\circ$  by a Norelco goniometer. The diffractogram chart recorder rate was  $2^\circ 2\theta$  per cm. This diffractometer was not capable of analysing

at lower than  $2\theta$  angles.

Each sample slide was glyconated on a large holed porcelain plate in a dessicator at  $60^{\circ}\text{C}$  for 12 hours according to the method outlined by Vemuri (1967) and then analysed for changes in peak position (applicable for determining montmorillonite).

Each diffractograph for the 9 samples was analysed using Vermuri's (1967) method and/or powder diffraction tables for minerals. Also standard clay minerals were analysed for comparison. Vermuri's method of clay sample mineral identification used characteristic, usually high angle peaks to identify a mineral in a sample. Mineral identification can be aided by heat treatment of clay but this was not done in this study. The relative proportion of each mineral present was measured by the ratio of usually the 100% maximum peak for each mineral.

### 3.1.5 Thin section preparation

Due to the friable nature of the weathered granites many of the samples had to be impregnated with epoxy before cutting the thin section. The samples were allowed to dry without the aid of a vacuum. The occurrence of a fragmented appearance in some of the samples may be the result of cutting

and grinding of the susceptible minerals. However this may also be the result of soil forming processes fragmenting grains. Sample Ag described this texture as cataclastic. Plucking of micas and clay minerals seems to be a common feature in the more weathered sample thin sections.

Using these methods it was the purpose of this study to determine the mechanism of weathering of the granites.

## 3.2 Petrography

### 3.2.1 Introduction

The initial composition and texture of the bedrock prior to alteration due to weathering is of importance in the rate and type of reactions that occur. The final end products in the weathering process are thought to be independent of initial parent rock type however (Blatt et al., 1972).

Thus the investigation of the rock by thin section analyses defines the pathway of the reaction not the end products, which are influenced by other factors such as microclimate, ground water pH and other dissolved ion concentrations, topographic position. Comparison of results with

Table 2 Modal Analyses (values in percent)

Sample	Qtz	Plag	Perthite	Micro- cline	Sericite	Biotite	K Feldspar	Opaque	Other	
5a *	37.3	16	24.9	12.9	3.3	2.8	2.4	0.4	Micrographic Rutile Apatite	trace trace trace
5c	31.8	21.1	20.5	16.0	4.6	3.2	2.8	1.0		
5f	45.5	15.6	20.9	6.9	5.4	0.3	5.0		Micrographic Iron oxide	0.3 0.4
<u>Cores</u>										
Top	46.6	13.7	15.6	10.7	1.7	3.5	7.5	0.2	Micrographic	0.2
Middle	31.7	23.6	23.8	12.0	2.4	0.9	4.8	0.7		
Bottom	35.9	15.6	12.4	4.8	6.8	1.8	5.0	0.5	Iron oxide Epidote Chlorite	0.7 0.1 trace
21	36.5	12.9	24.5	17.1	4.2	1.8	2.5	-	Epidote Chlorite Iron oxide Muscovite	trace trace trace trace
31a*	37.3	16.8	23.9	11.5	2.3	1.7	4.4	0.6	Rutile	1.5
31d*	41.2	14.6	23.5	7.2	4.0	1.5	7.2	0.8		
A34g*	46.7	9.4	19.2	1.6	10.8	8	3.4	1.0		
B34c*										
D34c*										
C-34*	31.3	8.9	22.1	-	13.8	4.3	0.8	-	Fragmented with crystals - Iron oxide	3.5 14.8
35*	47.1	14.0	24.4	3.2	3.2	4.9	-	3.2		

mesonorm analyses was instructive in determining bedrock mineral variations also.

### 3.2.2 Modal analysis

A total of 12 fresh and weathered granite bedrock thin sections were analysed by the point count method to determine the changes in mineralogy between relatively fresh and altered bedrock. Of these, 9 were from the Big Bald Mountain area and the remainder from Pierce Mountain. These samples were thought to represent the variations in intensity of weathering.

At least 500 points were counted per thin section. The results of the analyses are illustrated in Table 2. Using these analyses a quartz-alkali feldspar-plagioclase ternary diagram (IUGS, 1973) was used to determine if the parent rocks were true granites (Figure 24). All the samples plot in the granite field; however there is a trend for the granites to be quartz and/or alkali feldspar rich. The variability of the Pierce Mountain samples may be the result of alteration or bedrock inhomogeneity.

The analyses and textural description (discussed below) allowed a base from which weathering intensity and typical reactions would be determined.

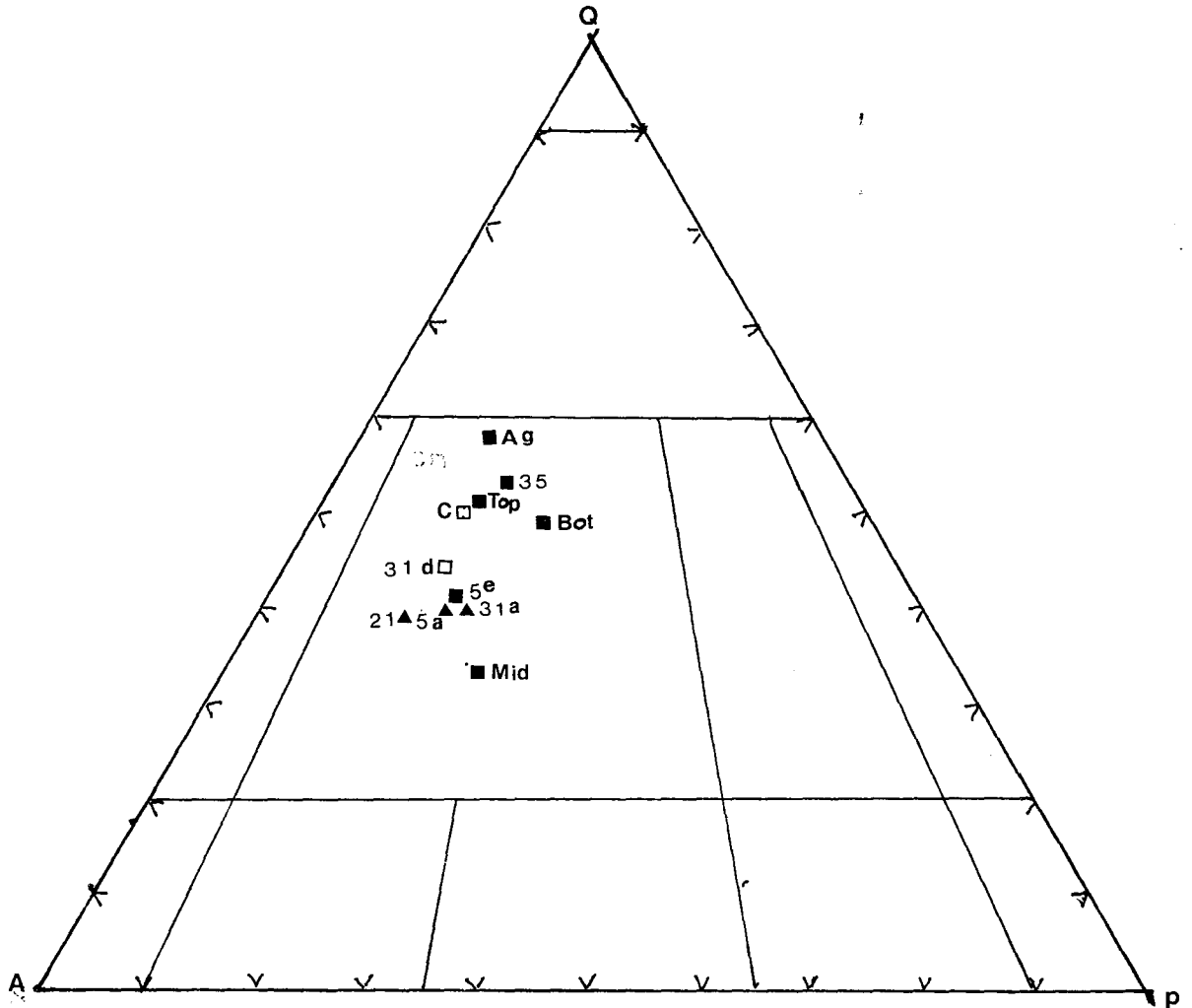


Figure 24. QAP diagram of modal analyses from both sites. Bedrock samples 31d, 5e, 31a, 21 and 5a are from Big Bald Mountain. Bedrock samples C, Ag and 35 are from Pierce Mountain.

In displaying the data on Figures 24 to 30 soil and rock horizons were used in place of sample numbers as follows:

A. Big Bald Mountain

Symbol	Location in profile	Samples
○	A horizon	8, 20a, 28a
●	B horizon	9a, 20b
□	C horizon	6, 9b, 20d, 20c, 22, 25, 31c, 31d, 5f
■	Grus	5e <sub>1,2</sub> , 12b, 14, 26b, 27, 28b, 30b, 32b
▲	Bedrock	5a, 5b, 5d, 7, 7a, 7c, 12a, 13a, 13b, 8a, 21, 31a, 31b

B. Pierce Mountain

Symbol	Sample type	Samples
○	Clay	Ba, Db, Ac
△	Grus	Bb, Ad <sub>2</sub> , Ad <sub>12</sub> , Ad <sub>1</sub> , Ae, Da, Aa, Ab
□	Regolith-rock	Bc, Af, Dc, C
■	Rock	Ag, 35

### 3.2.3 Normative analysis

A mesonorm program outlined initially by Barth (1959) was used. The advantage of this norm is it calculates biotite into the norm thus enhancing its value for portraying granitic rocks with respect to cation norm or CIPW norms. This is because biotite is a more realistic norm mineral for granites than pyroxene which would normally be calculated for the other igneous rock norms.

The mesonormative minerals calculated for each sample are tabulated in Appendix 2.

Quartz-albite-orthoclase diagrams were plotted for each site (Figures 25 and 26). Only the leached samples from Big Bald Mountain fell outside the granite field of Winkler and Von Platen's (1961).

The Pierce Mountain samples show two general trends:

- (1) samples falling within the granite field;
- (2) samples falling in the quartz rich field.

As a generalization the fresher samples (i.e. less altered) are in the granite field.

Comparison of mesonorm Q-A-P ternary diagrams (Figures 27 and 28) with modal analyses Q-A-P ternary plots reveals a relative increase in plagioclase and/or quartz content. These anomalies can be the effect of:

- (1) Perthitic intergrowths of orthoclase and albite



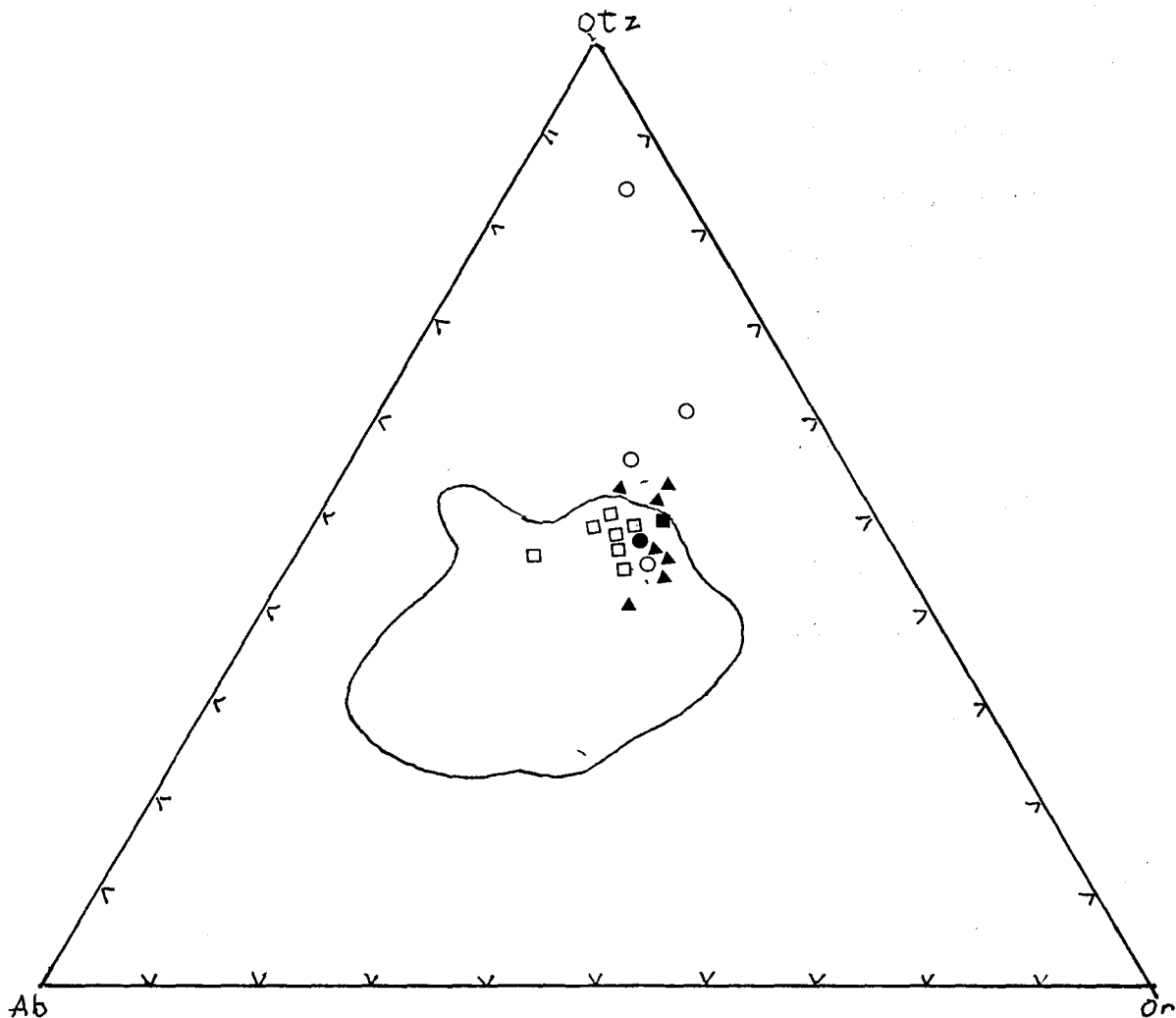


Figure 25. Q-Ab-Or mesonorm ternary diagram for Big Bald Mountain samples (including bedrock gus and soil samples). Solid irregular line is Winkler and Von Platen's (1961) area for granitic rocks.

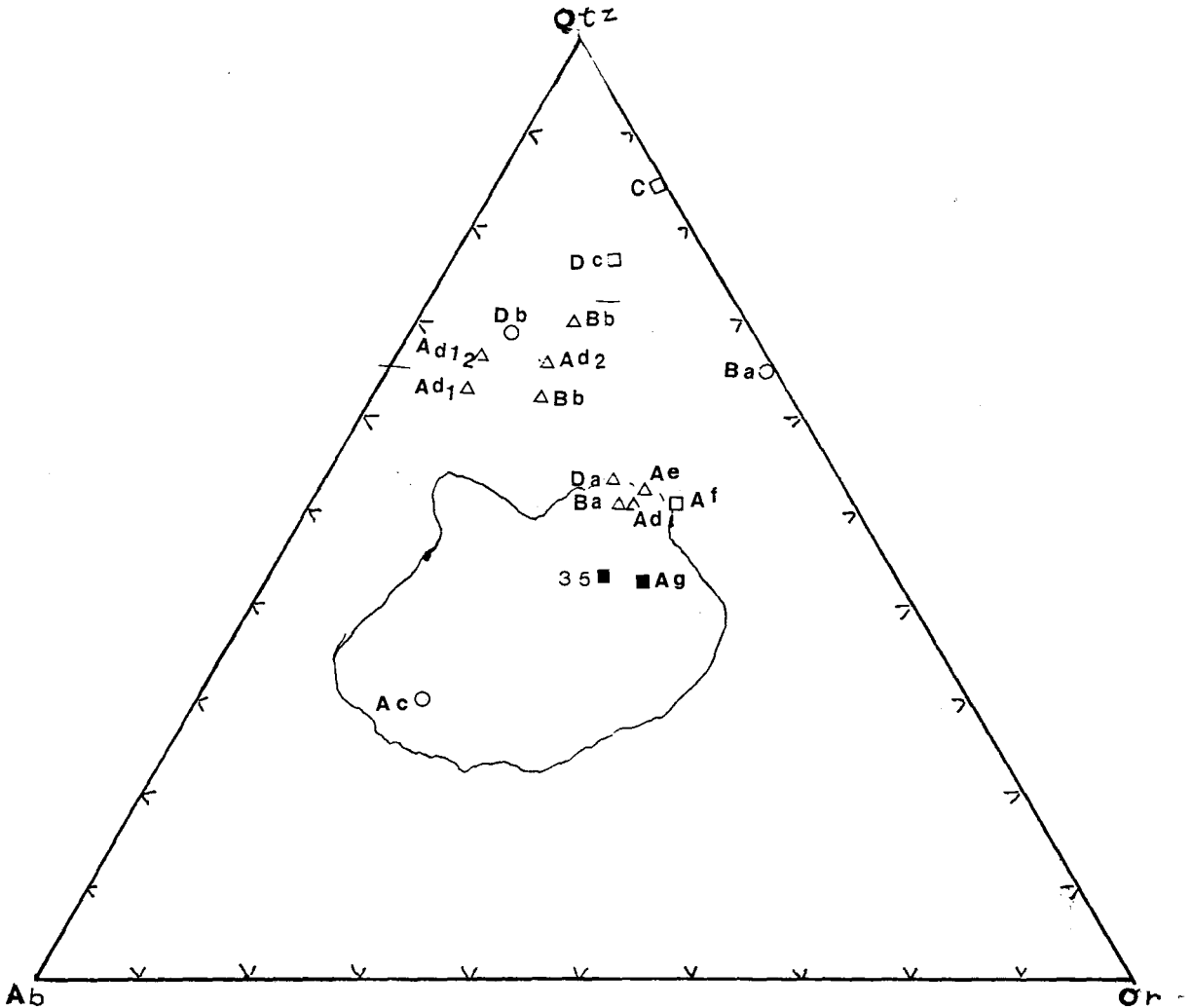


Figure 26. Normative Q-Ab-Or ternary plot for Pierce Mountain. Solid irregular line is Winkler and Von Platen's (1961) area for granitic rocks. Fresh bedrock samples fall in the area. However there seems to be little correlation with altered bedrock and gneiss samples. Indicative of inhomogeneity in the outcrop.

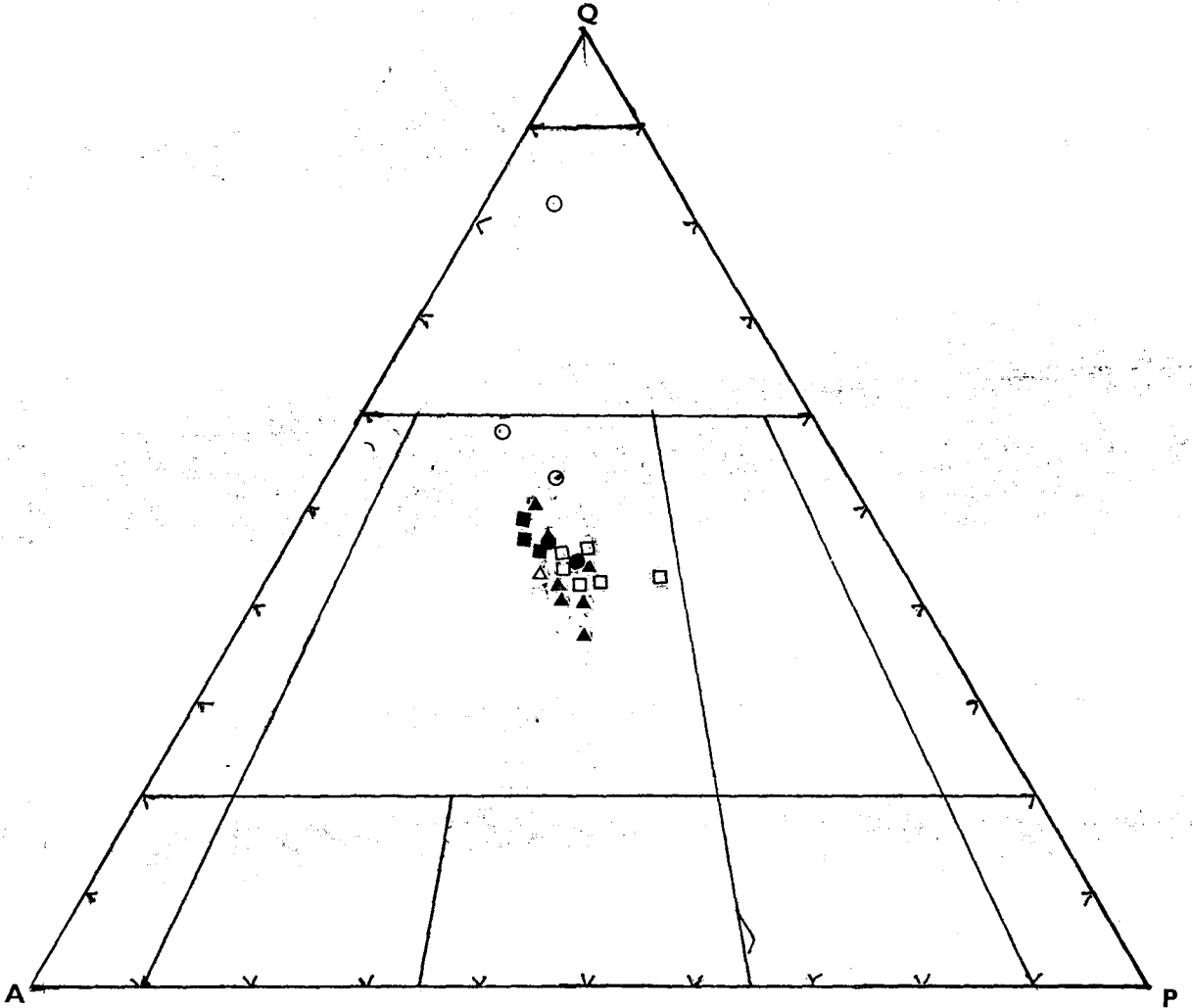


Figure 27. Mesonorm Q-A-P ternary plot for Big Bald Mountain bedrock grus and soil samples. Note they all are found clustered in the same area indicating that the grus is not significantly altered.

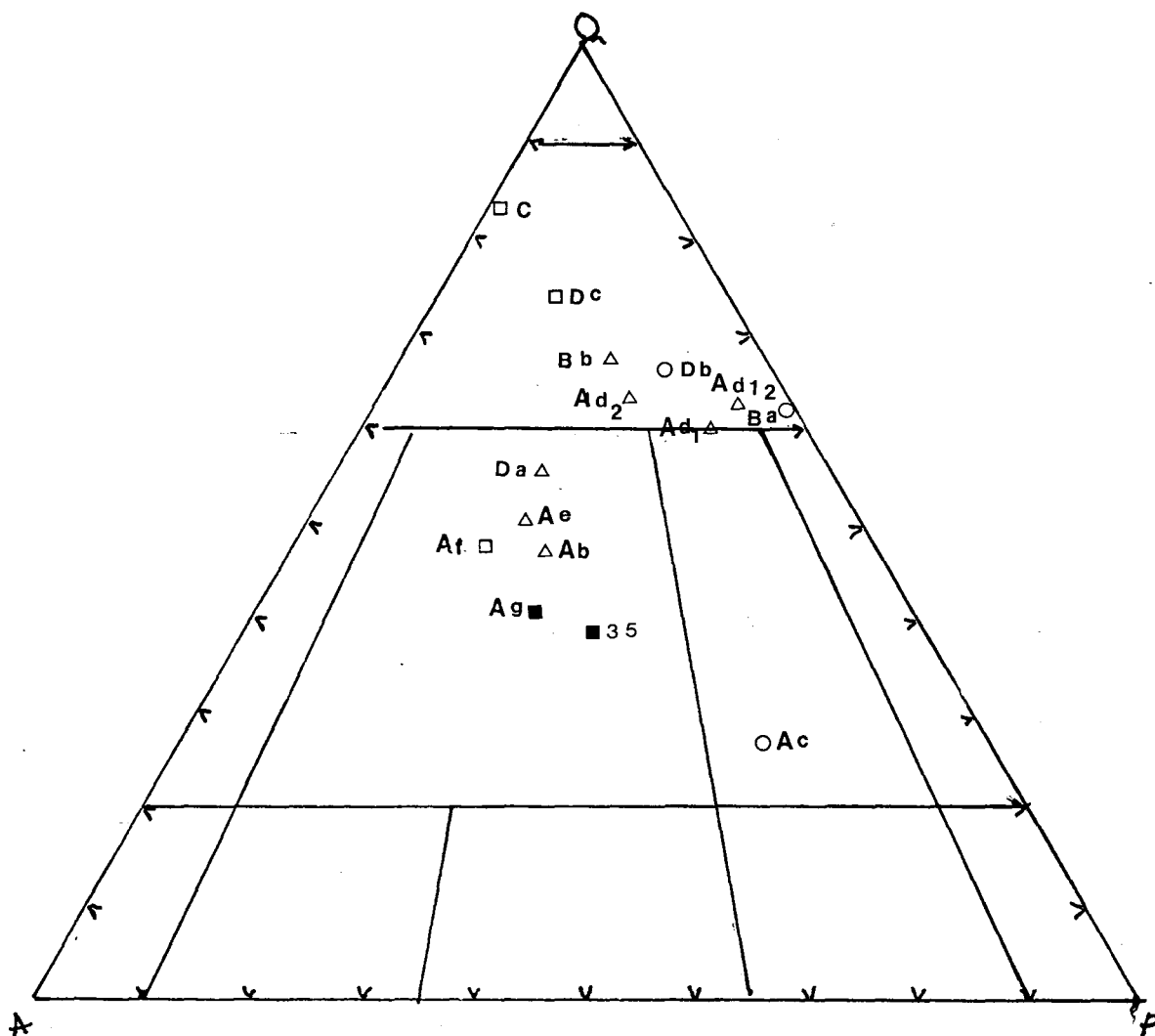


Figure 28. Mesonorm Q-A-P ternary plot for Pierce Mountain bedrock grus and clay samples. Note that samples sampled near the regolith bedrock interface fall in the granite field. Derived sediments fall in the granitoid field. Sample Ac is an anomalous clay sample.

giving erroneously high plagioclase content in the norm;

(2) The high quartz values are the result of normative analysis equating excess Si to quartz when in fact it is used in clay minerals and white micas.

In the K:Na:Ca ternary diagram (Figure 29) there is a general clustering of Ca poor, slightly enriched K samples. The clustering of bedrock and grus samples in the same area are indicative of the relative freshness of the Big Bald Mountain grus samples. Only leached samples show some depletion of Na and/or enrichment in K. The general trend for Ca poor samples is shown by the dominant plagioclase in modal analysis being albite, oligoclase.

The K:Na:Ca diagram for Pierce Mountain (Figure 30) shows a wide dispersion of samples about the unweathered sample #35. Note the trend for weathered samples to have a rapid decrease in calcium content.

Analysis of the mesonorm minerals indicates the following anomalies:

(1) There is a relative increase in  $\text{SiO}_2$  and corundum ( $\text{Al}_2\text{O}_3$ ) with the increase in weathering intensity. This could be the result of misidentification of clay minerals since the norm does not account for  $\text{H}_2\text{O}$  in norm-mineral estimation. Note that corundum was not found in thin section analysis. The presence of clay minerals would tend to increase the

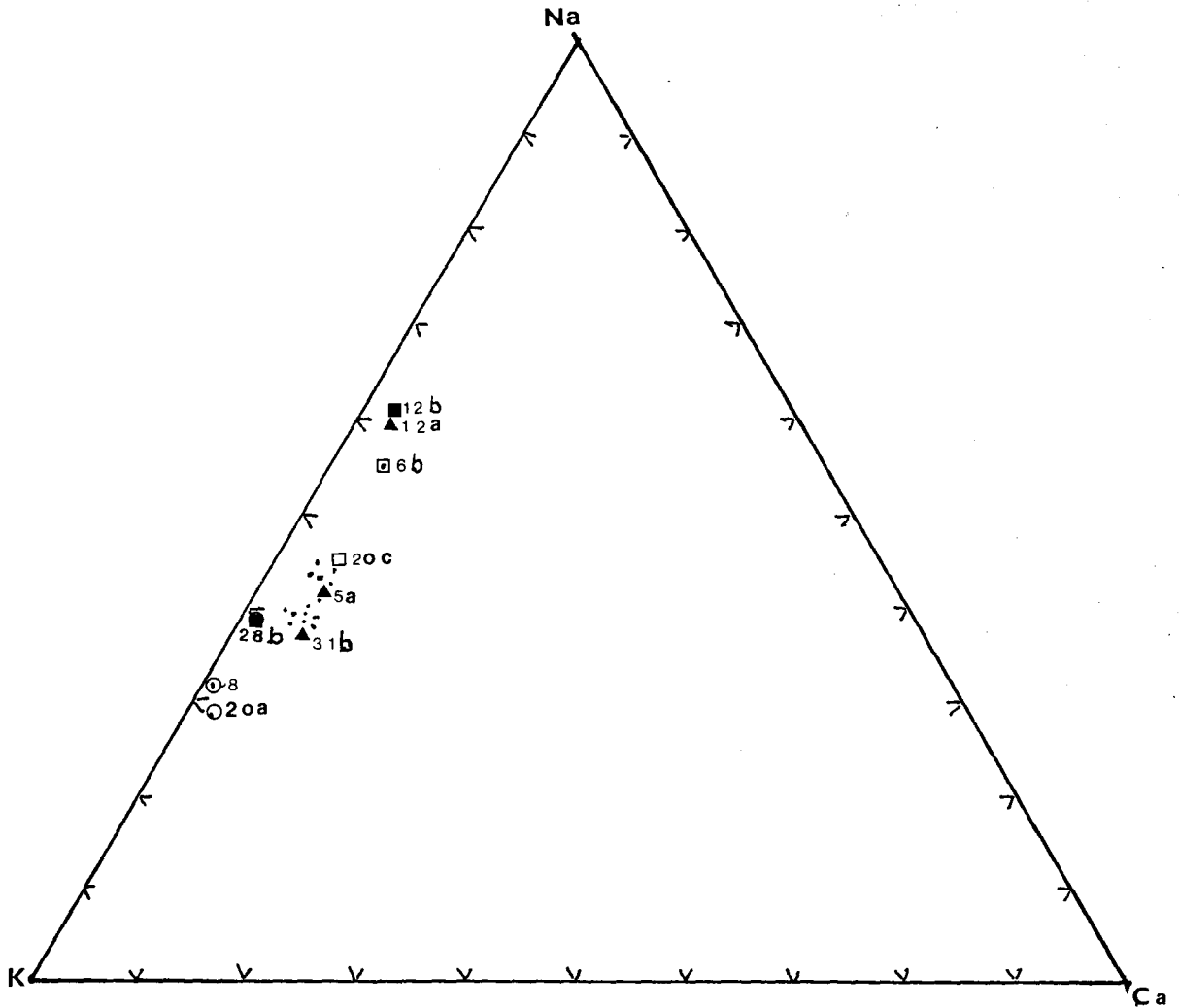


Figure 29. K-Na-Ca diagram for Big Bald Mountain samples calculated from mesonorm (after Barth, 1959). Samples include bedrock, grus and soil samples. Note the clustering of samples around sample 5a (bedrock). Also only the leached samples vary significantly from this trend (e.g. 8, 20a, 12a,b).

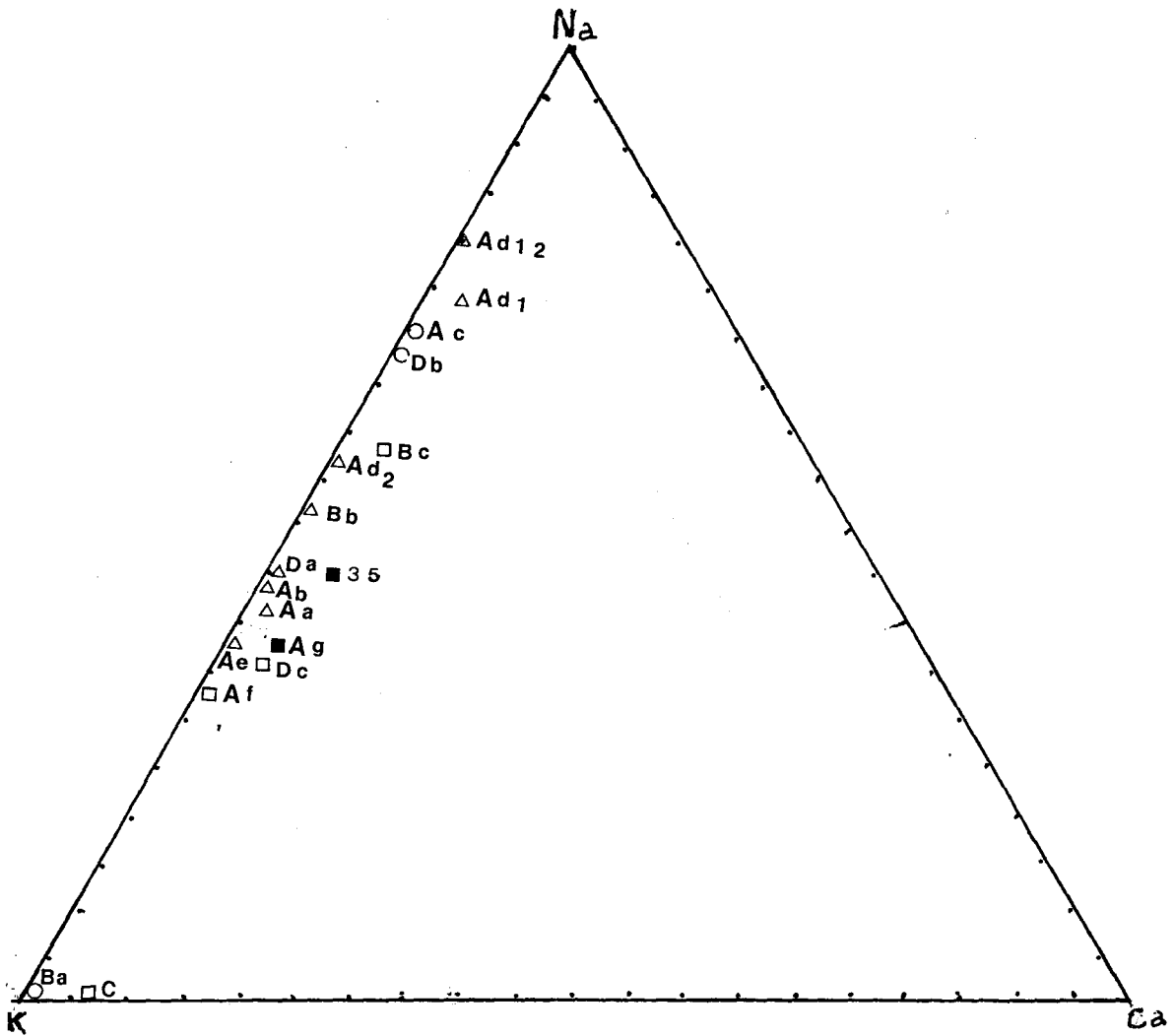


Figure 30. K-Na-Ca diagram calculated from mesonorm (Barth, 1959) for bedrock grus and clay samples. Note the wide spread of values about sample 35 (fresh bedrock). Also note the rapid depletion in Ca away from sample 35.

orthoclase percentage due to higher Si, Al and K content, but this is overshadowed by the effect of perthitic intergrowths on the norm mineral analysis. Thus the presence of corundum in the norm analysis suggests that alteration of feldspars is present (i.e. if not actually found in the rock).

(2) Another problem in using the mesonorm for weathered samples is it consistently underestimates biotite, most likely due to the norm calculating Fe as hematite or magnetite before biotite. There is a trend for highly weathered samples to be enriched in normative ilmenite and hematite with respect to magnetite. This may or may not be a true trend.

(3) Near surface soil samples show generally higher apatite occurrence. Rocks and deeper soil samples have no or little apatite. This may be a reflection of soil forming organic processes in effect in the weathering profile. Again, a misidentification of elements analysed with respect to mesonorm analysis.

Thus in conclusion, the use of the mesonorm as a representative approximation of minerals found in a weathering sequence of bedrock and grus-clays is truly not justified. Of course it was not made as a norm for weathered rocks, but for fresh metamorphic and granite rocks. However, some



information can be gained with respect to the intensity of weathering a sample has been subjected to, if one considers what and how the calculation of norm minerals are obtained. If for no other reason the mesonorm analysis was useful for the calculation of cation percentages.

#### 3.2.4 Textures

##### A. Hand specimen description

The Big Bald Mountain granite is a relatively homogeneous medium to coarse grain, pink granite. Surface relief of grains is generally high due to the preferential weathering of Ca feldspars with respect to quartz. A weathering rim is not immediately evident. This may be accounted for by the presence of microcracks, allowing deeper water penetration and/or the constant loss of grains when the interstitial grain - surface grain contact is broken.

The dominant minerals appear to be smoky quartz (often occurring as aggregates), pink K-feldspar and a white interstitial mineral which is most likely plagioclase. Black, seemingly unaltered tablets of biotite flakes are dispersed through the matrix. Hand specimen analysis would call this a biotite granite.

Samples 11a and 11c are exceptions to the above description. They are fine grain, pink, porphyritic rocks with eyes of quartz and what appear to be K-feldspar. Biotite is disseminated through the matrix. The rock forms a distinct leached white weathering rim unlike the rest of the batholith (see thin section, Figure 35)

#### Pierce Mountain

The "unaltered" bedrock is white-gray, medium grain granite or biotite granite. The K-feldspar is altered to a light pink-white mineral. Plagioclase has been altered also (easily powdered). The quartz has a smoky gray appearance. Black-brownish biotite is frequently enveloped by an iron oxide stain. It is dispersed as fine flakes through the rock matrix.

Alteration at this site is intense. Some still lithified rocks occur as greenish-pinkish massive rocks consisting of quartz and easily powdered fine grain minerals. Black-dark brown precipitated mineral occurs along joints within the rock. This "rock" no longer has the appearance of granite (e.g. sample Dc).

## Thin section textures

### A. Big Bald Mountain

The Big Bald Mountain granite is holocrystalline, hypidiomorphic granular, medium to coarse grain rock. It occasionally shows porphyritic texture due to phenocrysts of K-feldspar. Cataclastic like texture develops with varying intensity. This texture could be related to exfoliation jointing. Samples 5a and core top have limited fracturing, while samples 5c, 5f, 2l, core bottom, 3la and 3ld have more intense fracturing. Such fracturing may be the result of soil forming processes. This fracturing may be better described as an autoclastic texture. Figure 31 shows the effect of exfoliation on mineral grains. Note the subparallel orientation of the voids.

Minor fractures are seen radiating from the terminations of biotite crystals. This is best shown in Figures 32 and 33 (same thin section, plane and crossed nicols) in the central portion of the photo. These minor fractures may be exploited with further chemical alteration but at present show little relationship with feldspar alteration. Figure 35 is representative of samples 11a and 11c. Note the drastic textural difference with respect to other samples. It has a porphyritic texture and shows evidence of cataclastism by the rounding of

Figure 31. This shows the effect of exfoliation on mineral grains. Note the interlocking quartz grains (upper left corner of photo) thin section photomicrograph of sample 21 (X nicols).

Scale:   
3 mm

Figure 32. This shows the typical interlocking aggregates of quartz grains (lower right). Note the zoned plagioclase crystal (upper left) and the preferential alteration of the Ca-plagioclase core to the white metal. A large tabular grain of K-feldspar shows a sieve-like texture (lower central area). Core (bottom cut) thin section photomicrograph (X nicols).

Scale:   
4 mm

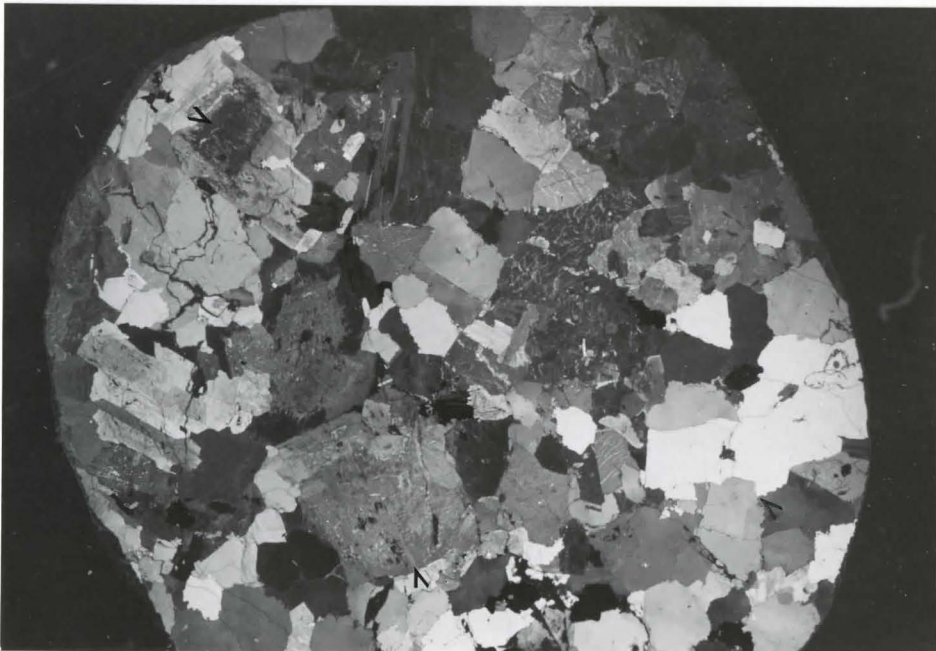
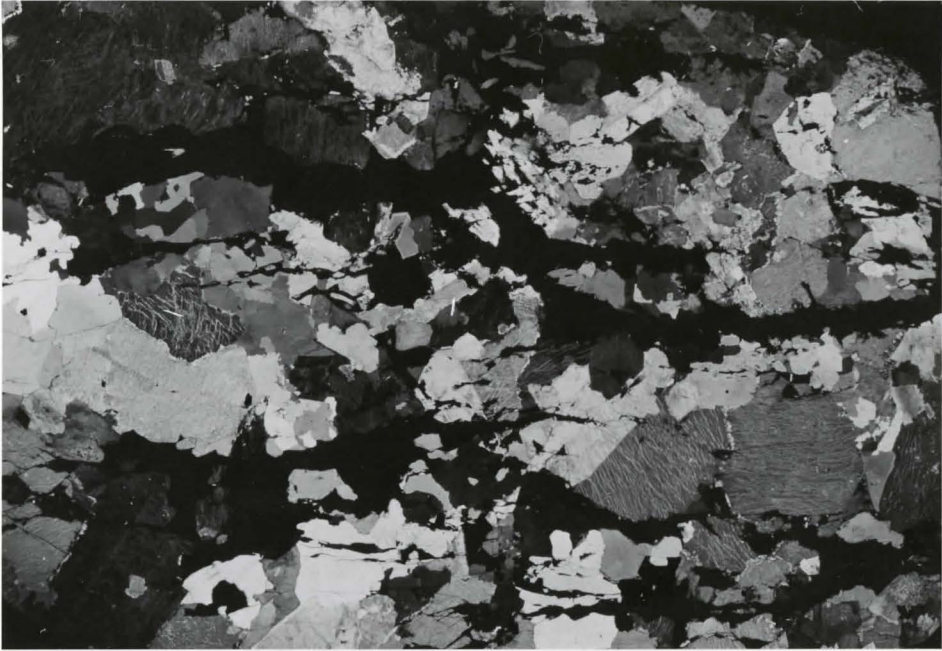


Figure 33. Note the small fractures radiating from the end of the lath-like biotite crystal. This photo also shows the difference in alteration between the unaltered clear surface of quartz (see 1) and the perthite which has preferential alteration of twin lamellae (see 2). (Sample 5a thin section photomicrograph, plane light).

Scale



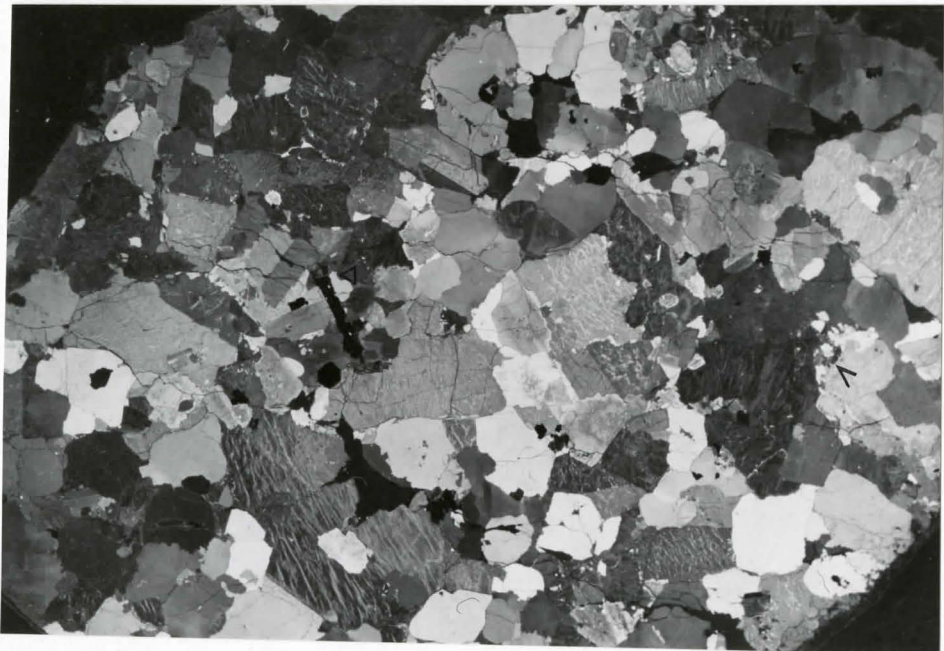
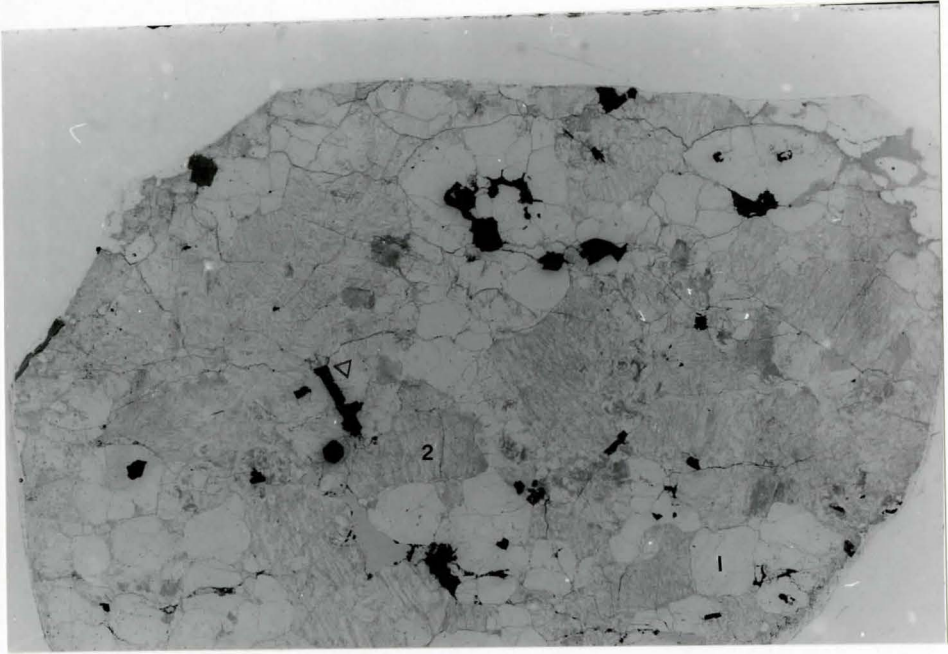
  
2.75 mm

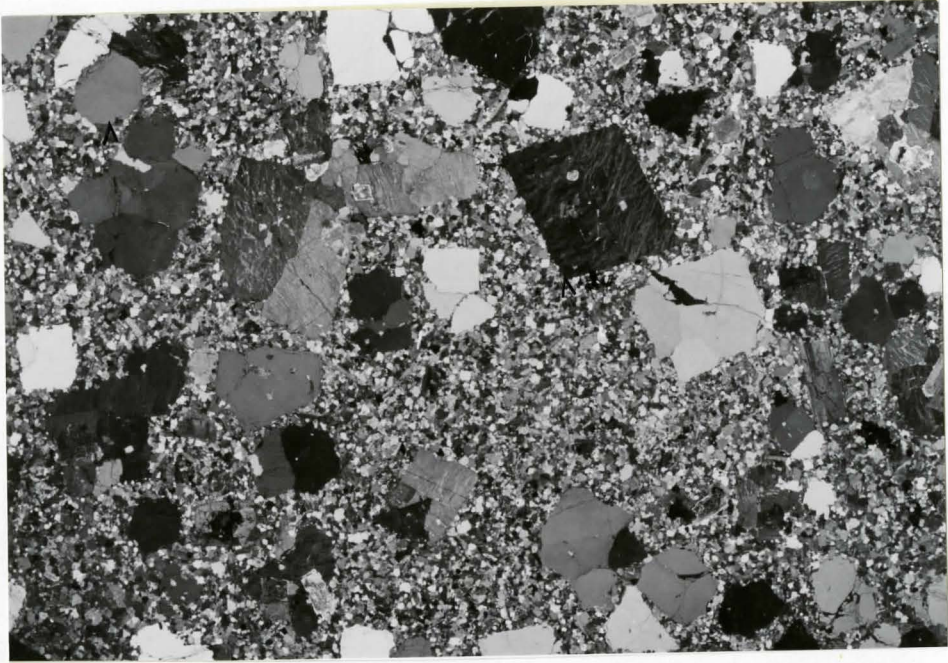
Figure 34. Sample 5a thin section photomicrograph, cross nicols. Note minor fractures radiating from biotite grains and the development of subgrains between K-feldspars (central right).

SCALE

  
2.75 mm








Scale   
3.5 mm

Figure 35. Sample 11a thin section photomicrograph (X nicols). Note the porphyritic texture of the marginal zone of the batholith. Quartz grains are frequently shattered some showing rounded character (upper left). Phenocryst of euhedral perthite has small inclusions of plagioclase and quartz (upper central area).



quartz grains. The same mineralogy, however, is present (i.e. perthite, plagioclase laths and quartz) as phenocrysts. The matrix is composed of fine grain quartz and feldspar aggregates. The rocks' resistance to chemical solution is enhanced due to the lack of porosity of the fine grain, but resistant and interlocking matrix.

The rate or susceptibility of the minerals present to alteration seems to be an indicator of weathering of the granite.

#### Minerals

After textural analyses of the thin sections, the following generalizations can be made about the minerals and their alteration.

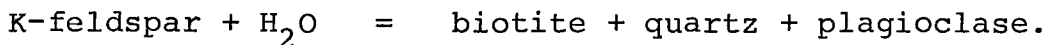
**Quartz:** Quartz occurs as anhedral frequently equal dimensional grains. Maximum grain size observed was 5 mm, but average size was 2 mm. It frequently occurs as clusters (Figure 32).

These grains often form sutured grain boundaries in these clusters. Also subgrain development along K-feldspar grain boundaries was found in a few thin sections (Figure 31). Some quartz grains are partially rounded, possibly formed due to autoclastism or soil process fracturing. Undulose extinction is very common. Quartz occasionally has inclusions of

muscovite or biotite.

The surface of the quartz is generally free of any alteration, but in the more intensely altered slides it has a mottled appearance. Note the difference in alteration between the perthite and quartz in Figure 33 (plane light).

**Perthite:** Perthite is thought to be the result of unmixing of sodic and potassic feldspars, possibly caused by autoclastism (Augustithis, 1973). Perthite is the dominant K-feldspar in all thin sections. It occurs as anhedral equant grains or subhedral columnar grains. Maximum grain size observed was 8 mm (section 5a), but average grain size was 3.5 mm. It frequently has one single Carlsbad twin. Intergrowth veinlets are commonly subparallel. Perthite frequently contains inclusions of quartz, zoned plagioclase (various sizes) and biotite. In a few instances all three are found as clusters in the perthite, possibly suggesting the following reaction has taken place:



Preferential alteration of the Na feldspar is shown by the darker buff surficial coating of what may be a clay mineral (kaolinite?, illite?). A few grains have a sieve

like texture due to sericitization (Figure 32, central lower area).

Microcline seems less resistant to alteration as there is a decrease in modal percent in the more altered samples. It also shows perthitic textures.

Plagioclase: It occurs as subhedral to euhedral laths interstitially between quartz and perthite grains. Average grain size is approximately 1.5 mm. Plagioclase displays polysynthetic twinning according to Carlsbad and albite laws when not altered. Plagioclase was determined to be oligoclase (10% An) as determined by Michel Levy test. However, a few grains per thin section had anomalously high extinction angles up to a maximum of  $24^\circ$  ( $\approx 44\%$  An). Note that alkalic granites are known to contain anorthite (Williams et al., 1954). A similar process may be in effect here.

Some grains have undulose extinction (sample 5c) but zoning is much more frequent especially when adjacent to K-feldspars.

Alteration takes place along twinning planes and/or Ca plagioclase cores of zoned crystals (Figure 32). White mica and/or to a lesser extent sausserite are usually the products of this alteration.

**Biotite:** Biotite occurs as euhedral hexagonal prisms or laths. The average grain size is less than 1.5 mm. Biotite is usually deep brown-green brown when not altered. It is, however, frequently oxidized or with further alteration occurs as secondary chlorite and a black opaque mineral (sphene?, magnetite?). The alteration occurs along grain boundaries or cleavage planes initially. Chlorite alteration is generally not extensive.

#### Accessory minerals

(1) Muscovite occurs as subradiating laths in quartz and perthite in thin section 5c.

(2) The occurrence of bright red rutile and hematite is associated with greater chemical alteration of the other grains. These minerals occur as fine granule like aggregates, and oxide stain in the void spaces caused by joint fracturing.

(3) Epidote results from the saussurization of feldspars. It appears as a dirty yellowish coloured mineral.

#### B. Pierce Mountain

There are at least three distinct mineralogies/textures developed at this site showing various degrees of alteration.

They are:

(1) The "non-altered" granite exposed at the base of this site. It is a medium grain, hypidiomorphic granular rock (Figure 36).

(2) The cataclastic medium grain, quartz-feldspar sericite rock (Figure 37).

(3) The severely altered quartz sericite sample in which quartz grains are intact but associated feldspars are completely replaced by white mica (sericite) (Figure 38).

These thin sections are discussed in detail below.

(a) Sample 35 (Figure 36)


This sample's texture and mineralogy closely approximate the textures seen at Big Bald Mountain. The sample is not completely unaltered, but it does show the original mineral type and form. It is the best approximation to the fresh rock that could be obtained at the site and thus it has great importance in the geochemical analysis (discussed later).

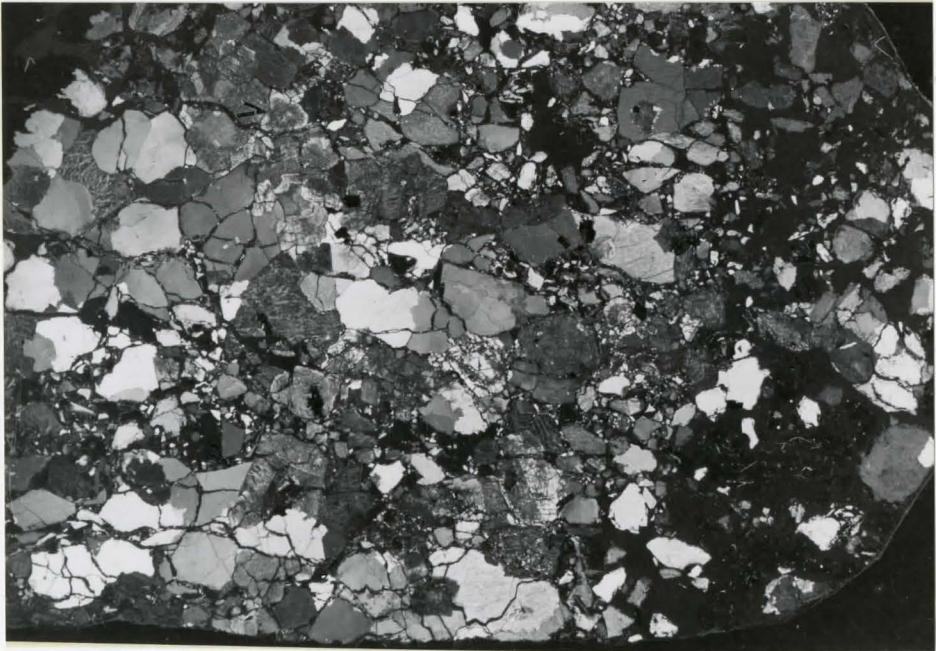
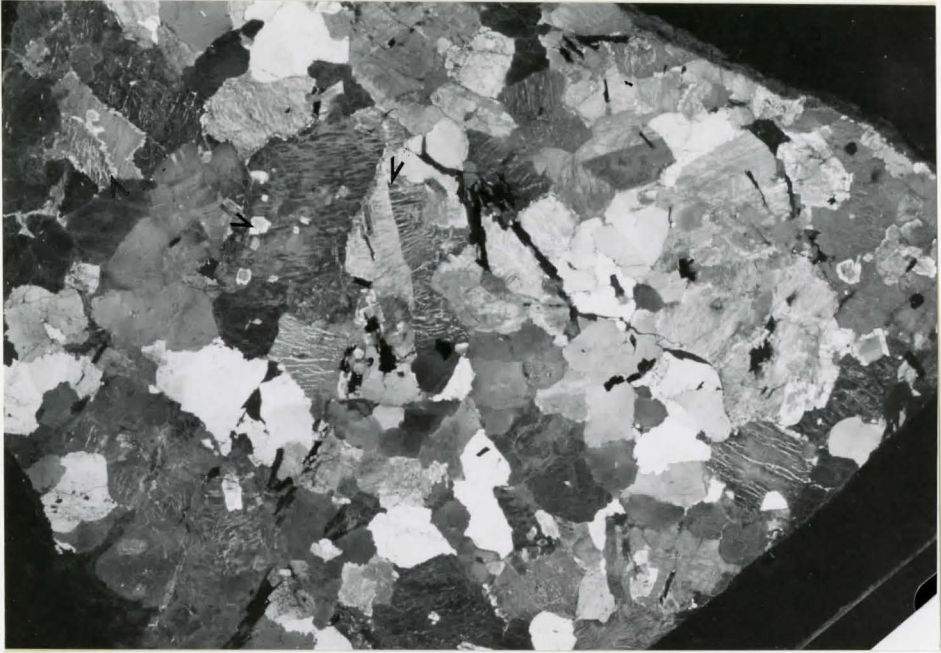
As previously stated sample 35 is a medium grain, hypidiomorphic granular rock. Fracturing is present but limited in extent and intensity. It most likely is related to exfoliation jointing present at the site. A sub-porphyritic texture is associated with larger subhedral perthite crystals which are surrounded by smaller anhedral aggregates of quartz and intergranular plagioclase.

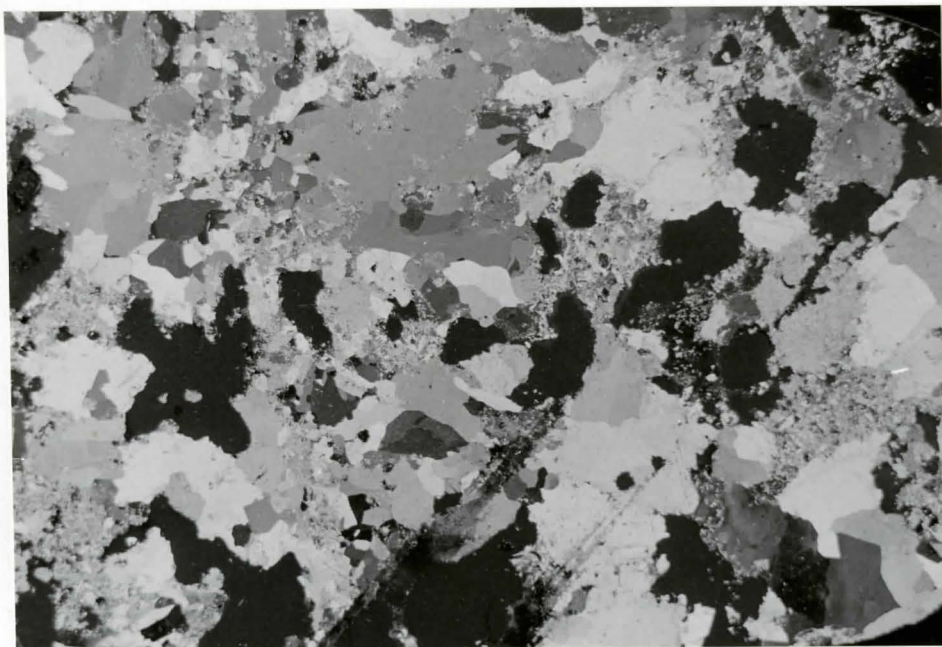
Figure 36. This shows typical hydromorphic granular, relatively unaltered texture of granite. Note the twinning of perthite (central portion) and the inclusions of zoned plagioclase in several of the larger crystals (upper central). Zoning of perthite crystals is also present (upper left). (Sample 35 thin section photomicrograph, X nicols).

Scale   
3.5 mm

Figure 37. This shows cataclastic texture of this weathered granite. Note the angular fragment of quartz (lower left) and zoned feldspar showing sericitization of the core (upper left). Large perthite grain cores are frequently plucked and/or fractured. (Sample A39g thin section photomicrograph, X nicols).

SCALE   
3.5 mm






Scale   
5.5 mm

Figure 38. Note the complete alteration of feldspars to white mica (sericite) leaving residual quartz in original aggregate clusters. Numerous voids present are most likely due to plucking of the soft minerals in thin section preparation. (Sample Dc thin section photomicrograph, X nicols).



The form and alteration of the minerals are discussed below.

#### Minerals

**Quartz:** It occurs as anhedral medium grain (1.5 mm average) crystals which have undulatory extinction. Alteration generally is not shown in the quartz grains.

**Perthite:** Perthite crystals show the characteristic intergrowth lamellae or veinlets which are oriented parallel to each other. It may have single Carlsbad twinning also. Commonly grains have several inclusions of zoned plagioclase or biotite/muscovite. Zoning of the crystals themselves was also found (Figure 36). Alteration of the perthite is limited to a buff brown surface coating (clay mineral?) and sericite. Again preferential alteration of the intergrowth veinlets is present.

**Plagioclase:** It occurs as subhedral laths usually less than 1 mm. Alteration is variable but it could be associated with the percent An composition. That is the more calcic cores of the crystals are frequently more altered.

**Biotite:** Biotite occurs as laths scattered throughout the section as intergranular crystals. Some minor fine fracturing seems associated with the expansion of the grains.

This is especially evident in areas where biotite laths occur as groups.

(b) Sample Ag

This thin section is dominated by the cataclastic fracturing of the grains (Figure 37). Angular fragments occur in fractures themselves. Also, networks of fractures occur along grain boundaries.

Mineral form and alteration

Quartz: Quartz grains average size was 2.5 mm. They show a distinct tendency to fracture brittly. The surface of the crystals still are not corroded.

Perthite: Perthite grains have a 2.5-3 mm average grain size. The grains are frequently fractured and highly pitted due to sericitization. In plane light, alteration is brownish. Small opaque inclusions, epidote and/or iron oxide also occur in the K-feldspar occasionally.

Plagioclase: The consistent alteration of Ca rich plagioclase is again seen in this sample. However complete obliteration of twinning is frequent in zoned crystals. Albite can be generally thought to be more resistant to chemical alteration.

Biotite: Biotite has an average grain size of 0.5 mm. The biotite appears to be oxidized to an orange-brown colour. Chlorite and associated opaque minerals are found in intense fracture zones.

(c) Sample Bc

This sample has no remaining evidence of the feldspars except for the skeleton produced by residual quartz. The feldspars are replaced by white mica (sericite) (Figure 38). The rock could be described as a quartz sericite porphyry now. Fracturing of quartz is common, but not usually intense enough to split the grains. A network of fine fractures occur along grain boundaries adjacent to voids, presumably once occupied by feldspar.

Mineral form and alteration

Quartz: Quartz occurs in two forms:

- (i) anhedral medium to coarse grain aggregates;
- (ii) fine grain, intergranular quartz aggregates dispersed with the white mica in the matrix.

The surface of the quartz is slightly mottled or corroded. Inclusions of white mica are found in the quartz especially along what appears to be former fractures. Some

quartz grains have triple junctions suggesting some pre-weathering deformation.

Radiating fine fractures occur in the quartz at the terminations of muscovite clusters. Undulatory extinction is very common.

Sericite: Sericite is found as:

- (i) Single muscovite grains in the quartz;
- (ii) Laths of fibrous radiating needle like laths in the quartz;
- (iii) Masses of fine grain crystals occasionally occurring in 4-5 mm aggregates in the voids.

Biotite is not present in its commonly lath like form, but occurs as amorphous looking anhedral clots in the sericite.

The occurrence of voids is a major feature present, most likely due to the preferential plucking of soft minerals in thin section preparation.

In conclusion a gradation in the intensity of weathering can be seen if the samples were taken from a homogeneous parent rock.

### 3.2.5 Summary of petrography

In summary the Big Bald Mountain samples generally showed limited alteration. Alteration trends could be distinguished however. These included:

- (1) The ability of quartz to remain unaltered.
- (2) The preferential weathering attack of feldspar grains along twin planes, perthitic lamellae, zoned plagioclase crystals, Ca rich core and the decrease in microcline with intensity of weathering.
- (3) The development of kaolin (?) on K-feldspars and the development of white mica on plagioclase crystals.
- (4) The importance of exfoliation in aiding the chemical weathering process.
- (5) The development of microfractures in the grains surrounding laths of biotite, due to the oxidation of the biotite crystals. Biotite eventually alters to chlorite.
- (6) In more intensely altered bedrock samples the development of hematite, rutile in the fractures is common. Also the reaction of biotite to chlorite often develops opaques adjacent and/or near the crystals.
- (7) Grain size differences in the boundary shear zone granitoid rock show more intense chemical weathering of feldspars in the fine grain matrix with respect to the porphyritic feldspar grains. However the interlocking

character of these feldspars and quartz tend to prevent deep percolation of water into the core of the bedrock, which seems to be the case for the majority of the medium to coarse grain granite of Big Bald Mountain. Note that a different style of weathering is produced typical of chemical dissolution (i.e. development of weathering rind) with respect to the physical disintegration modified by chemical alteration typical of the coarse grain granite.

#### B. Pierce Mountain

In comparison with Big Bald Mountain, Pierce Mountain bedrock samples are:

- (1) A slightly finer grain texture.
- (2) A much greater range of alteration has developed and is distinctly more related to chemical decomposition than Big Bald Mountain.
- (3) Generally, more variability in original composition (?) possibly the result of hydrothermal or metasomatic alteration.
- (4) Lacking in the occurrence of microcline.
- (5) Cataclastic textures of altered samples may be intense.
- (6) The original non-altered samples are very similar in texture and mineralogy.
- (7) With increased alteration the perthite becomes pitted

with sericite and/or saussurite.

(8) Plagioclase alteration is often intense enough to obliterate twinning with sericite.

(9) Alteration continues to "completion" (?) for this climate producing sericite and residual quartz.

In these samples biotite is amorphous looking oxidized mineral with iron oxide surrounding grains.

### 3.2.6 Discussion

There is evidence that the chemical weathering process is being aided by other factors in both areas.

Mineralogically, the development of perthite (at both sites) instead of separate orthoclase and albite crystals, suggests the rock has been subjected to some process which caused disequilibrium in the rocks' cooling history. In the case of Big Bald Mountain, the development of perthite may have been influenced by tectonism as evident by exfoliation. Pierce Mountain perthite may have developed due to hydrothermal or metasomatic alteration of the late stage intrusive batholith.

No matter how the perthite was caused its presence may make the rock as a whole more susceptible to chemical weathering, due to the numerous intergrowth lamellae acting

as planes of weakness in the mineral.

### 3.3.1 Grain size analyses

Grain size analyses of the weathered bedrock and soil is an important descriptive method which may indicate:

- (a) Whether the sample was transported or if the sediment developed "in situ".
- (b) Some measure of the intensity and processes involved in the weathering of the parent granite.
- (c) Whether small scale colloid migration through the weathering profile has taken place.

This information may be gained by interpreting the weight per cent data when displayed in the form of:

- (a) Histograms;
- (b) Probability plot and statistical analysis;
- (c) Rosin's law probability plot.

### 3.3.2 Histograms

The weight per cent data obtained from sieving was plotted in equal class intervals of  $0.5 \phi$  from  $-3.0 \phi$  to  $>3.5 \phi$ . A total of 18 samples were plotted. Note that the last value (i.e. usually  $3.5 \phi$ ) represents the total fine



fraction. The advantage of using a histogram is that the modal class can easily be visualized, a feature not necessarily true for cumulative percent methods.

In general the grain size analyses of regolith grus and clay pocket show a positively skewed relationship. However there is a relationship in grain size distribution with respect to the samples' position in the weathering profile.

#### A. Big Bald Mountain

Three distinct profiles develop corresponding to the A, B, and C soil horizons. The trend may be accounted for by the degree of chemical decomposition and mechanical disintegration that the bedrock has undergone (Figure 39).

##### A horizon

Leached samples from the A horizon (e.g. 20a, 8, 12a) have a depletion of coarse grain sizes and a strong tendency toward a strong positive skewed grain distribution profile. Note the addition of clay and silt fractions and also the dominance of the -1.5 to 2.0 phi class intervals. This may be a reflection of the average grain size of quartz in the granite (i.e. approximately 2.5-3.0 mm). Note that quartz is the main relic mineral in the leached zone.

### B horizon

B horizon samples have a distinct coarsening of grain size with respect to the leached zone. The predominance of the 1.5  $\phi$  grain size still reflects the effect of parent bedrock on grain size. The coarser fraction may reflect the occurrence of exfoliated rock fragments in the soil material (e.g. samples 12b, 20b).

The kurtosis of the B horizon peak is much wider for the B horizon with respect to the A horizon.

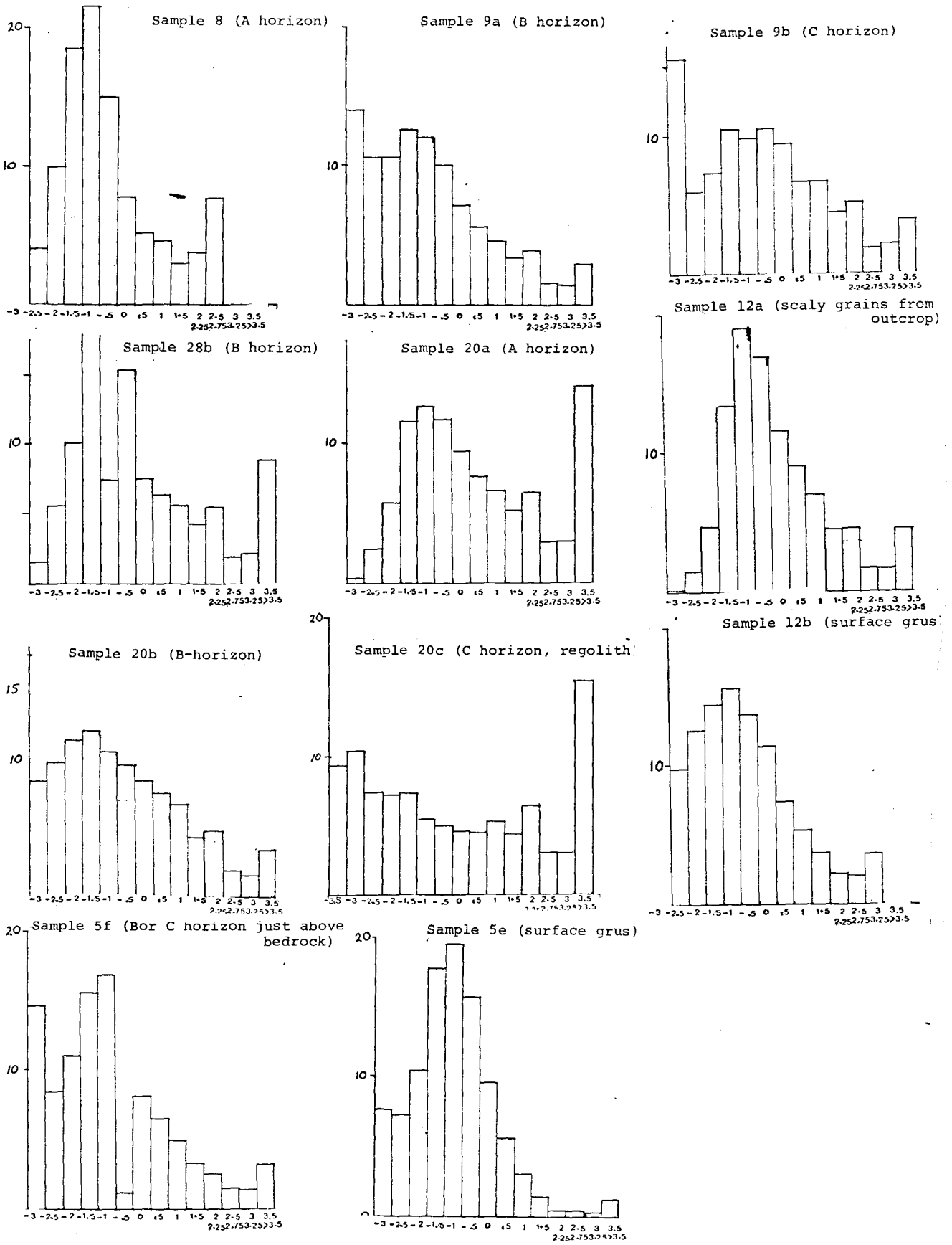
### C horizon

C horizon samples are characterized by a J-type positively skewed distribution. These samples do not have a distinct peak which may indicate a lack of physical disintegration and/or chemical breakdown of minerals and rock fragments (see samples 20c, 9a). Sample 20c has a somewhat anomalous 15% clay-silt fraction which may suggest a migration of clays (colloids) to the rock regolith boundary or alteration of the exfoliated regolith "in situ".

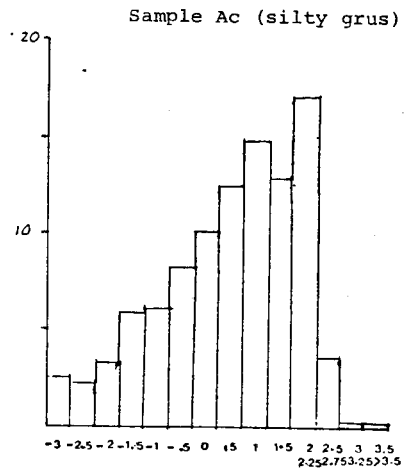
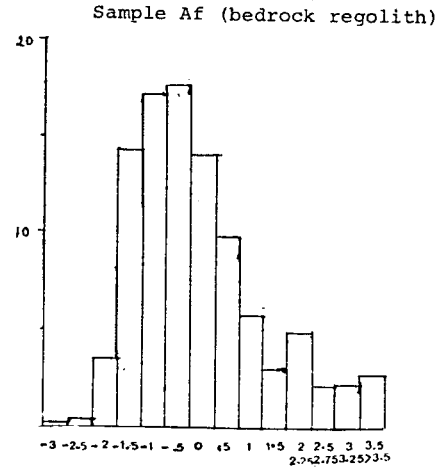
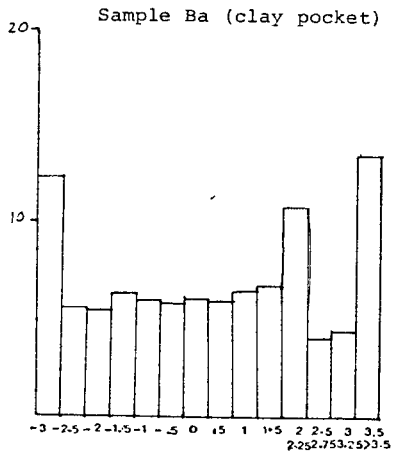
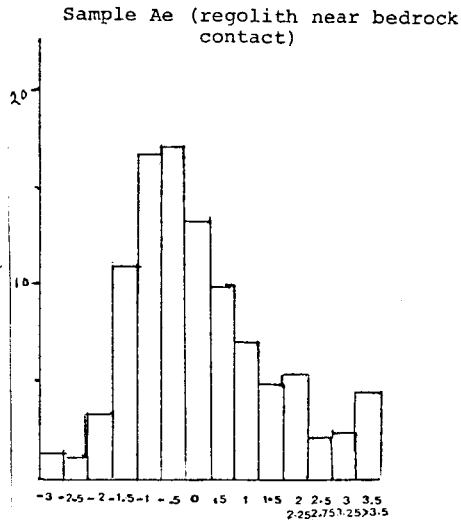
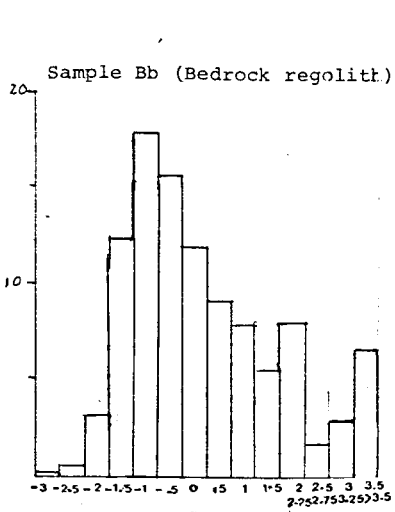
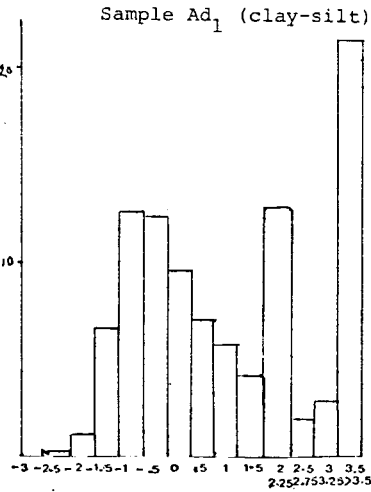
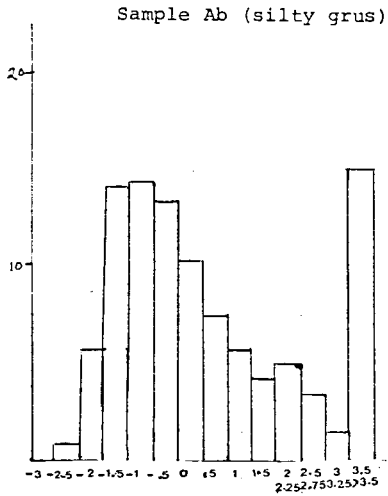
Samples 12a and 12b were taken from weathered outcrop itself and grains lying on the surface as grus. Note that sample 12b has a distinct coarser fraction with respect to 12a. It could be concluded from this distribution that grains do not fall off individually, but as exfoliated platy rock fragments.

Figure 39

(A) Big Bald Mountain: Grain Size Histograms (weight % vs.  $\phi$ )



(B) Pierce Mountain: Weight Percent vs. phi Histograms



In summary, there is a tendency for samples to have a minor fining of sediment and a major depletion of coarse fraction with increased weathering/leaching.

#### B. Pierce Mountain

Again, the majority of samples show a positive skewed trend (Figure 40). There is a distinct difference in grain size distribution between samples taken from the friable bedrock and those of the clay pockets (e.g. sample Ba vs. Bb). In general, there is a depletion of the coarse tail with respect to Big Bald Mountain, possibly indicating the friability of the rock and thus the greater degree of alteration.

A definite sequence or transition from the rock regolith samples to clay samples can be distinguished by the modal variations.

(1) Rock-regolith samples show a well defined positive skewness mode 1-1.5  $\phi$  which reflects average residual grain size (i.e. mostly quartz and potassium feldspar; e.g. samples Af, Bb, Ae).

(2) With greater alteration there is a general decrease in modal values, but the positive skewed trend is still present. There is a large increase in clay-silt percentage. These observations indicate minimal breakdown into secondary products.

Samples Ab, Ad, reflect this trend with different intensity.

(3) The redistribution of all grain sizes to approximately equal proportions and the drastic decrease in the skewness of the distribution are two characteristics of this profile exhibited by sample Ba. Also a very large clay/silt content is developed (i.e. approximately 33%). This reflects a final stage alteration grain size distribution profile of secondary and relic minerals as shown by the near normal distribution developed.

The occurrence of a coarse fraction when not present originally, may reflect the recrystallization of quartz grains to quartz aggregates, possibly with higher mobility of Si with greater chemical alteration. An anomalous negative skewed distribution for sample Ac has a mode of approximately 1 to 1.5. This could be explained by inhomogeneity in the bedrock profile. Note the distinct absence of clay and silt fractions, a factor which forbids a theory of fining with an extreme degree of alteration.

Thus the profile most likely reflects a finer grain rock type with the bedrock, not very evident in the field due to the intense weathering alteration.

### 3.3.3 Cumulative probability plot

A cumulative probability plot and Inman (1952)

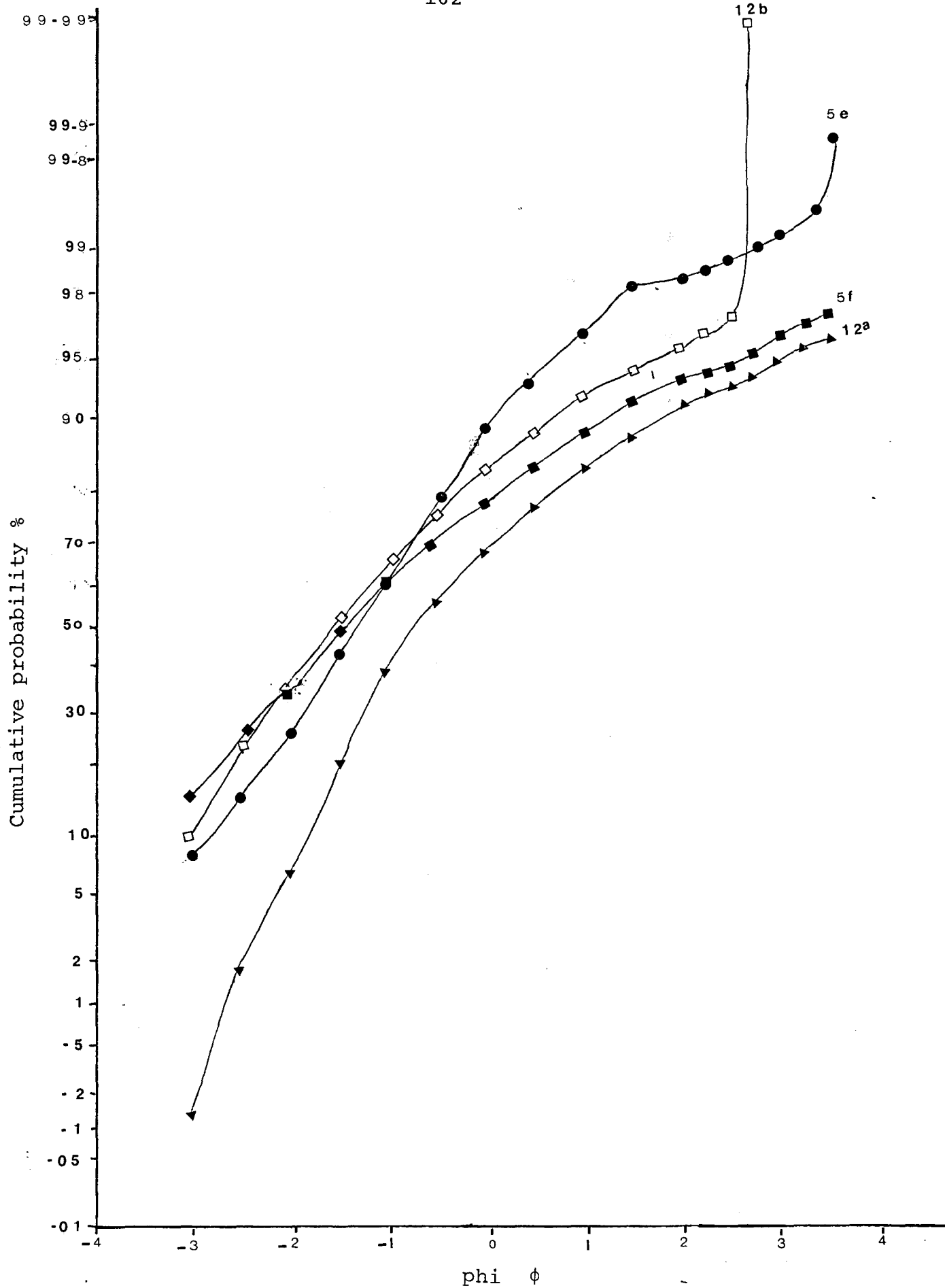
statistics were carried out to illustrate the degree to which grain size distributions are normally distributed. Deviations from normality thus indicate a different process acting on the deposit rather than the assumed abrasion and sorting transport processes.

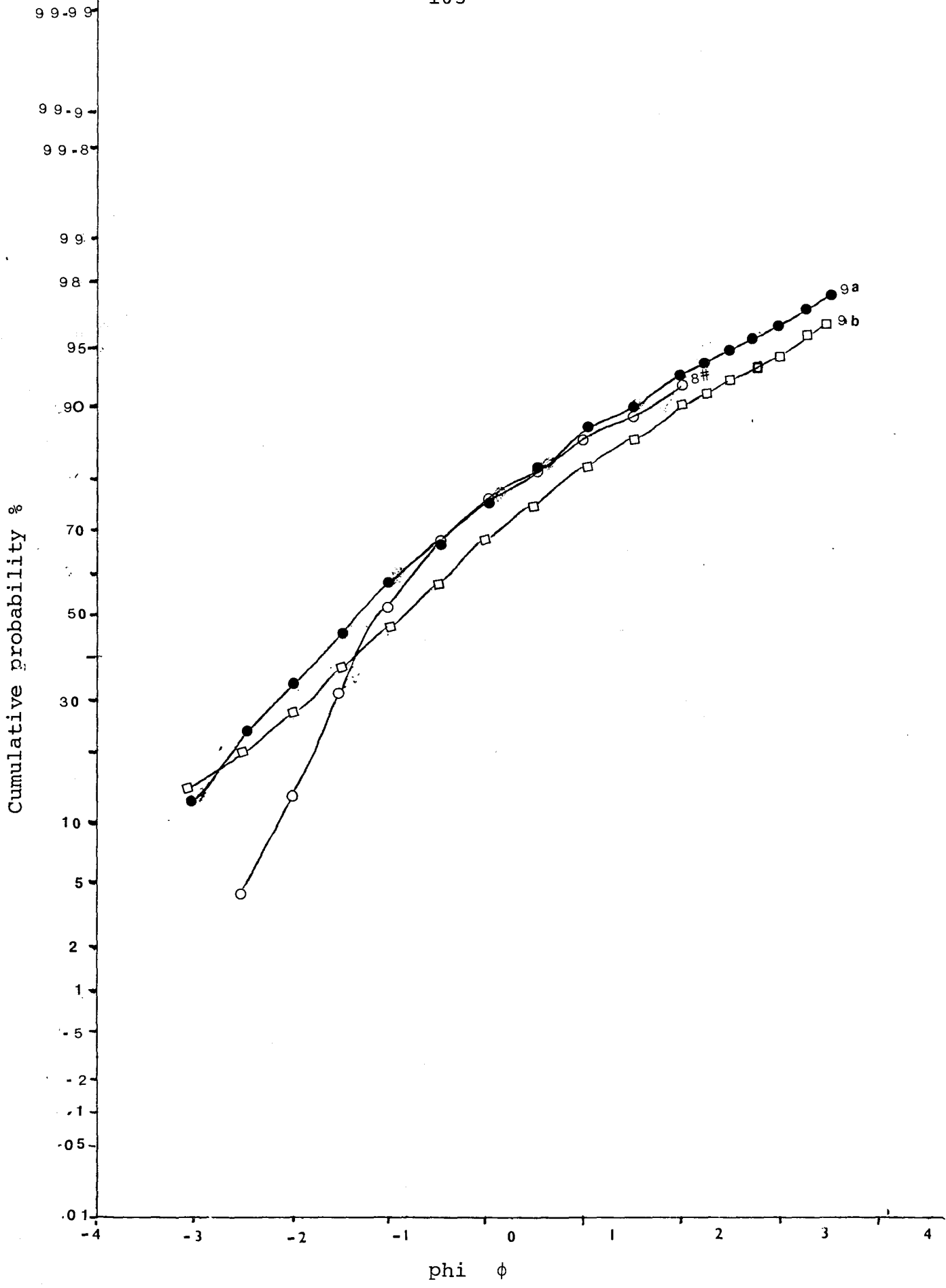
Kittleman (1964) determined that when Roslin's distribution curves are plotted on normal probability paper the Roslins distribution curves would vary significantly from linearity. In fact, a Roslin Probability Distribution when plotted on probability plot is concave down to the lower right hand corner of the graph. This indicates the positive skewed trend of Roslins curves where there is a general depletion of fines. This form was seen for most of the samples analysed (Figure 41). The tendency was for more altered samples (Figure 41B, samples Ab, Aa, Ad<sub>1</sub>) to have greater curvature and two distinct slopes. One representing a steep "well sorted" coarse grain size distribution and the other a horizontal trending distribution suggesting poor sorting of grains, as would be expected in an "in situ" weathering profile.

Note sample Ba is anomalous in that it approximates a moderately sorted normal distribution with a slight fining

Figure 41A. Cumulative probability plots for  
Big Bald Mountain samples







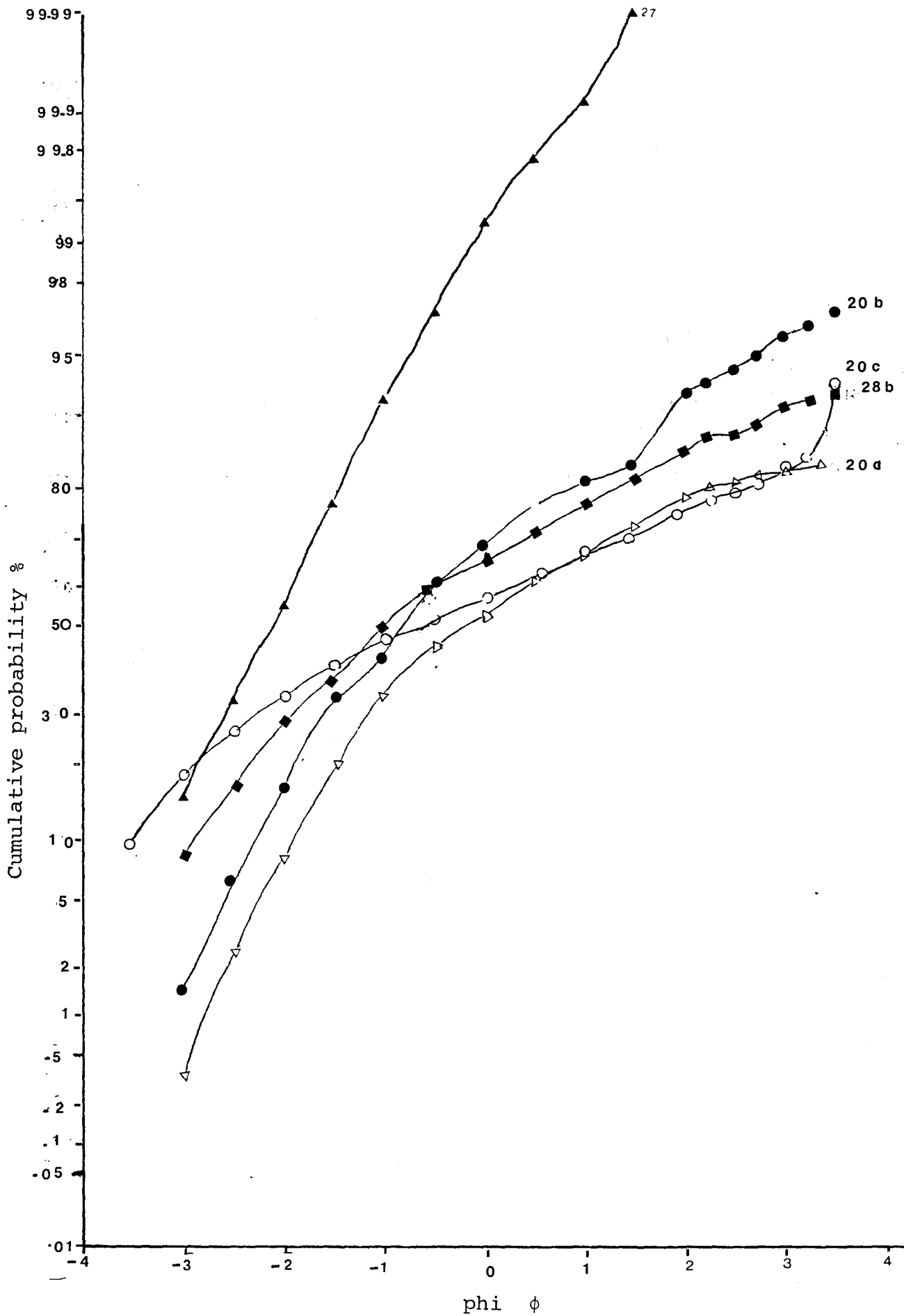
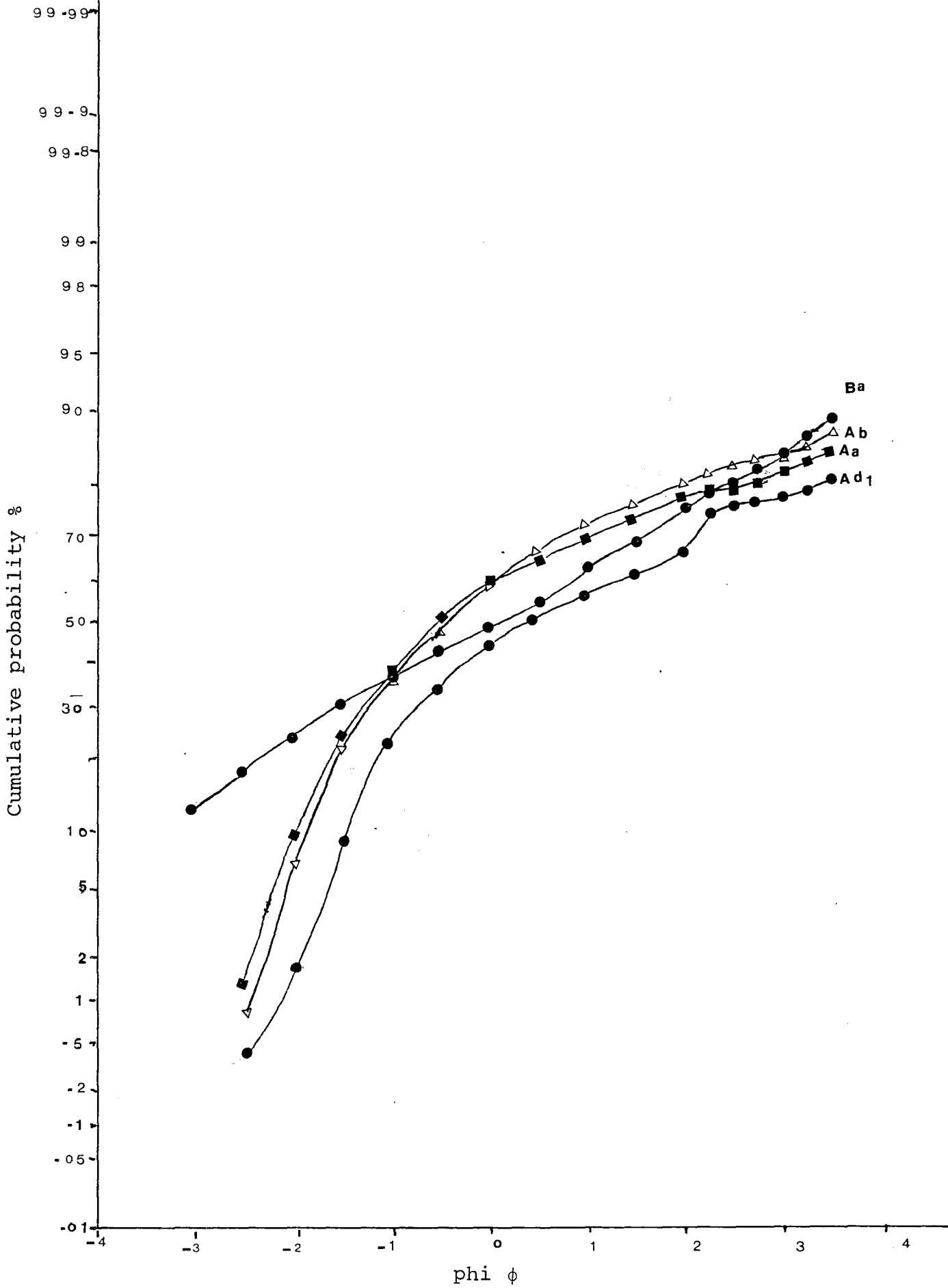
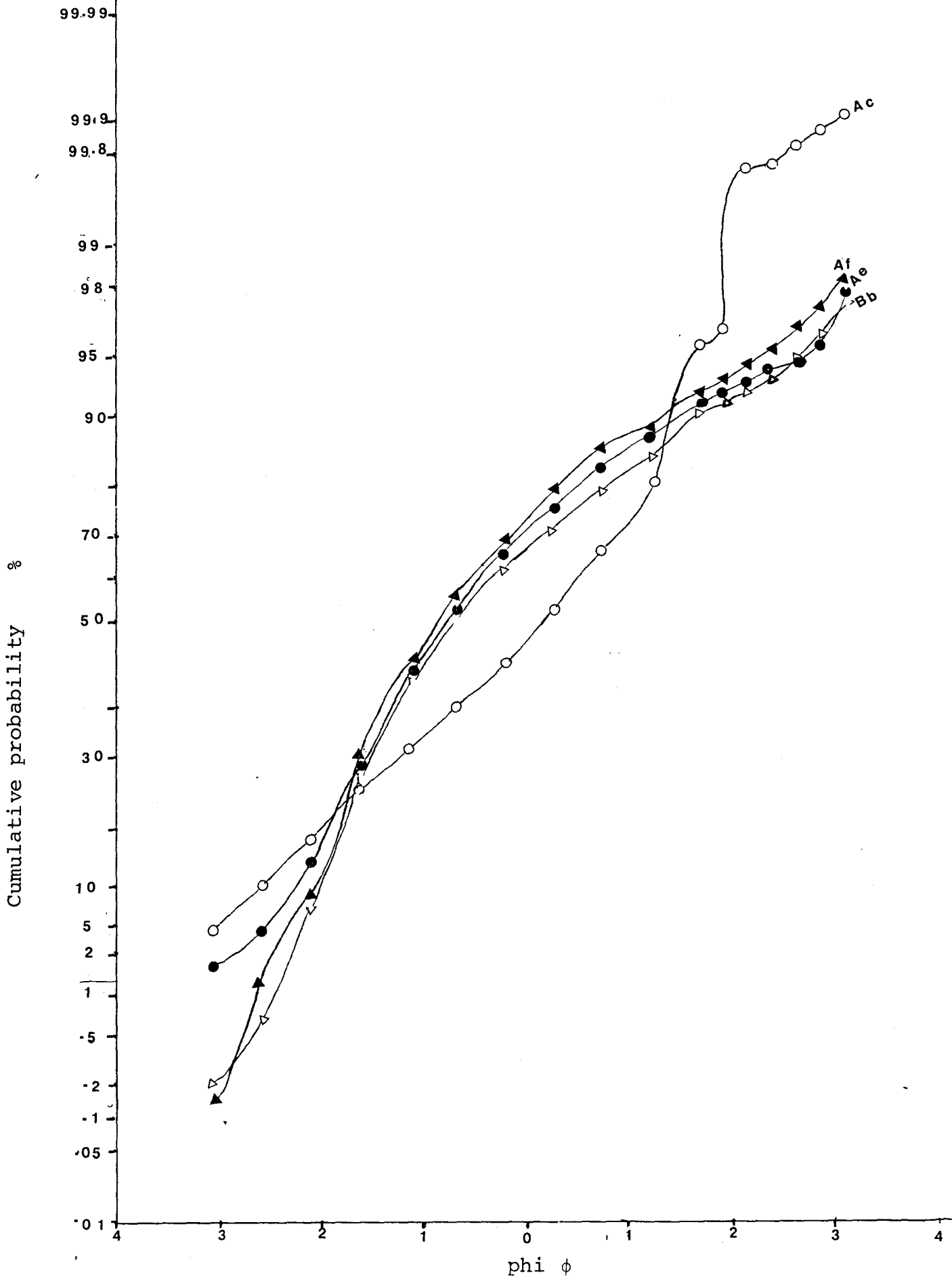


Figure 41B. Cumulative probability plots for Pierce  
Mountain samples





tail. Sediments which reflect disintegrated bedrock-regolith (i.e. sandy grus) approximate an S-shape cumulative probability of overlapping population distributions. This could be accounted for by a combination of clay fraction with grus population distributions.

Note that as a whole, the line is more vertical than weathered samples, indicating a better degree of sorting. This sorting difference may be an indication of alteration intensity.

Note also sample Ac shows the opposite trend to the other samples, indicating an increase in fines up to clay silt grain sizes, where this grain size is depleted.

#### Big Bald Mountain (Figure 41a)

In the Big Bald Mountain samples a similar trend of greater curvature indicates a two population sample can easily be distinguished for leached samples such as 20a, 8, 12a. This distribution is less distinct in B and C horizon soil samples as shown by the degree of curvature of the probability distribution better approximating a straight line (still skewed, however).

Samples 5e, 12b and 20b are anomolous in that they have a very distinct break in the distribution in the fine fraction indicating a decrease in fines as in the Rosin law

distribution. Thus a two population sample may be defined.

Sample 27 approximates a normal distribution of moderately well sorted sediment defined in coarse sand fraction. Thus this sample may have been transported by some fluvial system or possibly by solifluction downslope from Big Bald Mountain ridge. This sample is important as it represents a deep accumulation of grus (subangular-angular granule size quartz and potassium feldspar) in the incised valley-plain area. This is to the east of Big Bald Mountain (see site location Figure 21).

Inman (1952) statistical analyses were performed on the cumulative probability distributions (Table 3).

(a) Big Bald Mountain

From the median values ( $\phi$  50) of the samples, it could be generalized that samples representing leached profiles or surface quartz feldspar accumulations have medians greater than 1.00  $\phi$ . Those representing B and C soil horizons have medians generally less than 1.00  $\phi$ .

Skewness except in one sample is positive in leached samples having values greater than 0.3 and in B and C horizon samples less than 0.3 (Note maximum skewness is 1.00; Folk, 1966).

The analogy is very approximate and no systematic



variation can be discussed. Sample 12a however shows an abnormally high skewness (68) and kurtosis value (0.96), as would be expected from quartz, feldspar grains knocked off a "scaly" high grain relief granite outcrop.

(b) Pierce Mountain

Generally much better trends can be seen from the Pierce Mountain samples (Table 3). There is a decrease in median grain size from regolith-rock samples to highly altered clay pocket samples (samples Af, Ad<sub>1</sub>, respectively). The range in median size varies from 1.58 (Ac) to 0.50 (Ad<sub>1</sub>). The dispersion is generally greater for altered sediments (e.g. Ad<sub>1</sub> and Ba) versus regolith-grus samples (e.g. samples Af, Ae).

Again, highly altered clay pocket samples tend to approximate normal distributions while grus-regolith samples are usually positively skewed.

Thus Inman's (1952) statistics tend to have reasonably good correlation with histogram and probability plot analysis despite the inherent difficulties in the method.

Table 3 Inman Statistics

Sample	$\phi_{16}$	$\phi_{84}$	Md = $\phi_{50}$	Mean ( $M\phi$ )	Disper- sion $\theta\phi$	Skewness $\alpha\phi$	Kurtosis
BIG BALD MOUNTAIN							
8	-1.93	0.59	-1.13	-0.67	1.26	0.37	*
12a	-1.60	1.10	-0.67	0.25	1.35	0.68	0.96
20a	-1.68	3.50	-0.20	0.91	2.59	0.43	*
28b	-2.12	1.85	-0.78	-0.14	1.99	0.32	*
5e*	-2.45	0.24	-1.35	-1.10	1.35	0.18	*
5f	-1.95	0.60	-1.15	-0.68	1.28	0.37	*
12b	-2.75	0.09	-1.55	-1.33	1.42	0.16	*
20b	-2.55	1.50	-1.05	-0.53	2.03	0.26	*
9b	-1.65	1.10	-0.63	-0.28	1.38	0.25	*
9a	-2.90	1.60	-0.47	-0.65	2.25	-0.08	*
PIERCE MOUNTAIN							
Aa	-1.91	3.49	-0.50	0.79	2.70	0.48	*
Ab	-1.61	2.95	-0.47	0.67	2.28	0.50	*
Ac	-1.40	1.62	-1.58	0.11	1.51	1.12	0.49
Ad <sub>1</sub> *	-1.15	3.51	0.50	1.18	2.33	0.29	*
Ae	-1.53	1.55	-0.55	0.01	1.54	0.36	0.74
Af	-1.72	0.91	-0.62	-0.40	1.32	0.16	0.78
Ba	-2.60	2.90	0.19	0.15	2.75	-0.02	*
Bb	-1.47	1.57	-0.50	0.05	1.52	0.28	0.62

Note: For normal distribution curves Inman (1952) statistics for skewness and kurtosis should have values of 0.00 and 0.65, respectively.

\* Kurtosis values could not be determined due to  $\phi_{95}$  or  $\phi_5$  values were not obtained for the phi range analyzed.

### 3.3.4 Rosin law probability plot

Rosin law distribution paper plots a straight line for the grain sizes of many crushed and weathered materials. Rosin used linear regression and F-statistics to determine linearity of the size frequency distribution (Kettleman, 1964). Kettleman (1964) also notes that if the distribution is not ideal (as identified by kurtosis and skewness in normal distribution) the resulting distribution curve will not define a straight line on either of the probability graphs.

In summary, Rosin's probability plots account for the positive skewness of most weathered profiles thus producing a straight line.

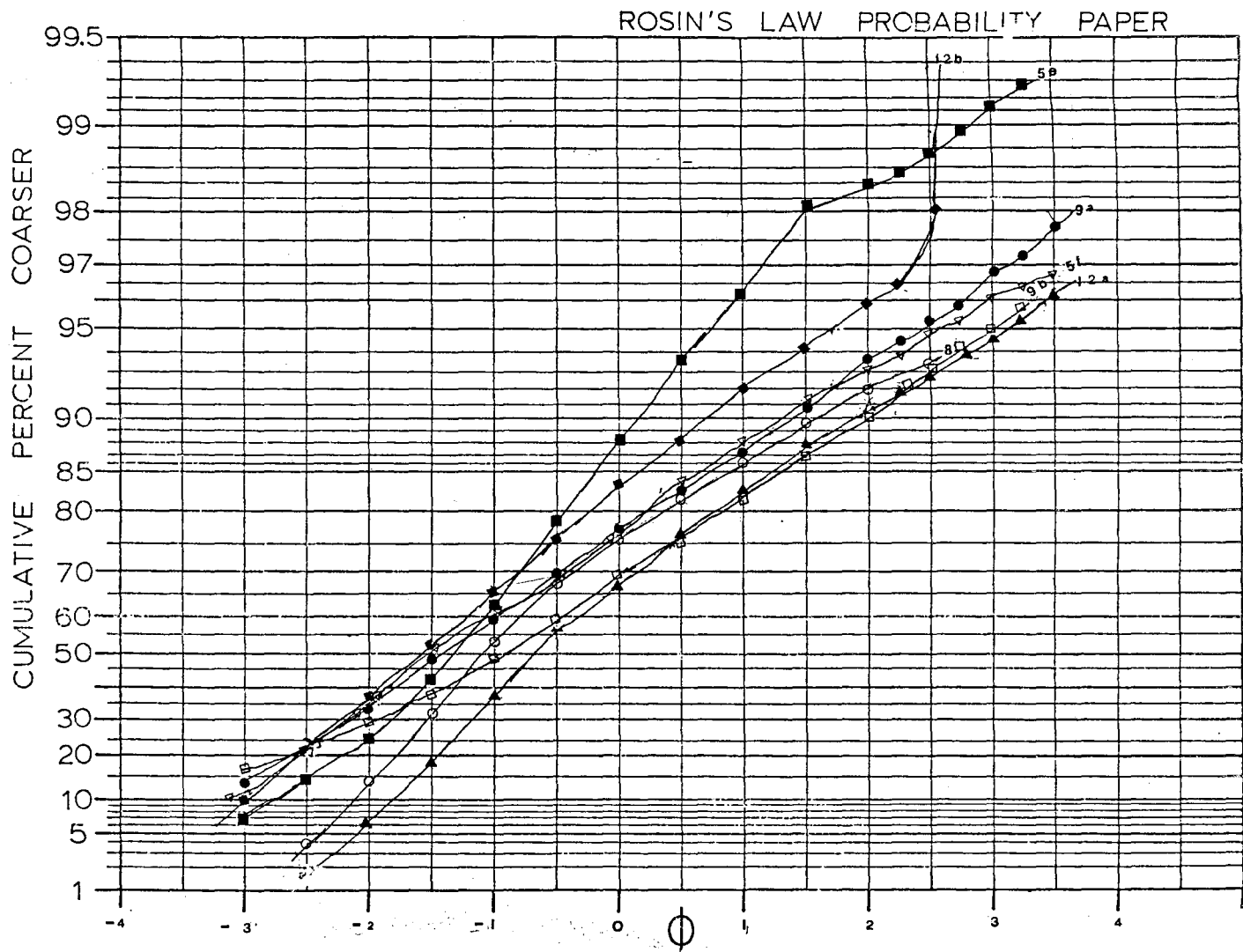
#### Big Bald Mountain

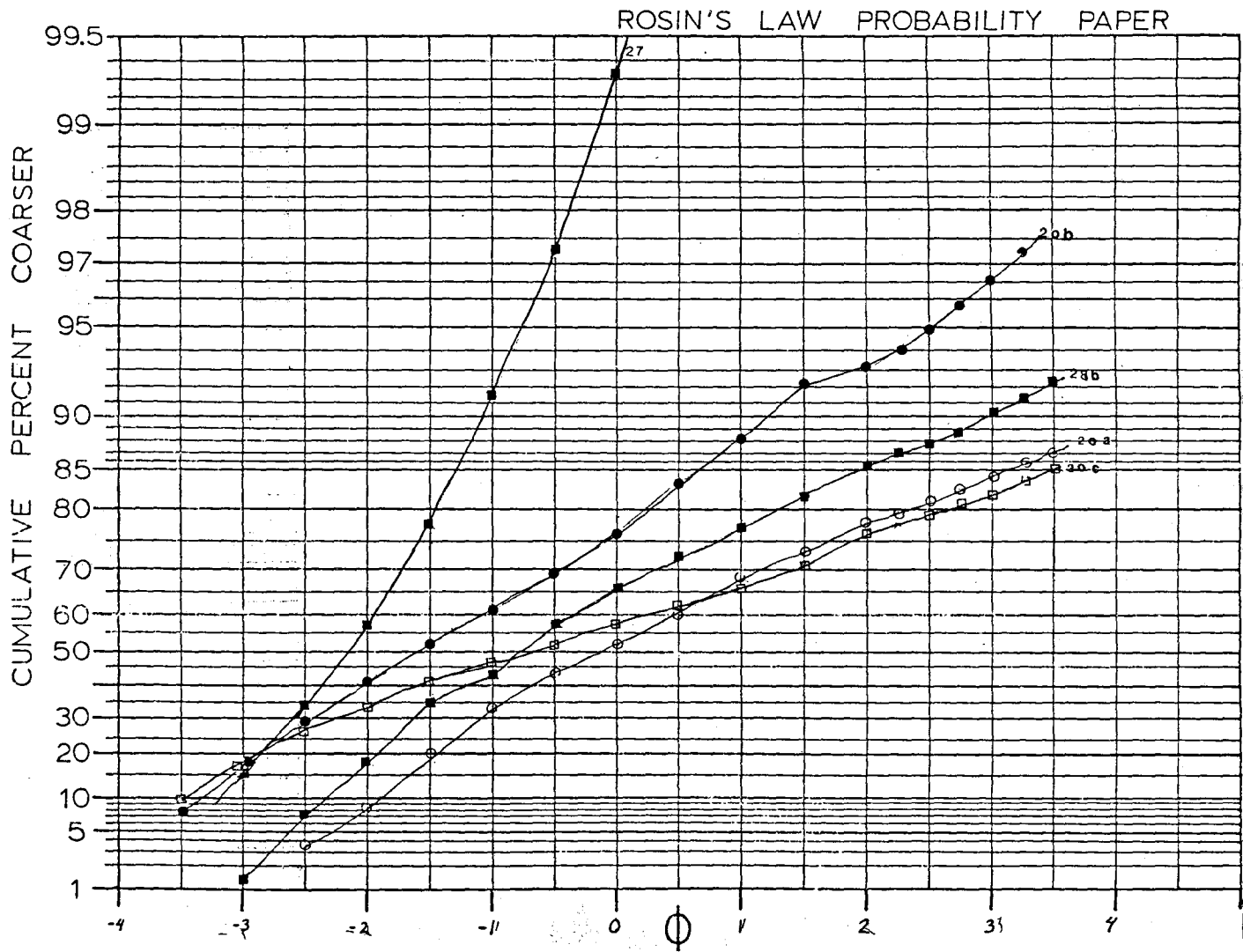
As already determined, many of the samples are skewed positively. Thus deviation from the straight line should not be expected (Figure 42a). In general the grain size cumulative probability plots follow a straight line relationship for Big Bald Mountain soil grus samples.

#### Pierce Mountain

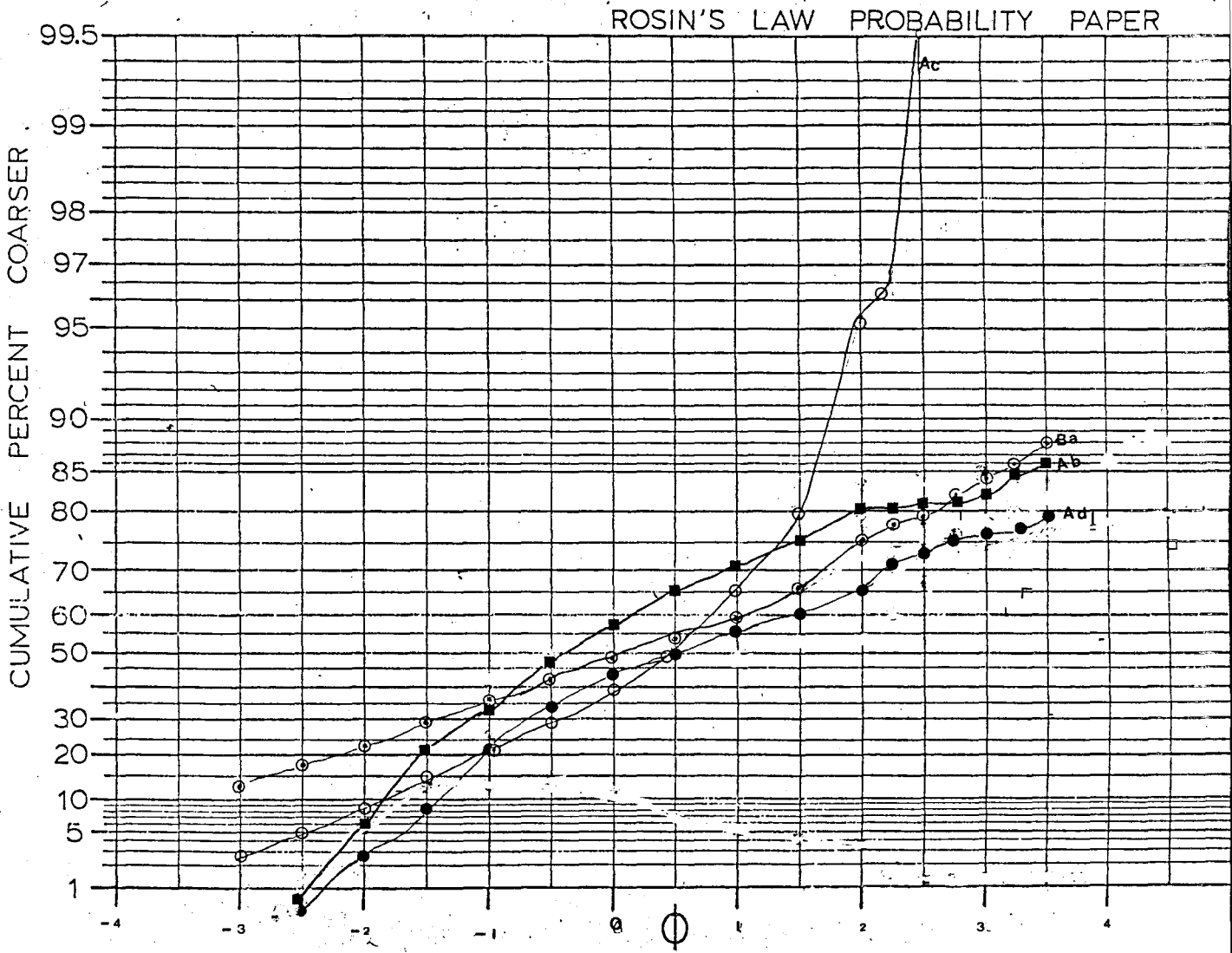
Two general trends can be seen in Figure 42b, which seem to correlate with weathering/alteration intensity. Samples Ba, Ab, and Ad<sub>1</sub> represent the clay rich sediment.

Figure 42A. Rosin law cumulative probability plots vs. grain  
size for Big Bald Mountain samples



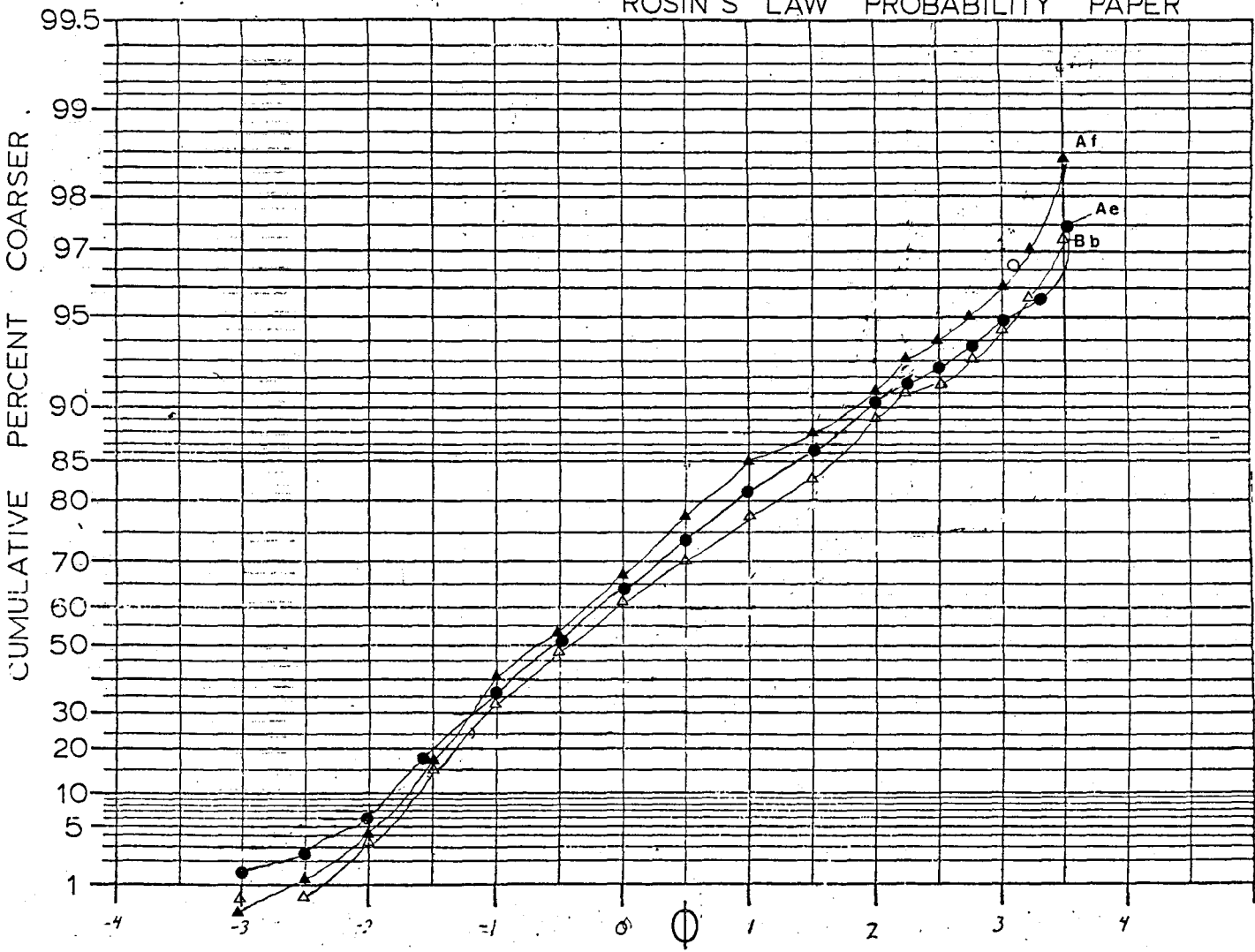


Rosin's law cumulative probability plot vs. grain size for  
Pierce Mountain





ROSIN'S LAW PROBABILITY PAPER



Note that sample Ab still has a coarse, rich tail which the clay pocket samples no longer have. Otherwise the samples approximate a straight line on the Rosin's probability paper (Figure 42b).

Again, sample Ac is anomalous, suggesting a normal distribution profile, but it does not fit well on either probability distribution plots due to the skewness of the distribution.

### 3.3.5 Discussion

In summary of findings from different methods of analysis we can conclude that grain size analysis can be used as a relative indicator of weathering intensity.

It can be seen from this study of grain size distributions that there are two types of granite regoliths produced. These are:

(1) Sandy-granule size regoliths which have generally a low silt clay fraction (i.e. <9%). This is thought to be produced more by the physical disintegration of the bedrock with slight modifications by chemical hydrolysis and oxidation of minerals in the bedrock. This size distribution characteristic of sandy regoliths (grus) is notable at the Big Bald Mountain site. Note that the leached surface A soil horizon

produces a distribution which is comparable to clay pockets found at the Pierce Mountain site.

(2) The clay pocket material as found at Pierce Mountain site which shows an addition in fine size fraction and depletion in coarse size material. These pockets are characterized by clay-silt (i.e.  $>3.5 \phi$ ) content of up to 33%. Such concentrations of fines have been suggested by Eden and Green (1971) to be indicative of hydrothermal alteration. This is one line of evidence that the alteration of the granite at Pierce Mountain is not entirely due to climatic weathering processes.

Sample Ac persisted to be anomalous throughout all methods of analysis of grain size distributions. This may suggest the host parent rock at the site is not a homogeneous rock.

The Pierce Mountain site shows the best correlation with intensity of weathering variations with grain size distributions which may be attributed to areas of preferential percolation of ground water along joints.

### 3.4 X-ray diffraction

A summary of peak intensity and d-spacings for the 9 samples analysed is illustrated in Table 4. Glycolation of samples determined that montmorillonite was not present, or if present, only in very limited amounts.

The following conclusions can be made on the clay minerals produced due to the alteration of the granite.

#### A. Big Bald Mountain

In the leached A horizon (sample 20a) the dominant clay minerals are vermiculite and mixed larger clays. This would be expected since the weathering products seen in thin section were chlorite and sericite. Chlorite is known to further alter to vermiculite upon intense weathering. Mix layer clays would develop from the sericite to produce illite, which may be further altered to produce a mix layer clay.

In sample 20B vermiculite and chlorite are both found as would be expected in the Fe oxide rich B horizon.

Sample 20c has developed a major peak that corresponds to gibbsite. This clay mineral is traditionally thought to represent intense weathering environments, but it has been found in other environments. Chlorite is subordinate to gibbsite but still important.

Sample 28b representing a grus accumulation has

kaolinite and gibbsite and illite present as strong peaks. The above are in order of decreasing abundance shown by peak intensities.

It appears that in regolith that gibbsite-kaolinite are produced with less dominant illite and chlorite. More leached profiles produce illite vermiculite clays.

#### B. Pierce Mountain

Samples Aa, Ab and Ad<sub>1</sub> have developed illite kaolinite as their major minerals with less dominant chlorite present. This sequence is from the same rock weathering profile where there are no major colour variations except in the clay pocket.

Samples Ba, Bb are anomalous. The major minerals produced are lepedotite-muscovite possibly illite, with minor kaolinite in sample Bb. This may suggest a different alteration due to ground water filtration. Ground water percolates along a joint beside the clay deposit.

Table 4 X-ray diffraction analyses

## A. Big Bald Mountain

d-spacing	I/I <sub>0</sub>	Shape of Peak	Mineral	d-spacing	I/I <sub>0</sub>	Shape of Peak	Mineral
SAMPLE 20A				SAMPLE 20c			
13.28	23	S	Verm *	19.15	14	B	Verm Cl
13.19	24	S	Mx	11.74	8	B	
10.52	5	M	Il	10.31	10	B	Il
8.88	4	M	Mx	9.95	15	M	Il
7.147	4	B	Verm	7.085	26	M	K Cl *
6.63	3.5	B	Or	4.99	13	B	Il
6.45	4.7	B	Or	4.825	100	S	Gib Cl *
5.855	3	B	Or Mx	4.425	18	B	Il
5.245	4	M		4.35	33	M	Gib *
4.985	4	B		4.30	22	B	Gib
4.45	9.2	M	Verm	4.24	17	B	Q
4.228	33	S	Q Or	4.12	5	B	
4.02	13	M		3.595	9	B	
3.925	5	B		3.54	17	B	
3.838	4	B	Or	3.535	15	B	
3.755	11	S		3.46	10	B	
3.655	8	S		3.34	75.2	S	Q Gib
3.46	13	M	Or	3.295	14	B	Gib
3.33	100	S	Q	3.23	7	B	
3.283	28	S		3.185	18	M	Gib
3.23	40	S		2.584	8	B	
3.175	41	S		2.558	7.5	B	Il
3.07	11	MB	Mx	2.453	15	M	Gib Il
2.95	10	MB		2.390	16	B	Cl
2.92	4	B	Or	2.381	14	B	Gib
2.88	10	M		2.279	9	B	Q
2.861	3	B		2.047	9	B	Gib
2.848	3	B		2.003	13	B	Cl Il
2.759	4	B	Or	1.996	14	B	Gib
2.604	4	B					
2.587	5	B					
2.573	6	B	Or				
2.553	12	M	Or				
2.52	6	B	Or				
2.444	8	M	Q				
2.276	8	M					
2.231	5	M	Q				
2.157	6	M					
2.123	8	M	Q				
1.997	4	B					
1.995	4	B					
1.94	6	B					

max. peak 55°

Other peaks correspond to lower d-spacing clays or high Ab or orthoclase feldspar

max. peak &gt;100°

Table 4/continued

d-spacing	I/I <sub>o</sub>	Shape of Peak	Mineral	d-spacing	I/I <sub>o</sub>	Shape of Peak	Mineral
SAMPLE 28b				SAMPLE 20b			
13.99	11	B	Mont Cl	14.2	24		Verm Cl *
10.17	26	B	Il	13.72	28		
9.86	39	M	Il *	8.4	19		Cl
7.89	16	B	Cl	4.84	28		Cl
7.51	35	B	Cl	4.45	19		
7.14	70	Mq	K Cl *	4.24	31		Q
5.00	30	S	Il	4.04	22		
4.83	35	M	Gib Cl *	3.78	16		
4.405	57	B		3.49	16		Cl
4.34	46	B		3.34	100		Q
4.24	36	B	Q	3.31	21		
4.16	21	B		3.23	16		
4.03	29	M		3.19	23		
4.01	25	M		2.96	16		
3.74	10	M					
3.66	34	M					
3.57	43	M	K				
3.47	22	B					
3.46	16	B	Gib				
3.33	100	S	Q				
3.18	50	S	Gib				
3.15	22	M					
3.06	11	B					
2.98	10	B					
2.564	28	M					
2.554	29	M					
2.44	10	B	Q				
2.38	12	M	K				
1.998	17	M					
1.990	22	M					

max. peak 35°

max. peak 30°

Table 4/continued

## B. Pierce Mountain

SAMPLE Aa				SAMPLE Ab			
d-spacing	I/I <sub>0</sub>	Shape of Peak	Mineral	d-spacing	I/I <sub>0</sub>	Shape of Peak	Mineral
13.645	7	B	Cl	12.63	13	B	Mx
12.40	8	B	Mx	9.94	10	M	Il
9.985	30	MS	Il *	9.01	9	S	
7.20	40	MB	K Cl *	8.51	9	M	Mx
7.117	38	MB	Cl K <sub>MD</sub>	7.40	75	B	H *
6.357	12	M	Ab	7.105	81	B	K <sub>MD</sub>
6.32	12	M	Mx	5.075	9	B	
5.893	6	B	Ab	4.975	16	B	
4.975	17	M	Cl	4.435	100	M	K <sub>MD</sub> H <sub>D</sub> *
4.84	15	M	Cl	4.385	85	B	
4.34	47	MB	K <sub>MD</sub>	4.215	43	B	
4.31	37	M		4.13	29	B	
4.253	36	M	Q	4.08	27	B	
4.123	15	B		4.01	44	M	
4.02	50	S	Ab	3.753	23	B	Ab
3.85	73	MS	Ab	3.725	21	B	
3.765	26	S	Ab	3.65	67	M	H <sub>D</sub>
3.665	47	S	Il	3.60	47	B	
3.573	29	B	K <sub>MD</sub>	3.57	49	K <sub>MD</sub>	
3.49	17	B	Cl	3.50	28	B	Cl
3.338	100	S	Q	3.34	47	M	H
3.185	98	S	Ab	3.185	74	S	Ab
3.15	39	M	Ab	3.16	31	M	
3.052			Mx	3.06	10	B	Mx
2.965	15	M	Ab	2.98	10	B	Mx
2.935	18	B		2.935	10	B	Ab
2.925	19	M	Ab	2.563	48	M	K <sub>MD</sub> H <sub>D</sub>
2.854	9	B		2.501	20	B	K <sub>MD</sub>
2.639	7	B	Ab	2.457	11	B	Il
2.555	29	M	K <sub>MD</sub>	2.382	15	B	K <sub>MD</sub>
2.506	17	B		2.346	20	B	K <sub>MD</sub> H
2.499	16	B		2.002	16	B	
2.381	15	B					
2.34	14	B	K <sub>MD</sub>				
2.314	11	B					
2.279	8	B	Q				
2.234	5	B	Q				
2.189							
2.126	13	B	Q				
2.120	9		Ab				
1.996	17	B					
1.990	15	B					

max. peak 67°



Table 4/continued

d-spacing I/I <sub>0</sub>		Shape of Peak	Mineral	d-spacing I/I <sub>0</sub>		Shape of Peak	Mineral
SAMPLE Ad <sub>1</sub>				SAMPLE Ba			
10.02	40	MS	Il *	10.28	91	S	Lep Musc
7.29	61	M	K <sub>MD</sub>	7.44	0.6	B	trace
6.35	8	B	Olig ? Ab	7.21	0.6	B	trace
5.01	20	M	Il *	6.78	0.6	B	trace
4.47	42	S	Il K <sub>MD</sub>	6.53	0.8	B	trace
4.35	24	B		4.99	52	S	Lep Musc
4.30	21	B		3.33	100	S	Lep Musc
4.27	25	M	Q	2.496	10	S	Lep Musc
4.04	47	S	Olig? Ab	1.998	44	S	Lep Musc
3.86	9.1	B	Olig? Ab				
3.78	23	S	Olig Ab				
3.67	54	S	Il				max. peak >100°
3.61	38	M					
3.59	38	M	K <sub>MD</sub>				
3.51	20	M	Olig				
3.35	100	S	Q Il				Muscovite 3T
3.19	80	S	Olig Ab				
3.16	32	S	Ab?				Tueniotite
3.07	7		Ab				
3.00	9	B	Olig Mx				
2.97	16	M	Olig				
2.94	13	M	Ab				
2.864	13	M	Il				
2.799	6	B					
2.567	42	S	K Il				
2.500	11	B	K				
2.46	8	B	Q				
2.45	8	B	Il				
2.394	11	B	K				
2.386	10	B	K				
2.359	10	B					
2.282	6	B	Q				
2.192	6	B					
2.181	6	B					
2.129	14	M	Q				
2.078	5	B	K				
2.002	20	M	Il				
1.989	8	B	Q K				
1.891	8	B					
1.888	7	B	Ab				
1.847	7	B	Ab				
1.820	13	M	Q				
1.786	7	B	K				
max. peak 68°							

Table 4/continued

d-spacing	I/I <sub>0</sub>	Shape of Peak	Mineral
SAMPLE Bb			
9.94	74	S	Il Lep Musc
7.44	52	B	Cl
7.29	61	B	Cl
7.14	56	B	K
6.74	14	M	
4.975	46	M	Il Musc Lep
4.445	31	BM	K Musc Il
4.30	14	B	Il Musc
4.215	17	B	K
4.01	19	M	Ab
3.885			Il Musc Lep
3.835			K
3.643	44.3	M	Il Lep
3.558	42	B	K Lep
3.52	18	B	
3.49	14	B	Musc
3.33	100		Il Lep Musc
3.175	18	B	Il Lep Musc
3.15	11	B	B
3.047	18	B	
2.917	11	B	
2.67	9	B	
2.58	9	B	Lep ?
2.559		B	Il K Musc
2.512	12	B	Musc
2.38	8	B	K Cl
2.123	8	B	Musc
2.085	8	B	K Musc
1.997	34	M	Il Musc Lep

LEGEND

## Minerals:

K - kaolinite  
 Q - quartz  
 Mx - Mix layer clay  
 Il - ilmenite  
 Cl - chlorite  
 Gib - gibbsite  
 Verm - vermiculite  
 Or - orthoclase  
 Ab - albite

OLIG - OLIGIOCLASE

max. peak 55°

## Accessory Minerals:

minor K  
 minor B  
 may be Li rich

## CHAPTER IV

### CHEMICAL WEATHERING

#### 4.1 Introduction to concepts of chemical weathering

The purpose of this chapter is to try to determine the chemical reactions and processes that take place in the weathering profile which result in the alteration of the parent rock.

The primary chemical weathering processes must be determined before products of weathering can be analysed. They are hydrolysis, hydration, oxidation and carbonation. These processes are seldom mutually exclusive.

#### Definitions (Steila, 1976):

**Hydrolysis:** is the process in which dissociated  $H^+$  and  $OH^-$  ions in water react with rock forming minerals.


**Hydration:** occurs when  $H_2O$  combines chemically with other molecules.

Oxidation: the process in which oxygen combines with rock compounds leading to weakening of the rock.

Carbonation: precipitation of  $H_2O + CO_2(aq)$  forms carbonic acid which will react with Na, Ca, K oxides to form carbonates.

Note that normal equilibrium mineral assemblages can not be used for soil formation (Keller, 1957).

Goldich (1938) produced a classic paper on the stability of minerals which influenced the discussion of weathering for decades after. His hypothesis that mineral stability was essentially a function of a reverse Bowen reaction series is still generally quoted to this day, i.e.

Olivine	Ca feldspar	 decrease in stability
Augite	Ca Na feldspar	
Hornblende	Na Ca feldspar	
Biotite	Na feldspar	
	K-feldspar	
	Muscovite	
	Quartz	

He established this sequence by determining the relative gains and losses of the minerals in a granite gneiss,

a diabase and an amphibole by assuming  $\text{Al}_2\text{O}_3$  was constant through the weathering sequence. This concept of determining the mobility of ions relative to a "stable" ion has been used extensively. (For example, Krauskopf, 1967, Harriss and Adams, 1966). Goldich believed that  $P_{\text{CO}_2}$  in the ground water was an important indicator of weathering intensity.

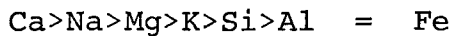
Other factors important in the stability sequence developed above are: temperature, ion concentrations of weathering ground waters, surface area of grain exposed to weathering, structured weaknesses in the mineral being altered (e.g. twin planes, exsolution lamellae, other lattice defects, presence or rate of development of amorphous clay coating on feldspar grains resulting in a decrease in the intensity and rate of chemical attack).

Thus it can be seen that the weathering process cannot be the result of any single parameter, but is a complex interaction of location, environment, climate and parent rock and age of profile developed. Associated with the age of the profile is the rate of erosion which often prevents the chemical weathering system to go to completion.

Harriss and Adams (1966) in a study of 5 granite weathering profiles concluded that the relative stability of the major granite minerals were plagioclase < biotite < K-feldspar < quartz. This relationship was independent of of physiochemical variations.

They also determined the major derived clay was a combination of kaolinite and illite, the relative concentration dependent on intensity of weathering. The major physical and chemical changes were between the weathered bedrock and soil developed above.

Blaxland (1973) confirmed the findings of previous workers when he concluded that the removal of major elements had the following order (stated in relative ease of removal):



He summarized his chemical analyses of a granite as follows:

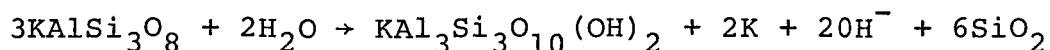
- (1) The slight increase in  $\text{SiO}_2$  with greater intensity of weathering was a function of the stability of quartz in the granite.
- (2) The  $\text{Al}_2\text{O}_3$  and  $\text{Fe}_2\text{O}_3$  contents have an inverse relationship with  $\text{SiO}_2$  concentrations with increased intensity of weathering, due to steady removal of feldspars, biotite and hematite.
- (3)  $\text{CaO}$  is steadily depleted also as the feldspar was altered to clay or sericite.
- (4) Finally he considered the variability of  $\text{Na}_2\text{O}$  and  $\text{K}_2\text{O}$  to be the result of original phase variations in the minerals themselves, not variations in the weathering profile.



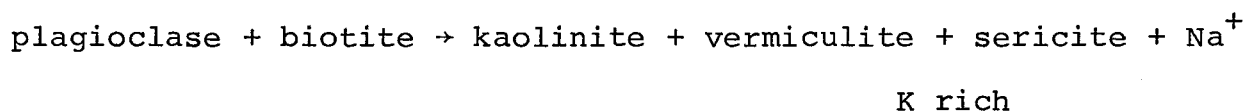
The order of appearance is thought to be constant.

Of particular application to this study, Tardy suggests that in temperate climates primary minerals weather slowly and intergranular joint solutions are dilute. Thus reaction completion is difficult and therefore mineral phase equilibrium is never attained.

Meunier and Velde (1976) determined that the early stages of granite weathering are characterized by the alteration of K-feldspar to muscovite, i.e.



However they determined that tectonically produced sericite had a different composition and was the result of the following reaction:



The mixing of the metamorphic and weathered sericite may result due to soil forming processes producing illite (Meunier and Velde, 1976).

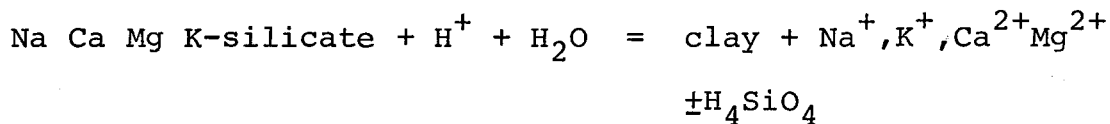
The diffusion of iron and Ti oxides around biotite grain edges is similar with this study's findings.

Now that some of the concepts of weathering have been established we can analyse the findings of this study.



Weathering index

The purpose of this section is to describe the chemical variations produced in the weathering profile. The basis for the variations lies in the general chemical weathering equation for silicate minerals, i.e.



The variations are based on the whole rock geochemical analyses of bedrock, grus, regolith and soil samples.

Many methods were used to determine chemical variations in the weathering profile. These included:

- (1) Deriving a weathering index (based on Parker, 1970).
- (2) Relating the weathering index to -
  - (a) depth;
  - (b) cation/Al cation percent ratios;
  - (c)  $[\text{Cation/Al}]_{\text{parent}} / [\text{Cation/Al}]_{\text{weathered}}$
- (3) Weathered vs. fresh cation percent ratios.

#### 4.2 Weathering index

A weathering index was used in this section as a base from which other cation changes could be evaluated. This weathering index was conceived by Parker (1970). The index is based on the assumption that the major process of weathering in normal humid climates is hydrolysis. Thus a mineral is altered by the exchange of Ca, Mg, Na and K for H with or without the loss of Si (Kramer, 1968). Parker states that if hydrolysis is the major process then the relative bonding strength to oxygen should be an important parameter in the determination of relative mobility of the ions. The relationship used in determining the weathering index was:

$$\left[ \frac{(\text{Na})_a}{(\text{Na-O})_b} + \frac{(\text{Mg})_a}{(\text{Mg-O})_b} + \frac{(\text{K})_a}{(\text{K-O})_b} + \frac{\text{Ca}}{(\text{Ca-O})_b} \right] \times 100$$

where  $X_a$  = atomic proportion of element X

$(X-O)_b$  = bond strength of element X.

The results of this calculation for bedrock grus and soil horizons are illustrated in Table 5. It was found that a "fresh" rock sample had values between 141-128, which decreased for weathered samples to values as low as 33. A few anomalous high values (e.g. 149) were determined for

Table 5.

Weathering Index  
[x]<sub>a</sub> / (x-0)<sub>b</sub> \* ratio

## A. Bald Mountain

Sample	Description	Symbol	Mg	Ca	Na	K	Weathering Index	Relative Degree of Alteration
5a*	Bedrock	▲	2.6	2.44	54.03	64.40	123.47	LM
5b*	Bedrock	▲	2.07	2.39	57.11	59.04	120.60	LM
5d*	Bedrock	▲	1.64	2.41	75.46	61.96	141.47	VL
5e*	Grus	■	0.78	1.91	55.31	62.80	120.80	LM
5e <sub>2</sub>		○	0.85	0.99	53.20	60.52	115.56	M
6b	C Horizon	□	4.68	1.83	74.34	43.12	123.97	LM
7*	Bedrock	▲	1.69	2.26	57.29	61.32	122.55	LM
7a*	Bedrock	▲	0.97	2.13	55.03	61.84	119.96	M
7c*	Bedrock	▲	0.71	2.37	61.34	59.48	123.90	LM
8	Horizon A	○	0.42	0.11	14.74	24.64	39.91	VH
8a	Horizon A	▲	0.99	1.47	65.17	59.64	127.27	L
9a	Horizon B	○	0.4	1.37	62.83	60.72	125.32	L
9b	Horizon C	□	1.09	1.31	62.74	56.80	121.92	LM
12a	Horizon A (Rb)	▲	0.07	0.81	46.6	61.44	108.92	H
12b	Grus	■	0.72	1.07	55.83	63.00	120.62	LM
13a*	Bedrock	▲	1.69	2.14	54.53	61.72	120.07	LM
13b*	Bedrock	▲	1.77	2.39	58.00	64.20	126.35	M
14	Grus	■	1.06	1.37	56.21	60.39	119.03	M
20a	Horizon A	○	0.40	0.78	30.60	57.49	89.27	H
20b	Horizon B	○	1.74	1.36	52.30	59.10	114.48	M
20c	Horizon C	□	2.42	2.12	51.06	54.82	110.42	M

Sample	Description	Symbol	Mg	Ca	Na	K	Weathering Index	Relative Degree of Alteration
20d	Horizon D	□	1.12	1.92	56.03	65.50	124.57	L
21	Bedrock	▲	0.79	1.14	60.57	61.70	124.19	L
22	Horizon C	□	2.68	1.69	59.15	51.90	115.40	LM
25	Horizon C	□	2.43	2.03	60.47	57.90	122.86	L
26b	Grus	■	2.37	0	51.28	62.12	115.76	LM
27	Grus	■	1.19	0.63	46.68	61.31	109.80	M
28a	Horizon A	○	3.96	1.02	45.14	51.34	101.46	MH
28b	Grus	■	1.33	0.56	49.55	62.10	113.54	LM
20b	Grus	■	0.93	1.19	54.03	59.68	115.80	LM
31a *	Bedrock	▲	1.11	2.54	67.94	64.68	136.27	VL
31b *	Bedrock	▲	1.16	2.41	54.66	65.36	128.58	L
31c *	Horizon C	□	2.26	1.38	63.54	51.24	118.42	L-M
			1.03	2.51	62.11	58.92	124.58	L
31d *	Horizon C	□	2.06	2.39	54.91	59.36	118.76	L-M
32b	Grus	■	0.92	0.92	73.95	60.88	136.66	VL-none

Table 5.

## Weathering Index

$$[x]_a / (x-0)_b^{\dagger} \text{ ratio}$$

## B. Pierce Mountain

Sample	Description	Symbol	Mg	Ca	Na	K	Weathering Index	Relative Degree of Alteration
Aa	Grus	△	0.867	0.934	49.53	55.96	107.29	M
Ab	Grus	△	0.534	0.074	49.59	58.58	108.78	M
Ac	Clay	○	1.374	0	111.08	37.48	149.93	VL-none
Ad <sub>1</sub>	Grus Clay	△	0.868	0.829	60.71	15.88	78.29	H
Ad <sub>1</sub> <sup>2</sup>	Grus Clay	△	0.528	0	69.95	16.80	87.28	H
Ad <sub>2</sub>	Grus Clay	△	0.874	0	47.60	29.13	77.61	H
Ae	Grus	△	0.666	0.037	44.71	60.03	105.45	M
Af	Grus R <sub>1</sub>	□	0.604	0.451	40.41	66.57	108.04	M
Ag*	R <sub>2</sub>	■	1.933	1.814	52.51	66.80	123.06	VL-none
Ba	Clay	○	1.844	0	0	65.07	66.92	VH
Bb	Grus	△	1.153	0	38.41	28.996	68.56	VH
Bc*	R <sub>1</sub>	□	1.1	1.386	56.03	30.36	88.86	H
C*	R <sub>1</sub>	□	1.41	0.757	0	31.48	133.65	VL-none
Da	Grus	△	1.20	0.453	51.93	52.67	106.26	M
Db	Clay	○	1.199	0	52.70	19.33	73.23	H
Dc*	R <sub>1</sub>	□	1.066	0.714	21.23	29.40	52.41	VH
35*	R <sub>2</sub>	■	0	2.9	66.71	58.60	128.21	VL-none

$\dagger [x]_a$  = atomic proportion of element x

$(x-0)$  = bonding strength of element x

clay pocket samples due to the high Na and/or K ratios. This would be the result of absorption of these ions into the "clay" of mica lattice.

The following ranges of weathering index were determined for samples from the Big Bald Mountain and Pierce Mountain areas:

A. Big Bald Mountain

<u>Sample</u>	<u>Weathering index range</u>
A horizon	39.92-101.47
B horizon	114.49-125.32
C horizon	110.43-128.59
Grus	109.81-136.67
Bedrock	119.97-141.48

B. Pierce Mountain

<u>Sample</u>	<u>Weathering index range</u>
Clay	73.23-149.93
( Grus	68.56-108.78
(	
( Regolith exfoliated bedrock	*52.41-108.04
Bedrock	123.06-128.21

\*except for sample C 33.65 anomaly

#### A. Big Bald Mountain

General inspection of the data reveal that the majority of the weathering index values are between 108-124. This indicates that the samples have not been significantly altered (i.e. relatively fresh) by hydrolysis. Three trends can be distinguished: (a) leached zone (A horizon samples have low values, i.e. generally less than 108); (b) B horizon, C horizon and grus samples have values close to or equalling fresh bedrock ranging from 110-136. The fact that the upper limit for each of these soil-disintegrated bedrock samples are essentially equal to the fresh bedrock value, indicates either the soil processes have not been effective in altering the rock, or the weathering index is not accounting for all the processes active in the disintegration/decomposition of the rock; (c) Bedrock samples generally have values above 120. Again because the bedrock and soil sample values overlap this suggests that chemical alteration is not the dominant process acting on these samples.

#### B. Pierce Mountain

Inspection of the weathering index values indicate that a much greater range of values is present at the Pierce Mountain site, indicating that the intensity of chemical

alteration is much greater here than the Big Bald Mountain area. Again three groups of values can be determined, but the subdivision is much more distinct.

(a) Samples with weathering index values in the 66-88 range. These include bedrock, clay and dominantly grus-clay samples. The occurrence of still lithified bedrock with such low values suggests that there is either hydrothermal alteration of the bedrock and/or inhomogeneity in the section. The fact that the grus samples have low values indicates that chemical alteration is an active process in the disintegration of the bedrock.

(b) Samples with weathering index values in the 105-108 range. Note the distinct separation between this group of samples with the previous samples. These samples are defined as grus or grus regolith samples. They represent samples which have been physically disintegrated but only moderately altered by chemical processes.

(c) Samples with weathering index values in the 123-133 range. They represent the fresh bedrock or slightly altered but still lithified bedrock samples. Note the similarity with the Big Bald Mountain bedrock samples.



It can be concluded that the weathering index does illustrate the intensity of chemical weathering at Pierce Mountain very well. It correlates, therefore, with the grain size or production of secondary minerals. A few anomalous values were observed however, which can be explained by:

(a) A strong depletion or leaching of ions in sample C (bedrock) or the bedrock never having these ions used in the index to any great extent, indicating inhomogeneity in the bedrock (e.g. this sample may respent or have within its matrix small quartz veinlets not distinguished in the field, due to alteration products coating the mineral).

(b) A strong adsorption of  $K^+$  and  $Na^+$  ions from some other source. For example, sample Ac may have been influenced by migrating ground waters rich in  $K^+$  and  $Na^+$  ions derived from weathering of the surrounding bedrock.

#### 4.3 Applications of weathering index

##### 4.3.1 Weathering index vs. depth

The weathering index was used to determine if there were any systematic changes in the weathering intensity with depth. Generally the amount of scatter was large for both

sites (Figure 43).

#### Big Bald Mountain

Due to the small deviation in the weathering index for the samples (i.e. between 110-130) any change in weathering intensity is hard to determine; however samples 20a, 20b, 20c and 20d (soil profile site) do show an increase in weathering index (i.e. approaching fresh rock) with depth. Thus in this case the weathering intensity seems to be related to degree of leaching in the soil profile.

#### Pierce Mountain

Since scatter of points is large there seems to be little correlation between depth and weathering intensity, except for the occurrence of fresh rock at the base of the section (sample 35). This may be taken as evidence of one of the following possible mechanisms of alteration:

- (1) hydrothermal alteration at or shortly after the time of emplacement of the granite intrusion.

This would be associated with volatile fluids migrating through the granite body altering the minerals in the process. The process need not alter the minerals immediately, but may make them more susceptible to chemical weathering when

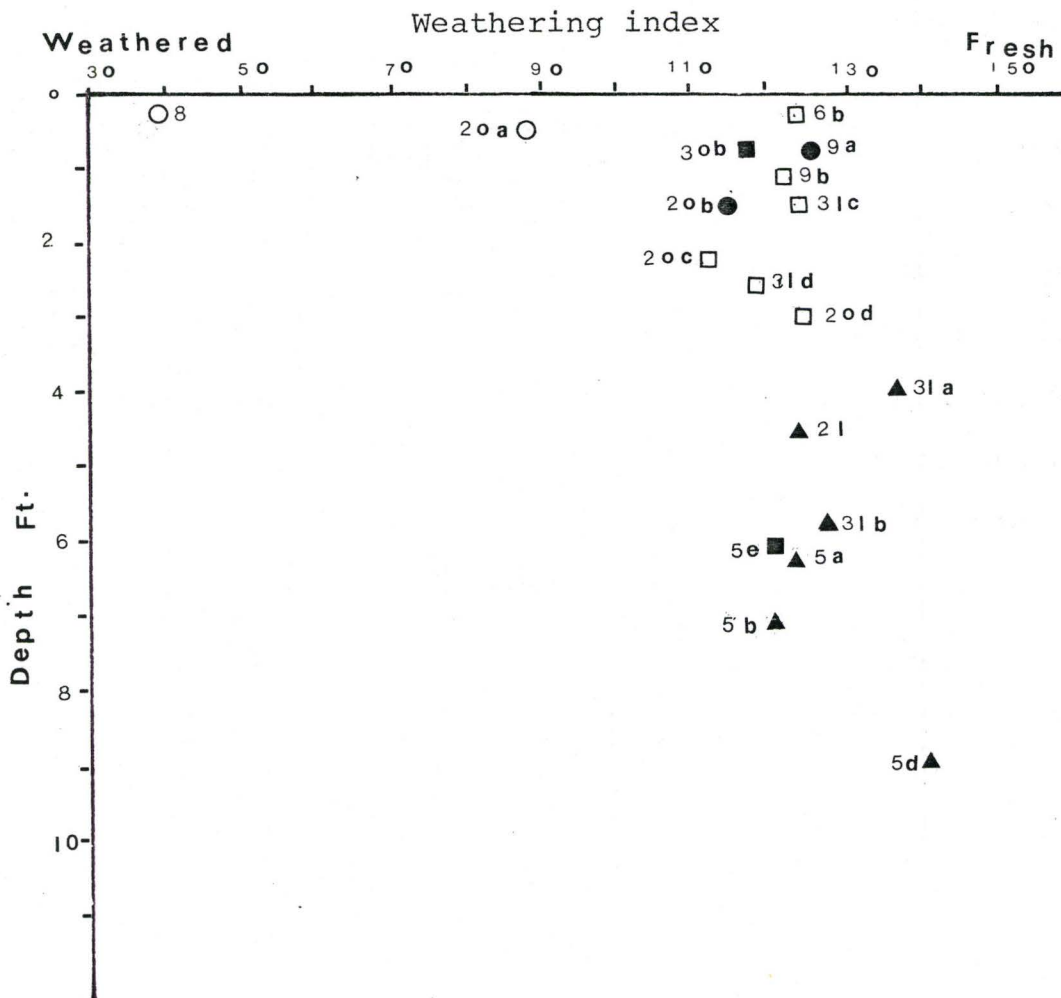


Figure 43A Depth vs. Weathering Index

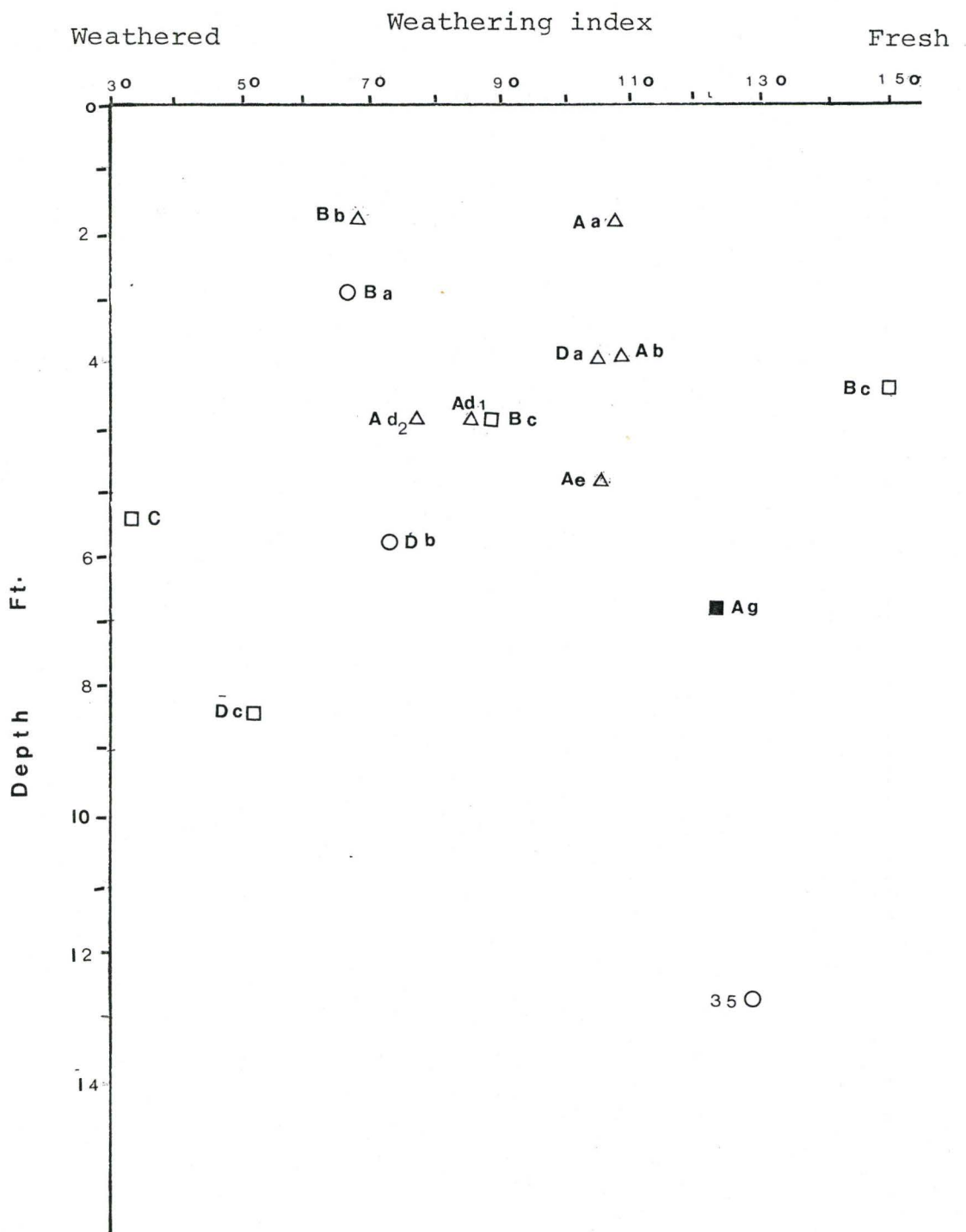


Figure 43B Depth vs. Weathering Index

exposed to the surface.

- (2) Metasomatic replacement of minerals possibly due to percolating ground waters migrating along jointing fractures.

#### 4.3.2

The relative mobilities of the cations in the weathering profile were determined by:

- (a) Graphing cation percentages with respect to weathering index for both sites. This method of displaying the data shows the quantitative variations in cation percent with greater intensity of weathering. However Pearce (1968) believes that such Harper diagrams may be misleading. He advocates the use of ratios to show the true variations between the components. The graphs for both sites for the major cations are illustrated in Figures 44A and 44B.

- (b) Calculating the ratio of  $[\text{Cation}/\text{Al}]_{\text{parent}}/[\text{Cation}/\text{Al}]_{\text{weathered}}$  and graphing this with respect to weathering index for each sample was also attempted to determine if there were any significant variations with the cation percent graph. Samples 31b and 35 were considered representative of fresh granite for Big Bald Mountain and Pierce Mountain,

respectively. This method assumes Al is constant in the weathering profile as suggested from the cation percent graph. Values of 1 for the above ratio illustrate that there has been no migration of the ion for the sample. Values less than 1 represent a net gain of the element and values greater than 1 represent a net loss of the element in the weathering profile. This method is better than the cation percent graph for illustrating the relative gains and losses in the sample for each element (Figs. 45A, 45B).

Both graphs essentially give the same information about the movement of cations in the weathering profile.

#### Big Bald Mountain

For this site the clustering of the weathering index values make the separation of the different soil-bedrock profiles difficult, but the following relationships can be distinguished.

Si - It can be seen that the bedrock samples are relatively stable with an increase in weathering intensity. Grus samples frequently show small net gain in Si, possibly due to the alteration of Ca plagioclase to clay minerals, thus depleting the sample of the mobile cation and concentrating Si. C horizon bedrock interface samples show a small net

depletion of Si or relatively stable concentrations of Si. This depletion of Si along the bedrock-soil horizon suggests this is an active zone in the weathering profile. Leached soil samples have a large net increase in Si due to the leaching of other cations and concentration of residual quartz.

Ti - A general trend of increased Ti with higher intensity of weathering is illustrated. Bedrock samples are relatively constant with a decrease in weathering index. There is an increase in Ti concentrations from grus to C horizon to leached soil profile samples, which show the greatest net gain of Ti.

Fe<sup>3+</sup> - Again bedrock samples are clustered in a finite range of Fe<sup>3+</sup> cation percents. Grus samples show a net depletion of Fe<sup>3+</sup> while C horizon samples have a net increase of Fe<sup>3+</sup> generally. Thus the distinction between grus and C horizon samples seems to be justified in this instance. Only one of the leached samples has a large depletion in Fe<sup>3+</sup>, the other samples have a net increase. This seems anomalous at first inspection, but could be explained by the fact that Fe<sup>3+</sup> is stable under most chemical weathering environments. The abundance of Fe in C horizon samples would be explained by the migration of Fe<sub>2</sub>O<sub>3</sub> colloids



to the bedrock-soil interface.

Al - For relatively fresh samples, including grus and bedrock, Al appears to be immobile. However more intensely weathered samples in the A, B and C soil horizons show some net depletion or gain of Al. This trend, however, is very approximate, as a direct correlation between weathering intensity and Al cation percent tends to cluster vertically.

Fe<sup>2+</sup> - No definite information could be gained due to scatter of data points.

Mg<sup>2+</sup> - The scatter of bedrock samples is quite large, but a general area of abundance can be defined. Grus samples are slightly depleted in Mg relative to bedrock. A group of bedrock samples which represent exfoliated samples has a near complete loss of Mg. Leached soil samples have a complete depletion of Mg. However one anomalous sample has a large gain which must be explained by influx of Mg from other sources (e.g. ground water percolation).

Ca - Even though weathering index values have a limited range, a distinct trend of Ca depletion from non-bedrock samples is found. C horizon samples have a relatively limited depletion. This slight anomaly may be the result of concentration of Ca in clays or carbonates along the bedrock-soil interface. Grus samples have a net loss of Ca as does A and B soil horizons. This could be



attributed to the preferential alteration of Ca rich plagioclase from the relatively fresh granite.

Na - Grus and bedrock samples are grouped in a definite range of Na cation percentages. This indicates that the albite or perthite feldspar is relatively fresh for the grus samples as suggested in the field description. Although the weathering index values are approximately the same as bedrock samples, C horizon samples have a net gain of Na cation percent. This could be accounted for by the inclusion of Na into the small percentage of clay produced. Again leached samples have a net depletion of Na from feldspars, mainly due to the higher intensity of chemical weathering.

K - Grus samples generally have a slightly lower weathering index than bedrock, but K cation percent is generally constant. Only a few leached horizon or bedrock-soil interface samples have a net depletion of K with or without a corresponding decrease in weathering index.

#### Summary

It is evident that even in the limited range of weathering index values for most of the samples that there are variations in cation abundance for the different samples in the weathering profile. However it is also evident that

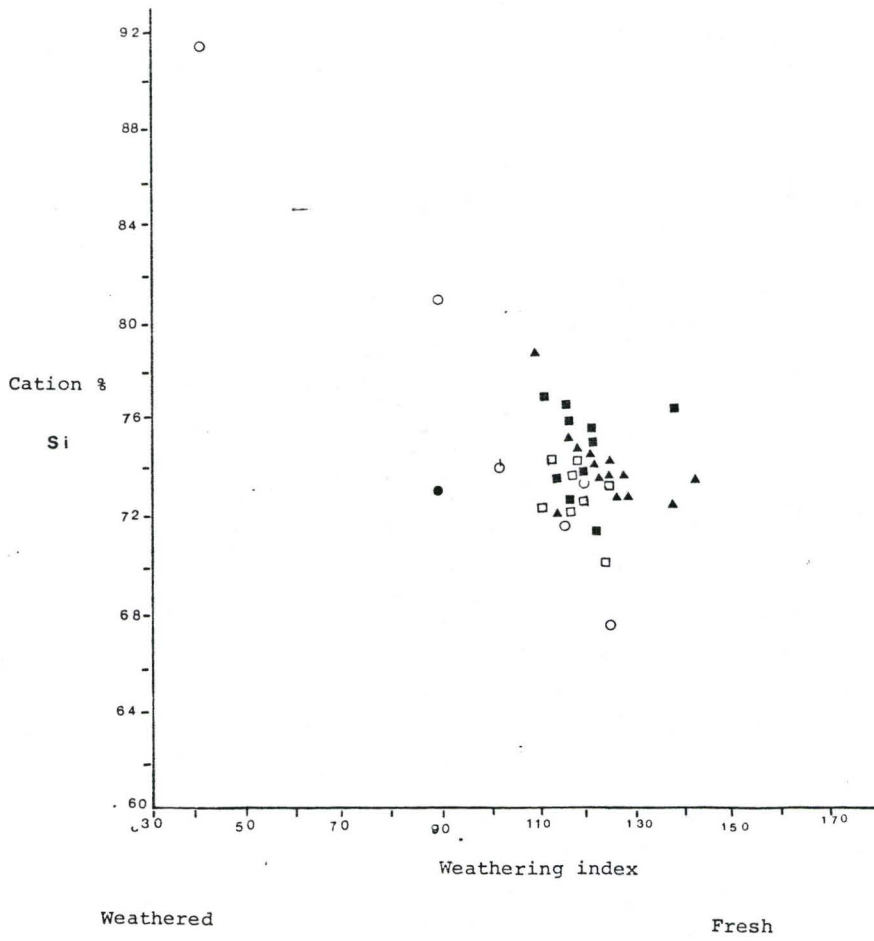
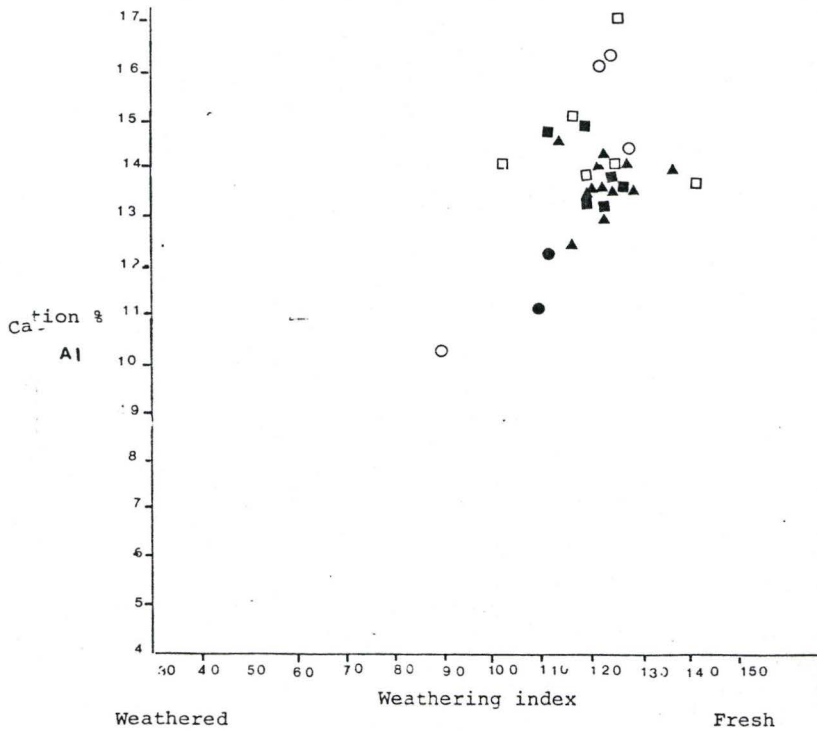


Figure 4 4 a Si % vs. Weathering Index



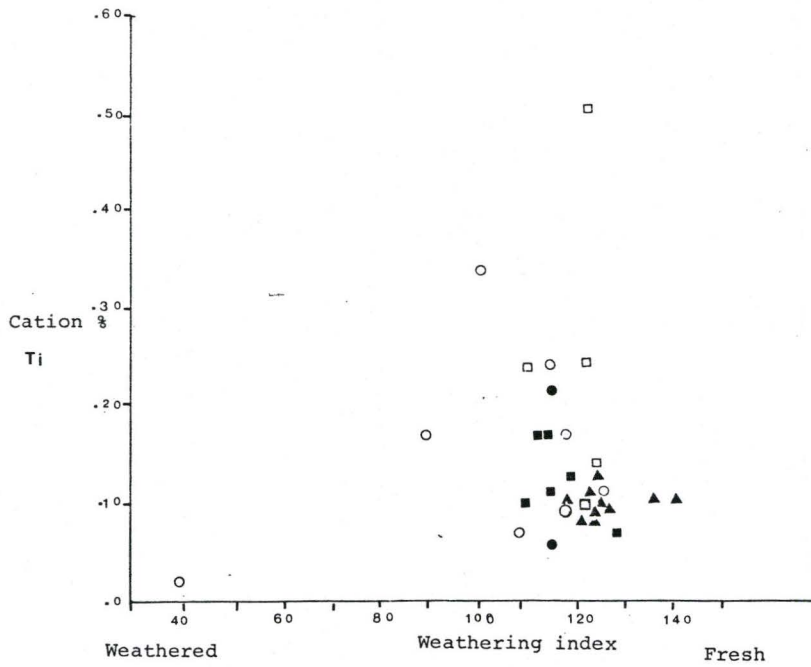


Figure 4 4 a Ti % vs. Weathering Index

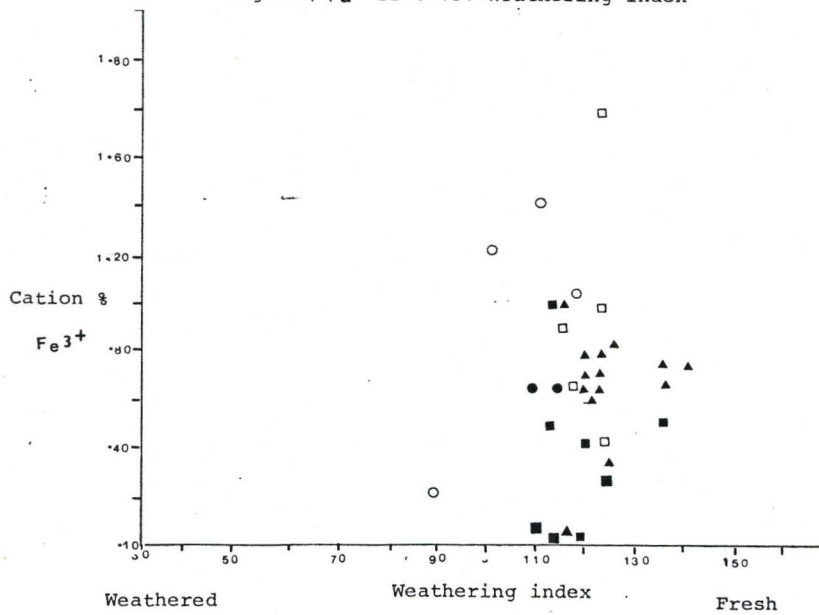


Figure 4 4 a Fe<sup>3+</sup> % vs. Weathering Index

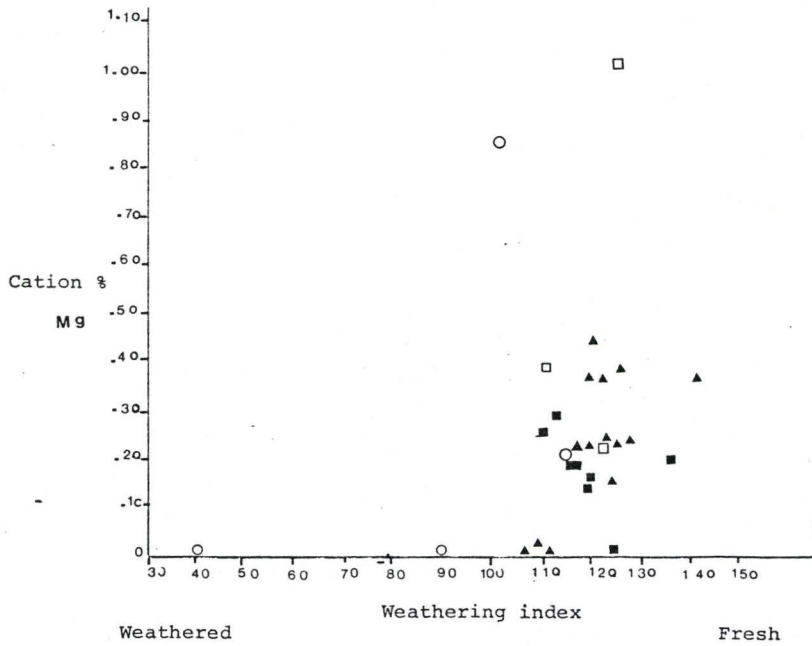


Figure 4 4 a Mg % vs. Weathering Index

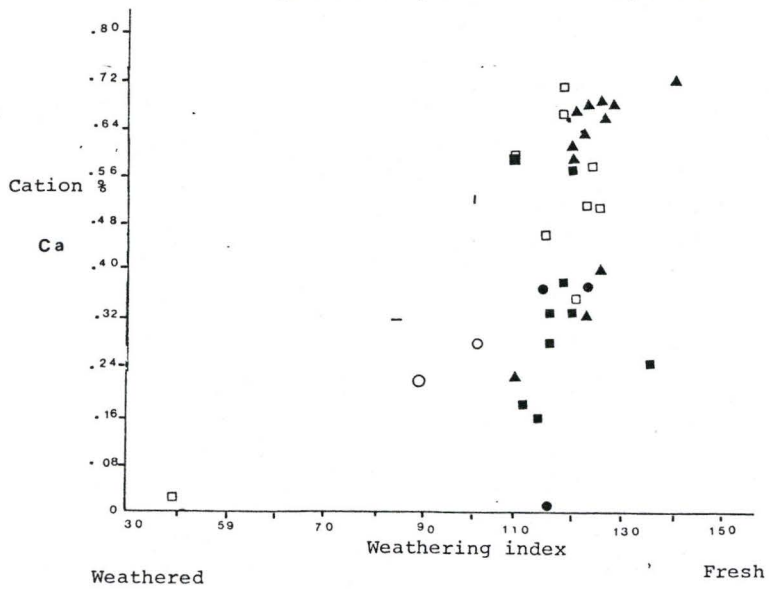


Figure 4 4 a Ca % vs. Weathering Index

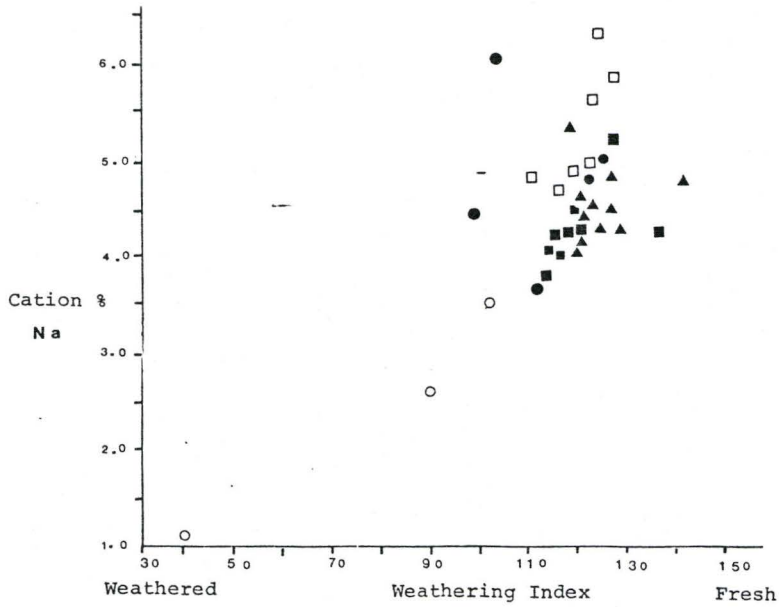


Figure 4.4a Na % vs. Weathering Index

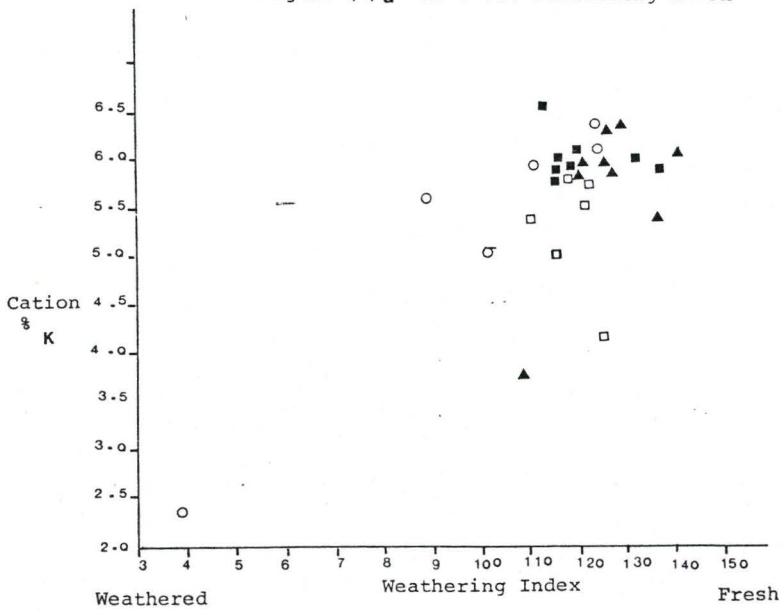


Figure 4.4a K % vs. Weathering Index

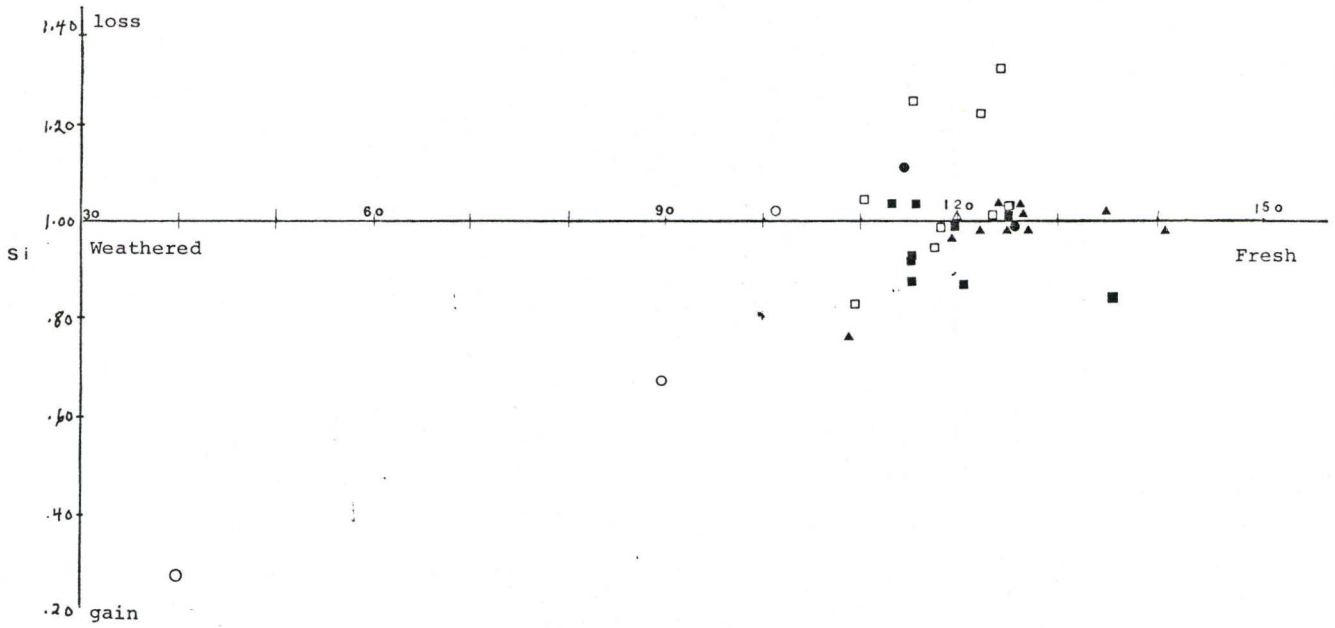


Figure 4 5 a.  $\frac{[Si]}{[Al]}$  parent/ $\frac{[Si]}{[Al]}$  weathered Cation % Ratio vs. Weathering Index

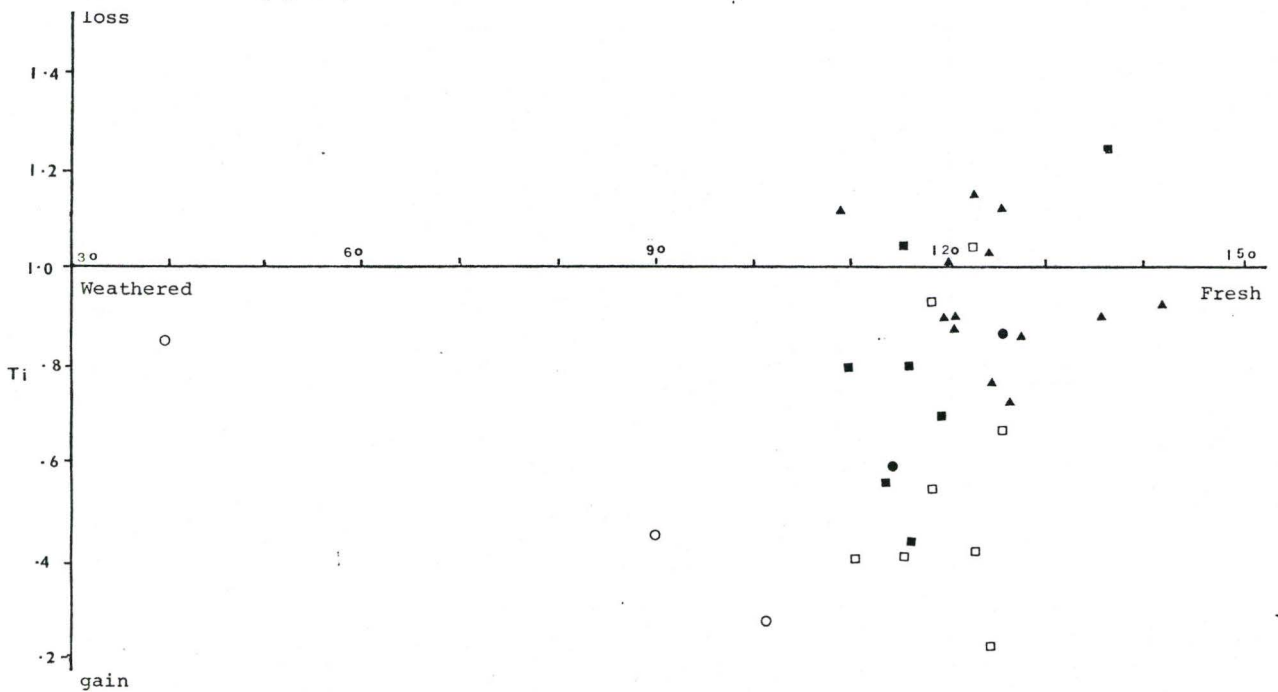


Figure 4 5 a.  $\frac{[Ti]}{[Al]}$  parent/ $\frac{[Ti]}{[Al]}$  weathered Cation % Ratio vs. Weathering Index

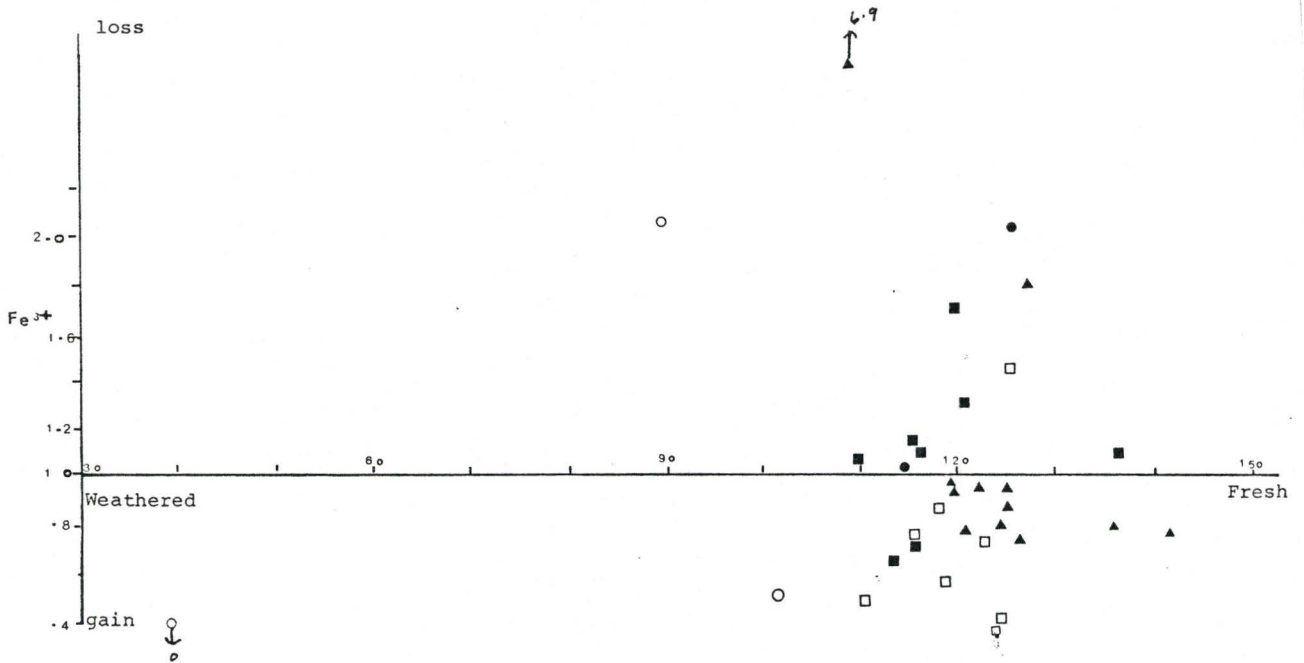


Figure 45 a  $\frac{[Fe^{3+}]_{parent}}{[Al]} / \frac{[Fe^{3+}]_{weathered}}{[Al]}$  Cation % Ratio vs. Weathering Index

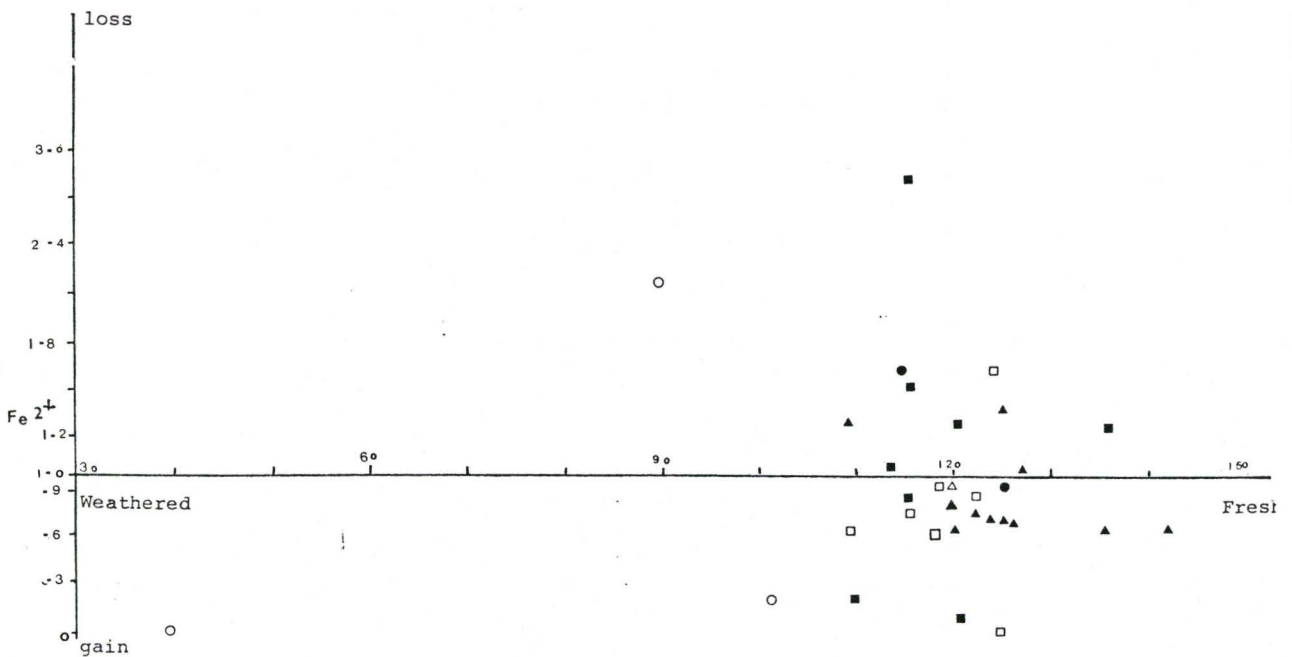


Figure 45 a  $\frac{[Fe^{2+}]_{parent}}{[Al]} / \frac{[Fe^{2+}]_{weathered}}{[Al]}$  Cation % Ratio vs. Weathering Index

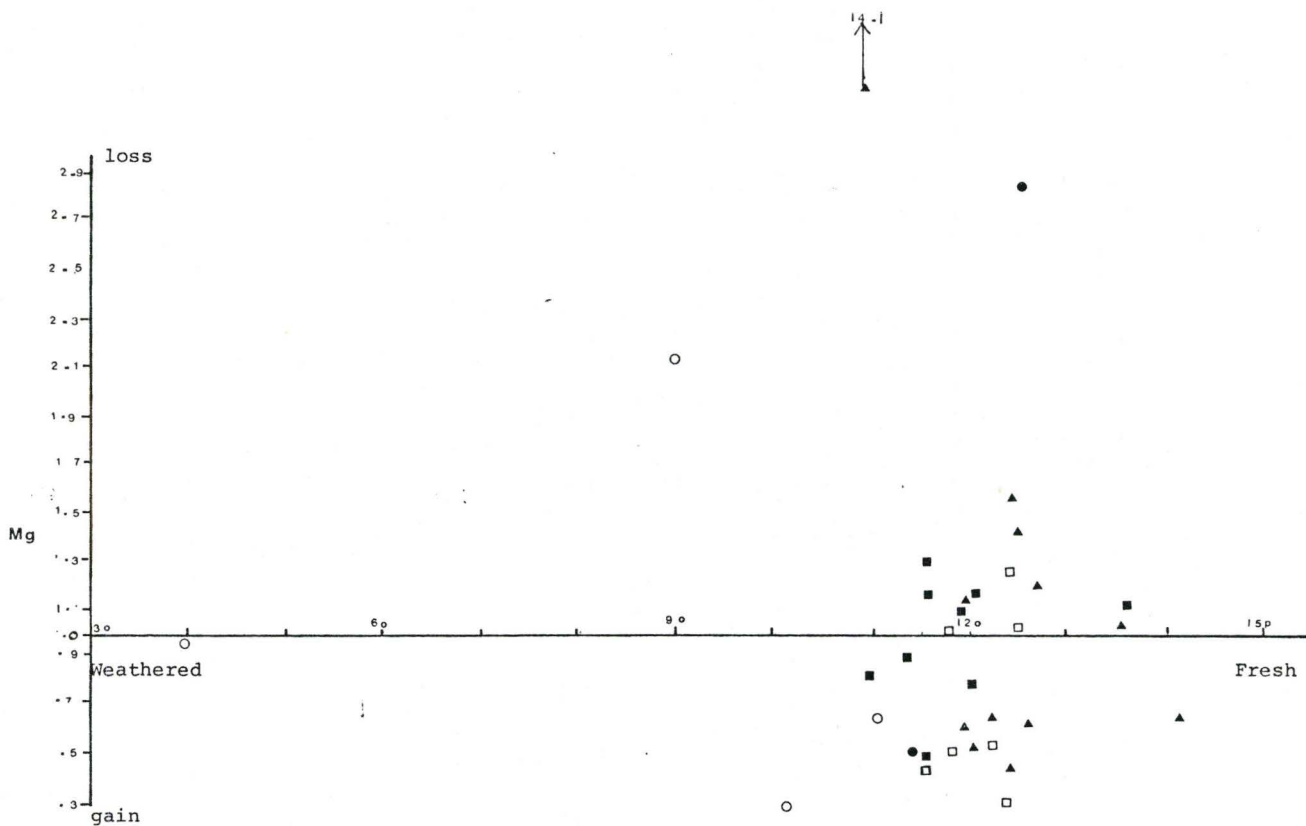


Figure 45a  $\frac{[Mg]}{[Al]}$  parent/ $\frac{[Mg]}{[Al]}$  weathered Cation % Ratio vs. Weathering Index

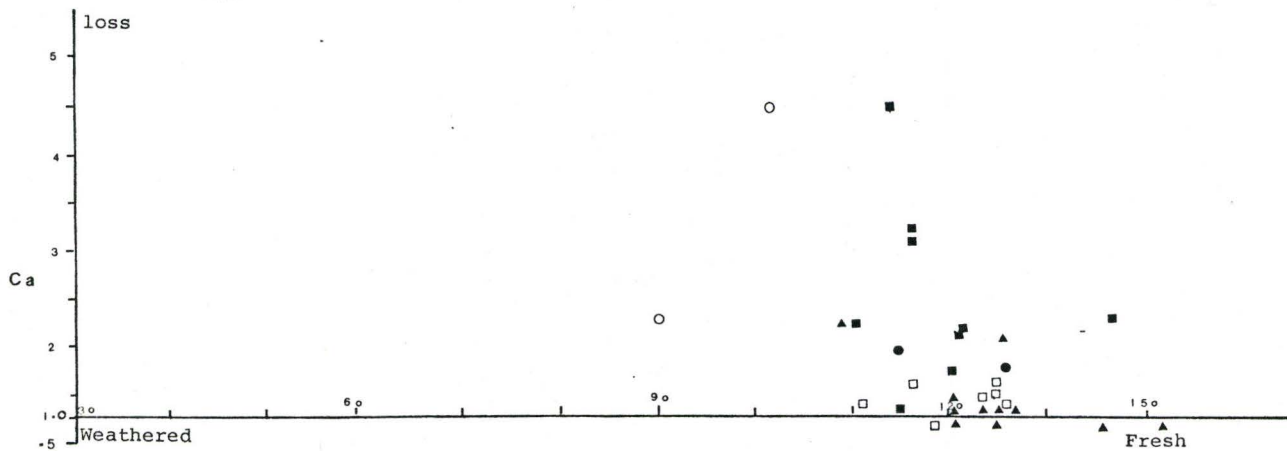


Figure 45a  $\frac{[Ca]}{[Al]}$  parent/ $\frac{[Ca]}{[Al]}$  weathered Cation % Ratio vs. Weathering Index



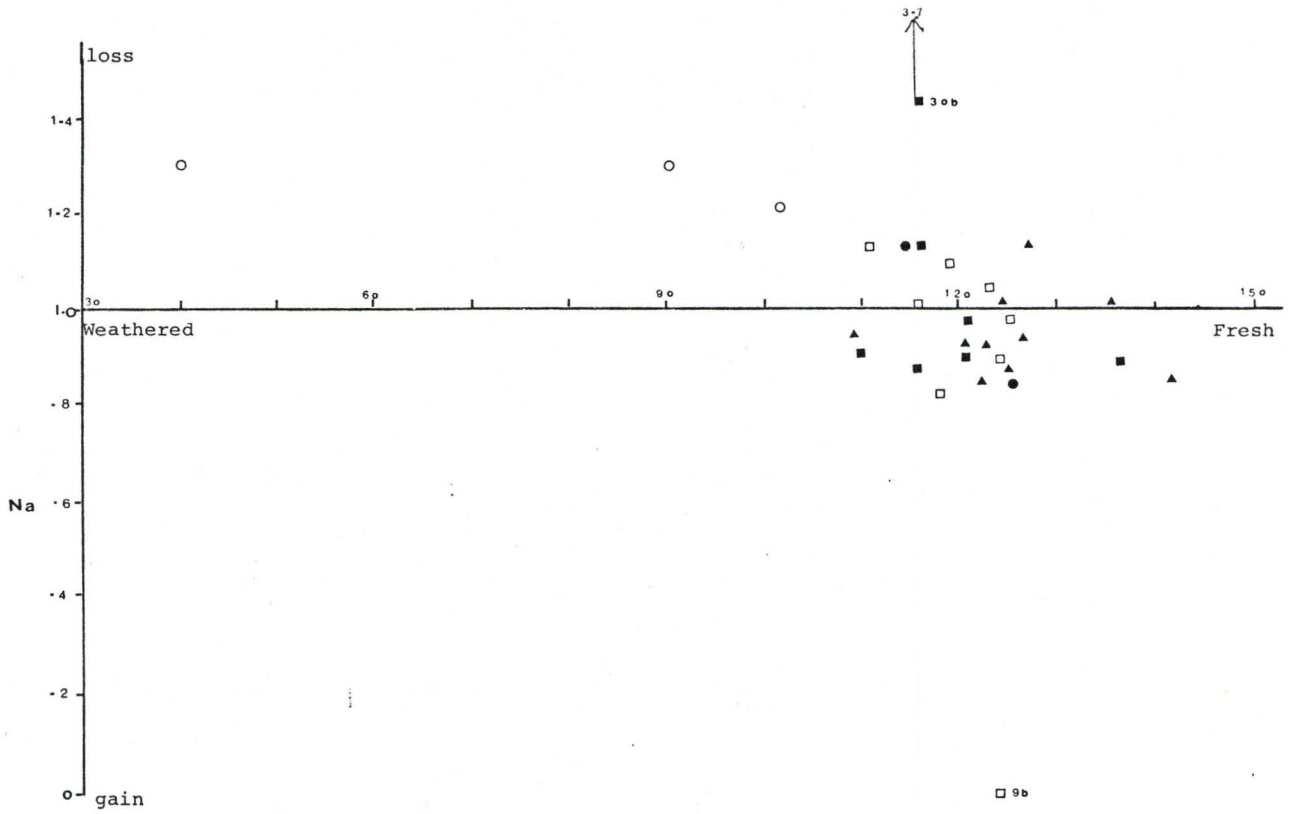


Figure 4 5 a  $\left[\frac{\text{Na}}{\text{Al}}\right]_{\text{parent}} / \left[\frac{\text{Na}}{\text{Al}}\right]_{\text{weathered}}$  Cation % Ratio vs. Weathering Index

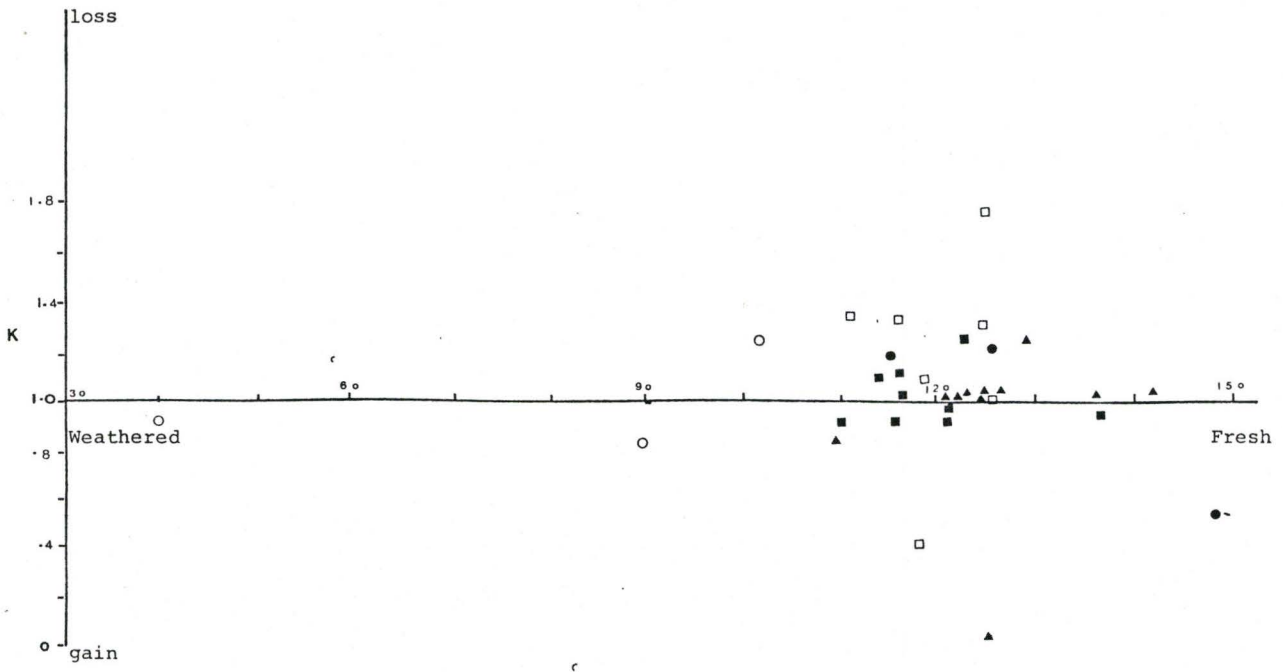


Figure 4 5 a  $\left[\frac{\text{K}}{\text{Al}}\right]_{\text{parent}} / \left[\frac{\text{K}}{\text{Al}}\right]_{\text{weathered}}$  Cation % Ratio vs. Weathering Index

only the most mobile cations, e.g. Ca, Mg, are significantly affected. As a generalization, it is also evident that leached and soil-bedrock interface samples have significant variations in cation percentages in the profile, while grus samples generally approximate bedrock sample cation percentages, thus indicating the relative freshness of the samples.

A weak trend of decreasing cation abundance with increasing weathering intensity is evident for the mobile elements Ca, Mg, Na, K. However this trend is interfered with by "clay" or mica minerals taking these cations into their structure. The migration of ions is related to the intensity of feldspar and/or biotite weathering which tends to be limited in most cases.

#### Pierce Mountain

There is a much greater range in the weathering index for this site, suggesting that chemical weathering processes are more important.

Si - Silica is relatively stable in the weathering profile (e.g. samples Ba and Ac are depleted in Si and bedrock; samples C and Dc are enriched in Si).

These variations may be the result of initial bedrock inhomogeneity prior to surface weathering. The majority

of the samples may be slightly enriched in Si with greater weathering intensity.

Al - The majority of the samples are stable with respect to Al. However clay samples Ba and Ac are enriched in Al, and bedrock-regolith samples C, Dc are depleted in Al. With the production of clay minerals one would expect a relative increase in Al.

Ti - Almost all the samples show an increase in Ti with decrease in weathering index. Regolith-grus samples are the least enriched, but clay pocket samples have larger increases in Ti. Sample Ag is anomalously high in Ti. This could be because sample Ag represents the bedrock-regolith interface, suggesting chemical weathering is intense at this site.

$Fe^{3+}$  - There is a general trend for  $Fe^{3+}$  to be depleted from the sample, except for samples below the colluvium and at the bedrock-regolith interface. Grus-clay samples tend to be abnormally depleted in  $Fe^{3+}$ . The above evidence suggests the following sequence of  $Fe^{3+}$  movement:

- (1) gain of  $Fe^{3+}$  from iron pan developing above the profile;
- (2) migration of  $Fe^{3+}$  possibly as colloids out of grus-clay samples;
- (3) slight reconcentration in clay pocket samples;

(4) deposition of  $\text{Fe}_2\text{O}_3$  at the soil-bedrock interface.

$\text{Fe}^{2+}$  - It is evident that the more intensely weathered samples (i.e. clay pocket and clay-grus samples) are completely depleted in  $\text{Fe}^{2+}$ , but some rock regolith samples are enriched in  $\text{Fe}^{2+}$ . The enrichment in  $\text{Fe}^{2+}$  may be the result of the element being used in the lattice of micas or chlorite produced in chemical weathering processes (i.e. from biotite).

$\text{Mn}^{2+}$  - Manganese is generally depleted in all samples, except those at the regolith-bedrock interface and those below the colluvium deposit. Samples representing regolith samples are only slightly depleted in Mn, while clay-grus, clay samples are completely devoid of Mn.

Mg - All the samples have greater Mg values than the fresh sample because the fresh sample has very low Mg abundance. This suggests that Mg has been brought into the weathering profile from another source. Clay samples are especially enriched in Mg. This may be the result of Mg being included in the clay structure or it may have been precipitated as an oxide along joint planes. Field evidence supports the second alternative.

Ca - Calcium has an intense depletion in the weathering profile. Only bedrock-regolith samples retain some Ca; the clay samples are completely depleted in Ca. Thus

in the production of secondary minerals from the feldspars all the Ca derived from the plagioclase is taken into solution and not incorporated into secondary mineral lattices.

Na - Again, bedrock regolith grus and anomalous samples C, Dc and Ac can be subdivided into distinct data point clusters. In general the samples are slightly depleted in sodium with increased weathering intensity. It is evident that the type of "clay" produced from feldspars will control the abundance of Na present. For example, sample Db is slightly enriched with respect to the regolith samples, but Ba is completely depleted in Na. This may be evidence of different ground water sources within the profile. Clay sample Ac is anomalously enriched in Na.

K - The majority of samples are depleted in K. However clay sample Ba and bedrock-interface samples are enriched in K, while regolith samples are only slightly depleted in K. The depletion of K is the result of hydrolysis of K feldspar where the cation is not taken into the clay structure. However, less altered samples are not depleted in K, indicating that even at relatively low weathering index values K feldspar is still stable.



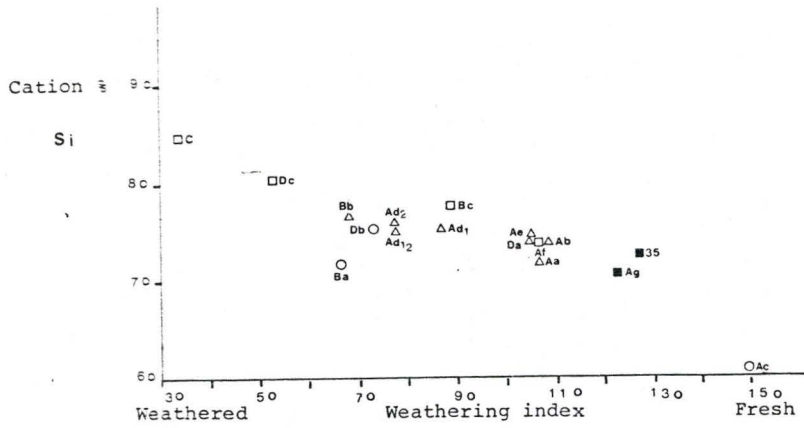


Figure 4 4 b Si % vs. Weathering Index

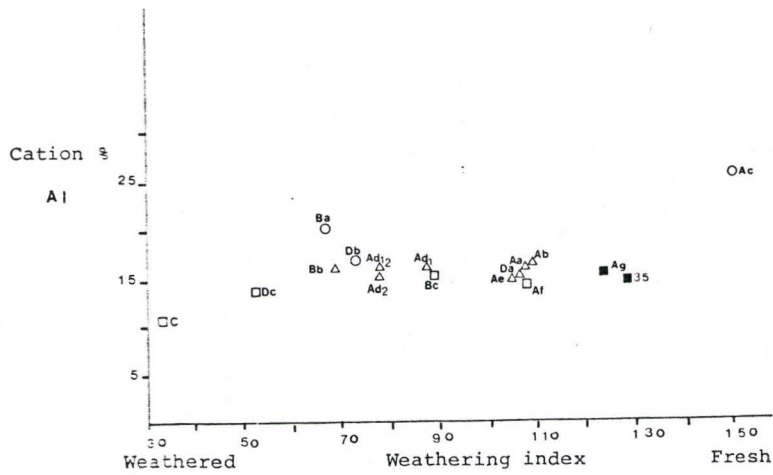


Figure 4 4 b Al % vs. Weathering Index

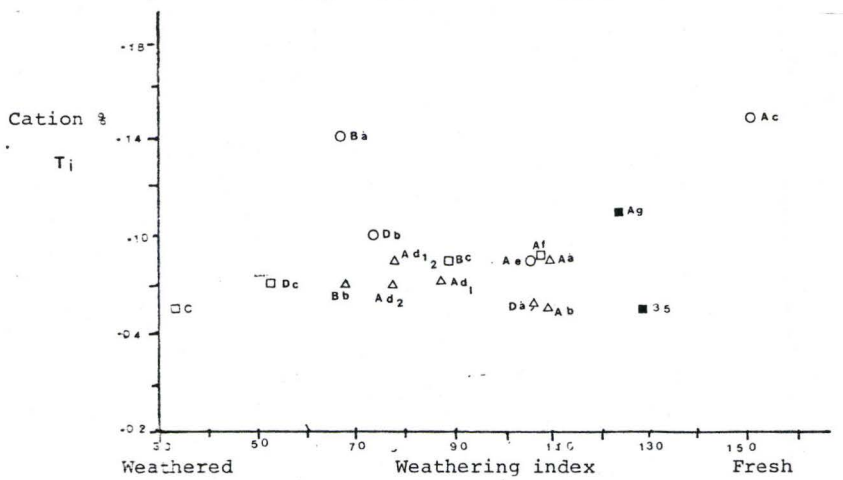


Figure 4 4 b Ti % vs. Weathering Index

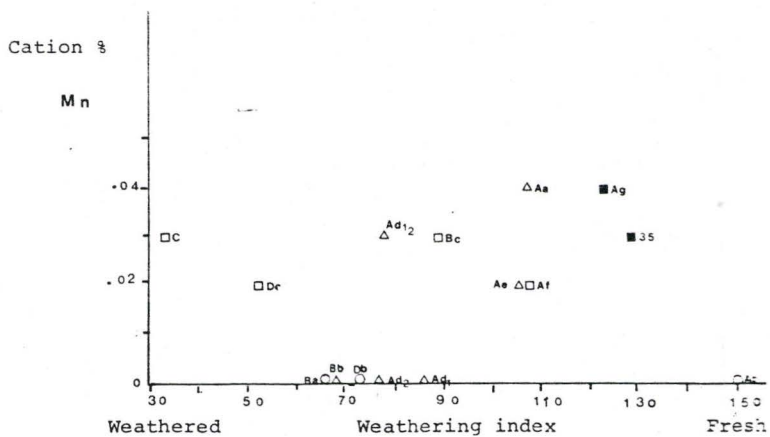


Figure 4.4 b Mn % vs. Weathering Index

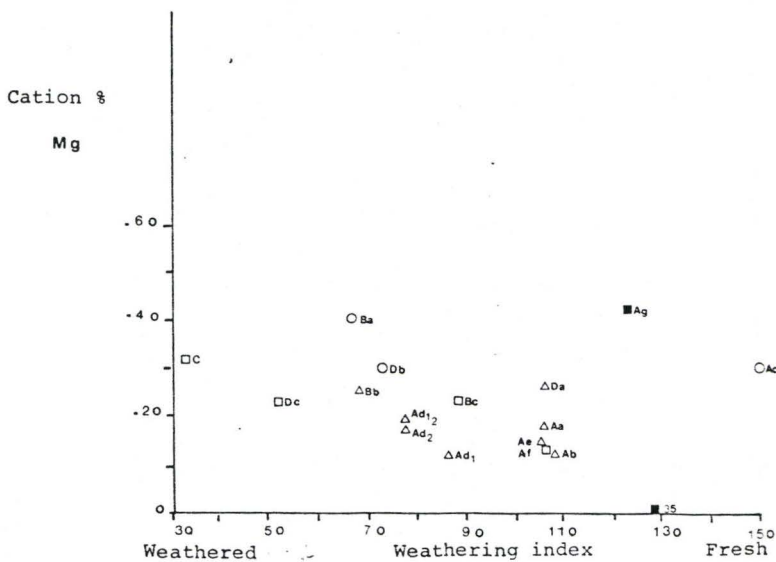


Figure 4.4 b Mg % vs. Weathering index

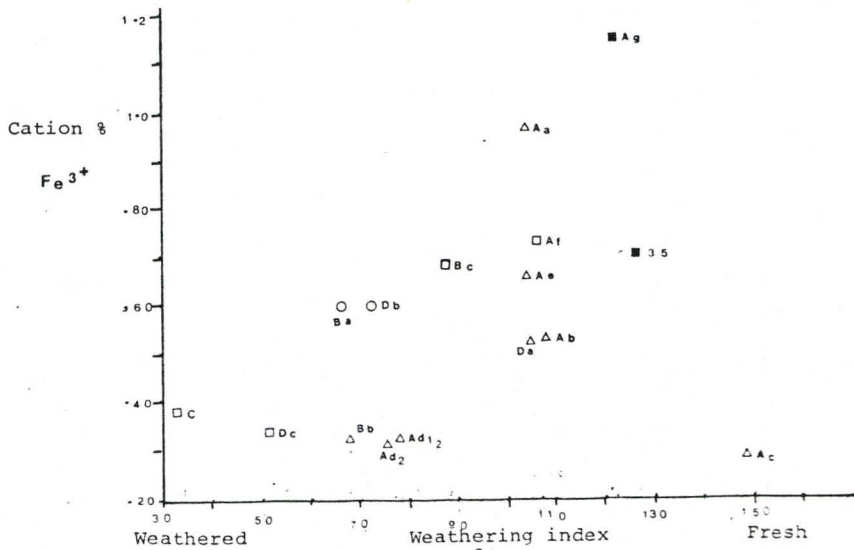


Figure 4.4 b Fe<sup>3+</sup> vs. Weathering Index

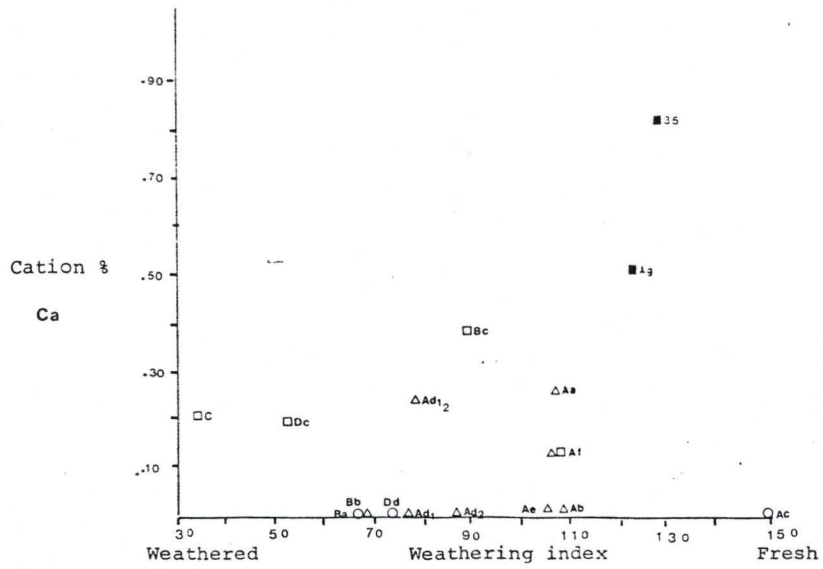


Figure 4 4 b Ca % vs. Weathering Index

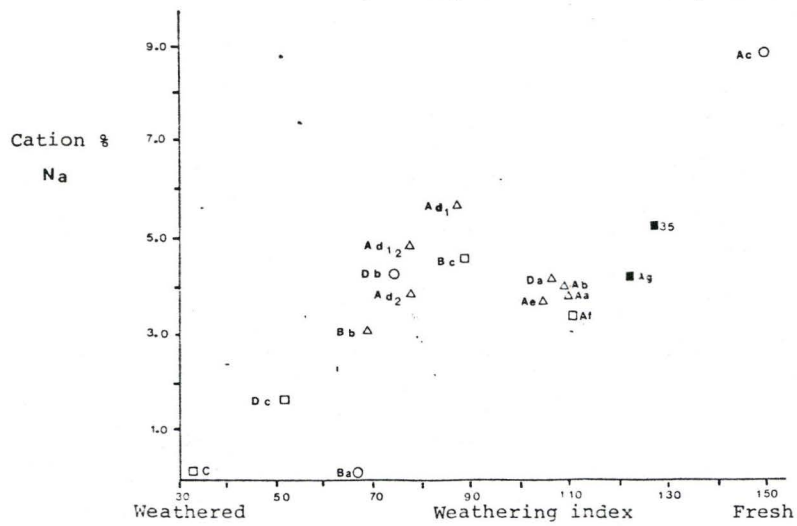


Figure 4 4 b Na % vs. Weathering Index



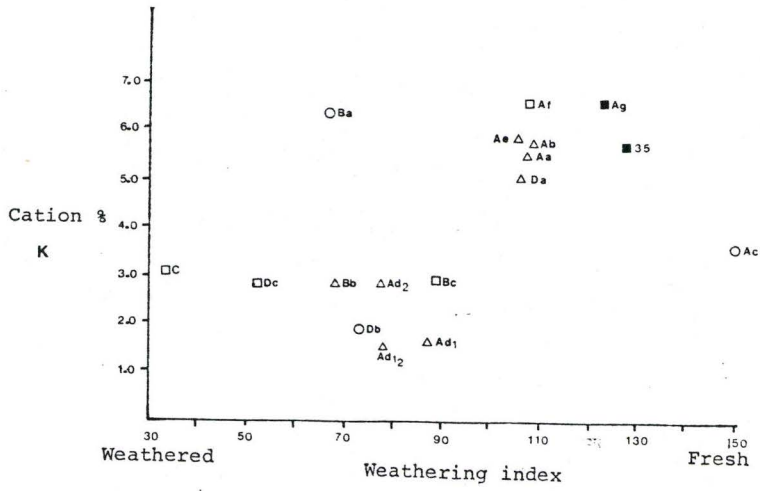


Figure 4 4 b K % vs. Weathering Index

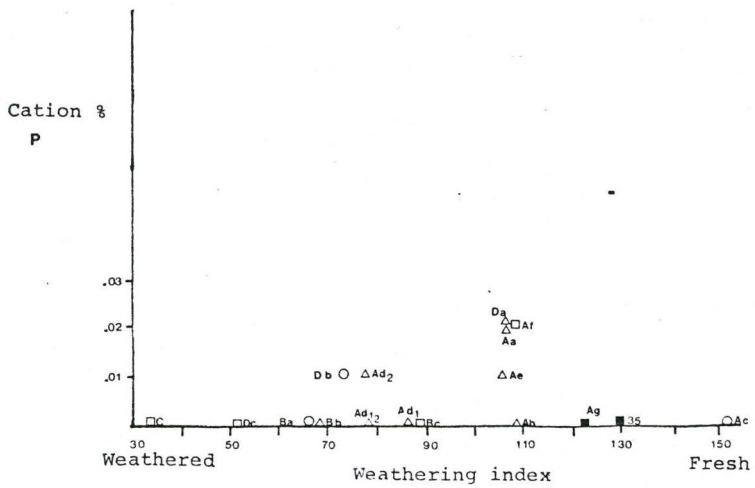


Figure 4 4 b P % vs. Weathering Index

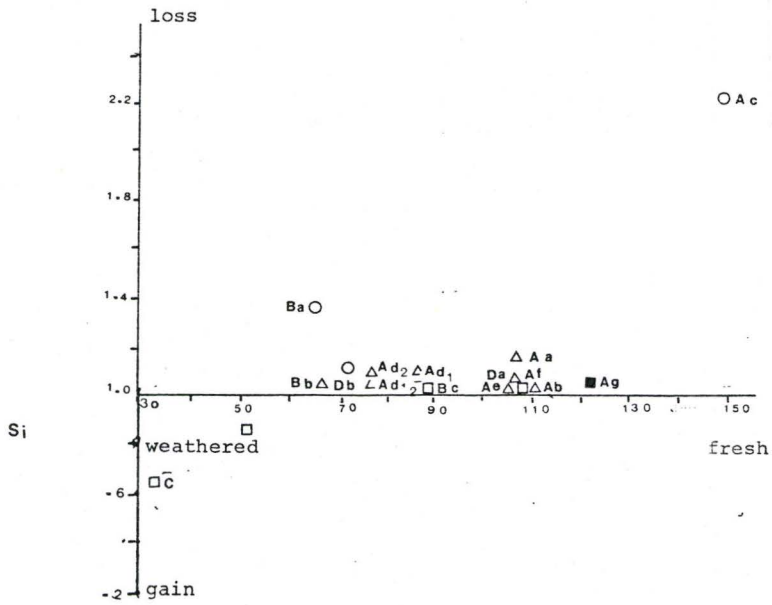


Figure 45b  $\left[\frac{Si}{Al}\right]_{parent} / \left[\frac{Si}{Al}\right]_{weathered}$  vs.  
Weathering Index

(B) Pierce Mountain

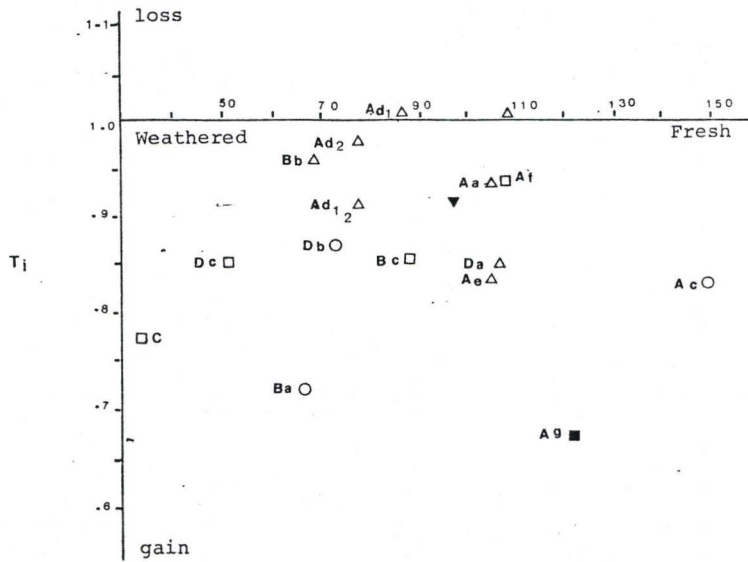


Figure 45b  $\left[\frac{Ti}{Al}\right]_{parent} / \left[\frac{Ti}{Al}\right]_{weathered}$  vs.  
Weathering Index

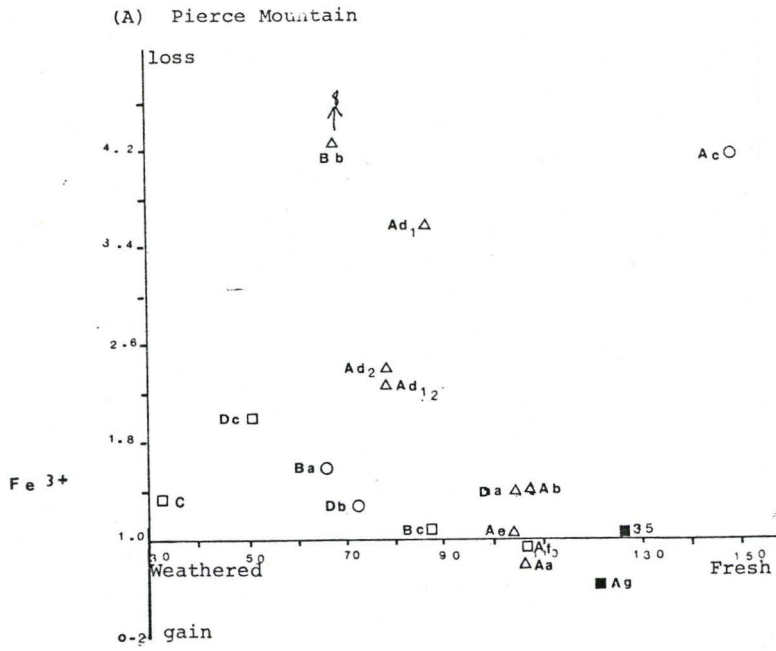


Figure 45 b  $\frac{[Fe^{3+}]_{parent}}{[Al^{3+}]_{parent}} / \frac{[Fe^{3+}]_{weathered}}{[Al^{3+}]_{weathered}}$  vs. Weathering Index

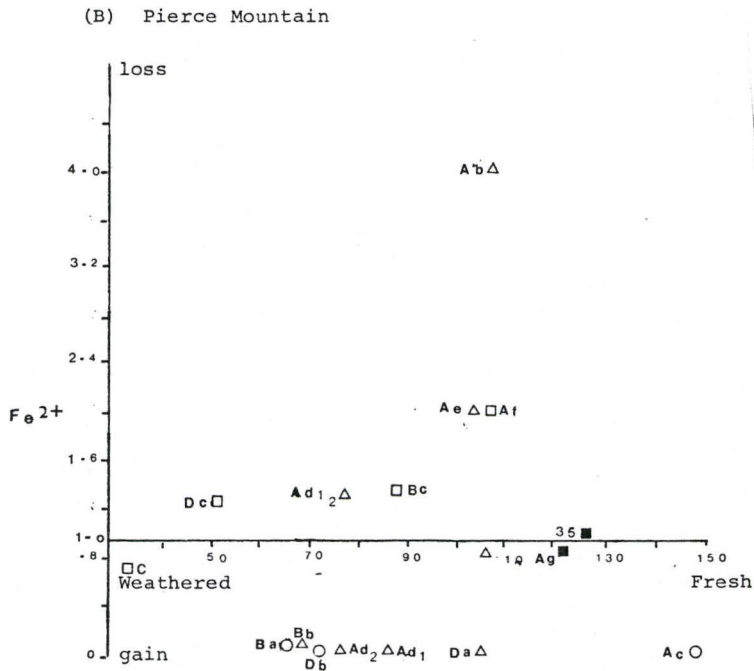


Figure 45 b  $\frac{[Fe^{2+}]_{parent}}{[Al^{2+}]_{parent}} / \frac{[Fe^{2+}]_{weathered}}{[Al^{2+}]_{weathered}}$  vs. Weathering Index

(B) Pierce Mountain

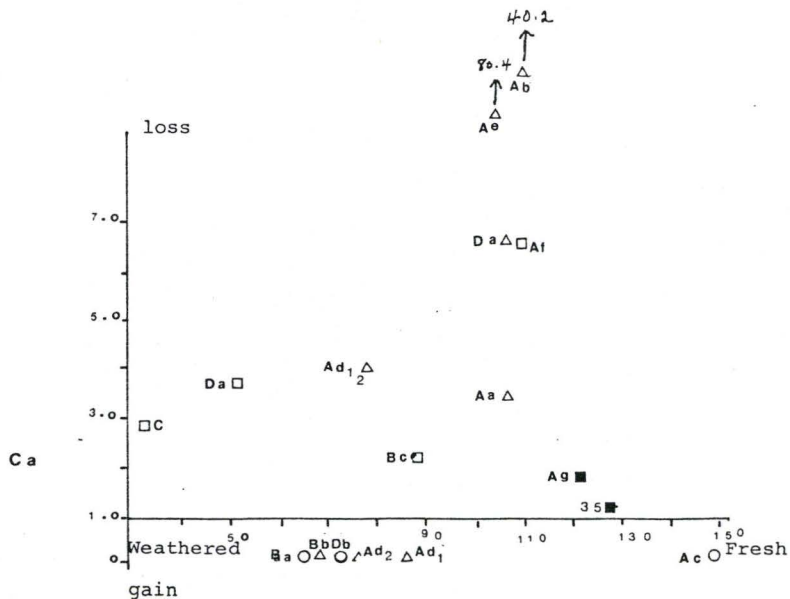


Figure 4 5 b  $\frac{[Ca]}{[Al]}$  parent /  $\frac{[Ca]}{[Al]}$  weathered

(B) Pierce Mountain

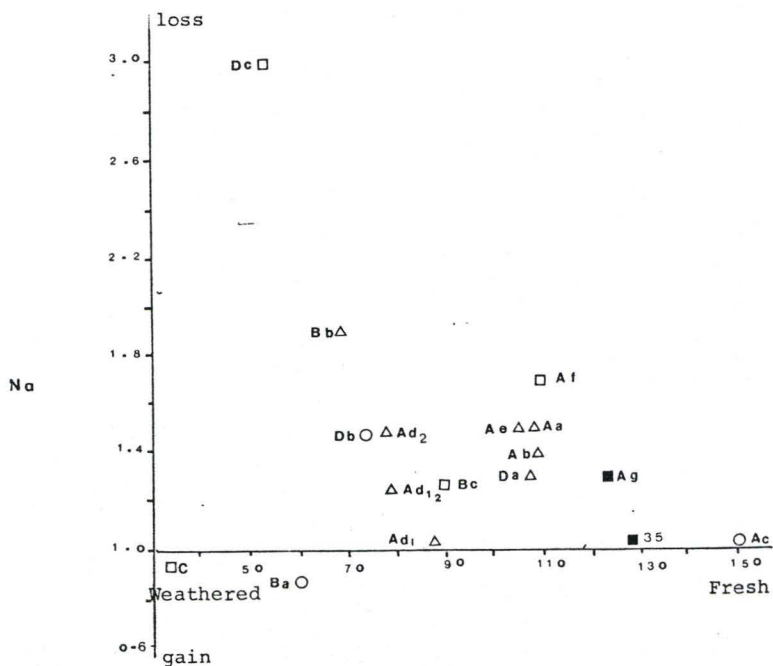


Figure 4 5 b  $\frac{[Na]}{[Al]}$  parent /  $\frac{[Na]}{[Al]}$  weathered vs. Weathering Index

(B) Pierce Mountain

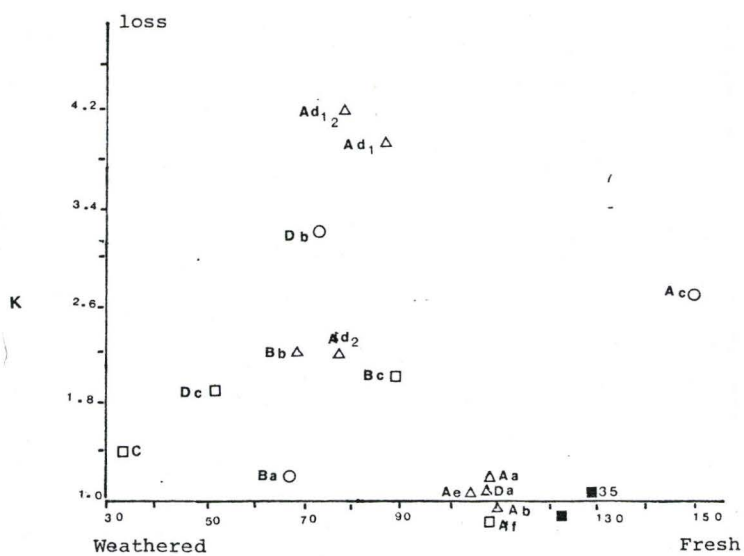


Figure 45b  $\frac{K}{Al}$  parent/ $\frac{K}{Al}$  weathered vs.  
Weathering Index

#### 4.4 Summary

Pierce Mountain samples have more variability between clay samples in comparison with leached soil horizon samples at Big Bald Mountain. This may be a function of differences in ground water ion concentrations altering the bedrock at Pierce Mountain, or initial inhomogeneity of the bedrock at Pierce Mountain.

The form of the sample (i.e. whether it is a clay or grus or regolith) is very important as an indicator of the mobility of an ion. This is shown by similar samples often making clusters of data points. Variations between these different samples can then be distinguished. Weathering index values are not as important because the mobile cations are frequently absorbed into secondary mineral structures. The depletion of many of the mobile cations demonstrated at Pierce Mountain were not in general evident at Big Bald Mountain, indicating that chemical alteration is more intense at Pierce Mountain.

Weathering versus fresh cation ratios were also determined for each element. The results are similar to those discussed previously, however. Appendix 4 tabulates the ratios and discusses the results.

As a generalization the geochemical evidence derived in this section tends to support evidence gained in the field and by other laboratory methods.

## CHAPTER V

## CONCLUSIONS

The following general conclusions can be made from the evidence presented.

(1) The physical disintegration/abrasion of the rock is of primary importance in determining the intensity of chemical weathering. This results in preferential weathering along zones of weakness (microfractures, unstable mineral assemblages, e.g. Ca plagioclase, twin and intergrowth lamella).

(2) It is the relative alteration of the feldspars that is of primary importance in granite weathering.

(3) The initial susceptibility of granite to weathering processes is dependent on the batholith geologic history. This would control the following parameters in the overall ability of weathering processes to alter the granite:

(a) relative time of emplacement which would in turn affect the mineral composition and grain size. It was found that the finer grain feldspars alter more readily than larger grains. It was also found that Goldich weathering index held true for both sites and seemed to be independent of physiochemical parameters. The following trend was found -

Ca feldspar < Na feldspar < K feldspar < muscovite < quartz;

(b) structures present in the granite such as the hierarchy of jointing discussed previously;

(c) pre-surface weathering alteration or weakening of mineral making them more susceptible to alteration. This factor is important because it prevents the estimation of the period of time required to produce the weathering profile.

(4) It is also evident that the chemical weathering end products do not depend on rock type but more general parameters such as climate, ground water composition, topography and several other parameters mentioned previously.



(5) The form, texture and physical condition of the bedrock and derived sediment directly reflect the intensity of weathering. This was found in grain size analyses where the following conclusions were made -

- (a) a sandy regolith (grus) is produced when chemical alteration is low to moderately intense. This results in a minor fining of sediments and major depletion of coarse fraction with increased alteration;
- (b) a clay regolith is produced when chemical alteration is intense. This eventually results in a major increase in clay silt and equal proportions of other grain sizes.

The geochemical trends discussed previously are related to the physical conditions of the weathered rock. Depending on weathering intensity and the ability of derived minerals to absorb cations from the ground water solution, the following cation mobility trend was found:

Ca(-) < Na(±) < Mg (±) < K < Al(±) = Fe (±) = Si (+) > Ti(+)  
 stability

Note that the above is a generalization since there

was much variability in cation migration with weathering intensity due to local conditions and position in weathering profile. Essentially the difference in chemical alteration between the two sites can be seen in the mobility of the cations. The following generalizations can be made:

Big Bald Mountain	$Ca < Na = Mg < K = Si = Al = Fe$
Pierce Mountain	$Ca < Mg < Na < K < Fe \approx Al \approx Si$

In conclusion, the Big Bald Mountain site is dominated by physical weathering processes such as jointing, possibly biotite expansion, which would allow kaolinization along cracks produced. Deep chemical alteration of the grains does not take place except in leached soil horizons and soil bedrock interfaces where chemical processes are active. Glaciation especially affected the Big Bald Mountain site by modifying weathering processes. The weathering profiles found are thought to be relics of former climate regimes. This may be supported by the presence of gibbsite in the weathering profile.

The Pierce Mountain site is likely to be closer to mineral phase equilibrium than the Big Bald Mountain site, due to the modifying effect of hydrothermal and/or metasomatic alteration.

Evidence for alteration processes other than surficial weathering include:

(1) Inhomogeneity in the section shown by colour variations, grain size anomalies, geochemical analyses, dispersion of data.

(2) Low weathering index values for bedrock.

(3) Concentration or depletion of cations not relating to the derived sediment physical properties.

(4) Variability of samples with depth with respect to geochemical and physical characteristics. There is strong evidence of lateral or down slope subsurface movement of ground water solutions.

It can be seen that the physical and chemical processes involved in rock weathering are intimately related and are dependent on a hierarchy of parameters, all of which must be determined with respect to their relative importance in producing the weathering profile.

## REFERENCES

- ALCOCK, F.J., 1935. Geology of Chaleur Bay region. Geol. Surv. Can., Mem. 183.
- ANDERSON, F.D., 1968. Woodstock, Melville and Coldstream map areas. Geol. Surv. Can., Mem. 353.
- ANDERSON, F.D., 1970. Geol. Surv. Can. Map 1220A.
- AUGUSTITHIS, S.S., 1973. Atlas of the Textural Patterns of Granite, Gneisses and Associated Rock Types. Elsevier Pub. Co., Amsterdam.
- BARTH, T.F.W., 1959. Principles of classification and norm calculations of metamorphic rocks. Jour. Geol., 67, 135-151.
- BIRKLAND, P.W., 1969. Quaternary paleoclimatic implications of fossil clay. Mineral distribution in a Sierra Nevada-Great Basin transect. Jour. Geol., 77, 289-302.
- BIRKLAND, P.W., 1974. Pedology, Weathering, and Geomorphological Research. Oxford Univ. Press, London, 285p.
- BLACK, L.A., EVANS, D.D., WHITE, J.L., ENSMINGER, L.E. and CLARK, F.E., 1965. Methods of Soil Analysis (Part 1). Am. Soc. Agronomy, Inc., Madison, Wisconsin.

- BLACKWELDER, E., 1927. Fire as an agent in rock weathering. Jour. Geol., 35, 134-140.
- BLATT, H., MIDDLETON, G.V. and MURRAY, R., 1972. The Origin of Sedimentary Rocks. Prentice-Hall, Inc., N.J., 634p.
- BLAXLAND, A.B., 1974. Geochim. Cosmochim. Acta, 38, 843-852.
- BOOS, M.F., 1937. Influence of primary structures on granite weathering. Abstr., Geol. Soc. Amer. Proc. No. 1936.
- BROWN, G., 1961. The X-ray Identification and Crystal Structures of Clay Soil. Mineralogical Society, London.
- BUSTIN, R.M. and MATHEWS, W.H., 1979. Selective weathering on granitic clasts. Univ. B.C., Dept. Geol. Sci.
- CARROLL, D., 1960. Rock Weathering. Plenum Press, N.Y., 203p.
- CHAPMAN, C.A. and RIOUX, R.L., 1958. Statistical study of topography, sheeting and jointing in granites, Acadia National Park, Maine. Am. Jour. Sci., 256, 111-127.
- CHAPMAN, R., 1898. Pre-glacial decay of rocks. Amer. Jour. Sci., Ser. 4., 5, 280.

- CHESWORTH, W., 1957. The origin of certain granitic rocks occurring in Glamorgan Township, S.E. Ontario. Ph.D. Thesis, McMaster Univ.
- CLEMONT, P. and DE KEMPE, C.R., 1977. Geomorphological conditions of gabbro weathering at Mount Megantic, Quebec. Can. J. Earth Sci., 14, 10, 2262-2273.
- DAVIES, J.L., 1972. Map - Geology of the Bathurst-Newcastle area, N.B.
- DERBYSHIRE, E., 1976. Geomorphology and Climate. Wiley and Sons, Inc., N.Y.
- DICKSON, M., 1974. The sieve method of size analysis. Tech. Memo 74-3, McMaster Univ.
- EGGLER, D.H., LARSON, E.E. and BRADLEY, W.C., 1969. Am. Jour. Sci., 267, 510-522.
- FOLK, R.L., 1966. A review of grain size parameters. Sedimentology, 6, 73-93.
- FREININGER, T., 1971. U.S. Geol. Surv. Prof. Paper 750-C, C65-C81.
- GEOLOGICAL SURVEY OF CANADA, 1960. Paper 60-15, Bulletin 149.
- GRANT, W.H., 1969. Abrasion pH, An index of chemical weathering. Clays and Clay Minerals, 17, 151-155.

GOLDICH, S.S., 1938. Jour. Geol., 46, 17-58.

GREINER, H.R., 1970. Geology of the Charls area, Restigouche Co., N.B. Min. Res. Branch, N.B. Dept. Nat. Res., Map Series 70-2.

HAMILTON, J.D., 1968. Information Circular, Dept. Nat. Res., Mineral Resources Branch.

HARRISS, R.C. and ADAMS, J.A.S., 1966. Geochemical and Mineralogical studies on the weathering of granitic rocks. Amer. Jour. Sci., 264, 146-173.

HELMSTAEDT, H., 1970. Structural geology of Portage Lakes areas, Bathurst Newcastle District, N.B. Geol. Surv. Can. Paper, 70-78.

INMAN, D.L., 1952. Jour. Geol. Pet., 22, 125-145.

ISHERWOOD, D. and STREET, A., 1976. Biotite-induced grossification of the Boulder Creek granodiorite, Boulder Co., Colorado. Geol. Soc. Amer. Bull., 87, 366-370.

I.U.G.S., 1973. Geotimes, October.

JAHN, ., 1976. In Progress in Geomorphology - Essays in Honour of David L. Linton, E.H. Brown and R.S. Waters. Inst. Brit. Geog. Spec. Pub., 7, 53-61.

- KELLER, W.D., 1957. The Principles of Chemical Weathering.  
Lucas Bros., Columbia, Mo., 110p.
- KETTLEMAN, L.R. Jr., 1964. Jour. Sed. Pet., 34, 483-  
502.
- KRAUSKOPF, K.B., 1967. Introduction to Geochemistry.  
McGraw-Hill, Co., N.Y., 721p.
- KONTA, J., 1969. Proc. International Clay Conf., 281-290.
- KRAMER, J.R., 19 . Mineral-water equilibria in silicate  
weathering. Int. Geol. Congr., 5, 149-160.
- LOUGHNAN, F.C., 1962. Some considerations in the weathering  
of the silicate minerals. Jour. Sed. Pet., 32,  
284-290.
- MARTIN, R.F., 1966. A chemical and petrographic study of  
granitic rocks of New Brunswick, Canada. M.Sc.  
Thesis, Penn. State Univ., University Park.
- MARTIN, R.F., 1970. Petrogenetic and tectonic implications  
of two contrasting Devonian batholithic associations  
in New Brunswick, Canada. Amer. Jour. Sci., 268,  
309-321.
- McALLISTER, A.L. and LAMARCHE, R.Y., 19 . Mineral deposits  
of Southern Quebec and New Brunswick. Excursion  
A58-C58. 24th Int. Geol. Congr.



- McCONNELL, D., 1961. Mechanism of weathering. Bull. Geol. Soc. Amer., 62, 700-701.
- McEWEN, M.C., FESSENDEN, F.W. and ROGERS, J.J.W., 1959. Jour. Sed. Pet., 29, 477-492.
- MEUNIER, A. and VELDE, B., 1976. Mineral reactions of grain contacts in early stages of granite weathering. Clay and Clay Minerals, 11, 235-239.
- MOORHOUSE, W.W., 1959. The Study of Rocks in Thin Section. Harper and Row, N.Y., 514p.
- OEN, I.S., 1965. Zeitschrift für Geomorphologie N.F., 9, 285-304. In Thomas, 1976.
- PARKER, A., 1970. An index of weathering for silicate rocks. Geo. Mag., 501-504.
- PEARCE, T.H., 1968. Contrib. Mineral. and Petrol., 19, 142-157.
- POOLE, W.H. and RODGERS, J., 1972. Field excursion A63-C63. Int. Geol. Congr., 29th Session, 28-29.
- POOLE, W.H., 1960. Geol. Surv. Can., Paper 60-15.
- RICE, A., 1976. Insolation named over Geology.
- RICE, C.M., 1974. Chemical weathering on the Carnmenellis granite. Mineral. Mag., 39, 304, 429-447.

- ROSE, B., ANDERSON, F.D., GREENSHIELDS, R.A., JOHNSTON,  
MacGREGOR, I.D., 1962. Tabeguque Map Sheet 210. Prelim.  
Map Series 37.
- RUXTON, B.P., 1968. Measures of the degree of chemical  
weathering of rocks. Jour. Geol., 76, 518-527.
- SHAW, E.W., 1935. Little S.W. Miramichi-Sevogle Rivers  
area, N.B. Geol. Surv. Can., Memoir 197.
- SKINNER, R., 1974. Geology of the Telagouche Lakes,  
Bathurst and Nepisiguit Falls map areas. Geol. Surv.  
Can., Memoir 371.
- SMITH, C.H., 1973. California Lake. Geol. Surv. Can., Map  
1341A.
- STEITA, D., 1976. The Geography of Soils. Prentice Hall,  
Inc., N.J.
- SUGDEN, D. and JOHN, ., 1976. Glaciers and Landscape.  
Edward Arnold Ltd., London.
- SUGDEN, D.E. and WATTS, S.H., 1977. Tors, felsenmeer and  
glaciation in northern Cumberland Peninsula, Baffin  
Island. Can. J. Earth Sci., 14, 2817-2823.
- TARDY, Y., 1971. Characterization of the principal weather-  
ing types by the geochemistry of waters from some  
European and African crystalline massifs. Chem.  
Geol., 7, 253-271.

- TARDY, Y., BOCQUIN, G., PAQUET, H. and MILLOT, G., 1973.  
Formation of clay from granite and its distribution  
in relation to climate and topography. *Geoderma*,  
10, 271-284.
- THOMAS, M.F., 1976. In *Geomorphology and Climate*,  
E. Derbyshire, ed. John Wiley and Sons N.Y.
- TORRENT, J. and BENAYOS, J., 1977. Origin of gibbsite in  
a weathering profile from granite in West Central  
Spain. *Geoderma*, 37-49.
- TODD, W.T., 1968. Paleoclimatology and the relative  
stability of feldspar minerals under atmospheric  
conditions. *Jour. Sed. Pet.*, 38, 832-844.
- TUPPER, W.M. and HART, S.R., 1961. Minimum age of the  
Middle Silurian in New Brunswick based on K-Ar  
method. *Geol. Soc. Amer. Bull.*, 72, 1285-1288.
- TWIDAL, C.R. and BOURNE, J.A., 1976. The shaping and  
interpretation of large residual granite boulders.  
*Geol. Soc. Austr.*, 23, 371-381.
- VAN WARNBEKE, A.R., 1962. Criteria for classifying tropical  
soils by age. *Jour. Soil Sci.*, 13, 124-132.
- VERMIERE, R., 1967. Tech. Memo 67-9. McMaster Univ.
- WHITE, W.A., 1945. *Jour. Geol.*, 53, 276-282.

WILLIAMS, H., TURNER, F.J. and GILBERT, C.M., 1954.

Petrography. W.H. Freeman and Co., San Francisco.

WINKLER, H.G.F. and VON PLATEN, H., 1958. Geochim.

Cosmochim. Acta, 15, 91-112.

WOLFE, ., 1961. Thesis, Queen's Univ.

WRIGHT, W.J., 1934. Preliminary report on granite industry,  
St. George. N.B. Dept. Lands and Mines, Mining  
Section.

## APPENDIX 1

## A. Big Bald Mountain - Major Element Analysis

Sample	SiO <sub>2</sub>	Al <sub>2</sub> O <sub>3</sub>	TiO <sub>2</sub>	Fe <sub>2</sub> O <sub>3</sub>	FeO	MnO	MgO	CaO	Na <sub>2</sub> O	K <sub>2</sub> O	P <sub>2</sub> O <sub>5</sub>	H <sub>2</sub> O	Rb	Zn
5a*	76.69	12.44	0.15	1.10	0	0.04	0.40	0.67	2.35	5.17	0.00	0.41		
5b*	78.12	12.10	0.14	1.11	0	0.03	0.32	0.66	2.50	4.77	0.00	0.27		
5d*	73.17	11.53	0.13	1.04	0	0.04	0.24	0.63	2.53	4.73	0.00	0.35		
5e <sub>1</sub> *	79.01	11.09	0.08	0.69	0	0.03	0.12	0.54	2.40	5.03	0.00	0.37		
5e <sub>2</sub>	79.50	11.00	0.07	0.70	0	0.02	0.13	0.27	2.30	4.83	0.00	0.60	0.023	0.000
6b	68.10	14.50	0.68	2.40	1.3	0.06	0.69	0.48	3.10	3.32	0.06	4.10	0.018	0.004
7*	77.41	12.16	0.11	0.94		0.04	0.26	0.62	2.49	4.92	-	0.32		
7a*	78.38	12.23	0.12	0.94		0.04	0.15	0.59	2.41	5.00	-	0.33		
7c*	77.64	12.09	0.12	0.97		0.03	0.11	0.65	2.69	4.78	-	0.24		
8	89.30	4.10	0.05	-	0.2	-	0.06	0.03	0.60	1.85	0.02	0.20	0.007	-
8a	75.40	12.70	0.15	0.50	0.6	0.03	0.15	0.40	2.80	4.73	0.01	1.00	0.025	-
9a	76.80	11.90	0.14	0.40	0.5	0.03	0.06	0.37	2.70	4.82	0.02	0.70	0.024	-
9b	68.50	13.30	0.13	0.00	1.1	0.02	0.15	0.33	2.50	4.18	0.04	5.90	0.021	-
12a	81.30	9.80	0.09	0.10	0.1	-	0.01	0.22	2.00	4.87	-	0.50	0.024	-
12b	77.70	11.50	0.12	0.60	0.3	0.02	0.11	0.29	2.40	5.00	-	0.60	0.025	
13a*	78.09	12.09	0.14	0.89		0.03	0.26	0.59	2.36	4.97	-	0.36		
13b*	75.64	12.45	0.18	1.22		0.04	0.27	0.65	2.50	5.11	-	0.45		
14	76.00	12.20	0.18	0.50	0.7	0.02	0.16	0.37	2.40	4.76	0.01	0.90	0.022	-
20a	82.80	8.90	0.23	0.30	0.1	0.01	0.06	0.21	1.30	4.51	-	0.40	0.018	-
20b	73.30	13.10	0.23	0.90	0.8	0.02	0.36	0.36	2.20	4.59	0.04	3.00	0.019	-
20c	74.00	12.90	0.33	2.00	0.0	0.05	0.27	0.57	2.60	4.31	0.04	1.40	0.020	0.002
20d	75.60	12.30	0.09	0.60	0.5	0.02	0.17	0.52	2.40	5.18	0.01	0.40	0.021	0.001

A. Big Bald Mountain - Major element analysis/continued

Sample	SiO <sub>2</sub>	Al <sub>2</sub> O <sub>3</sub>	TiO <sub>2</sub>	Fe <sub>2</sub> O <sub>3</sub>	FeO	MnO	MgO	CaO	Na <sub>2</sub> O	K <sub>2</sub> O	P <sub>2</sub> O <sub>5</sub>	H <sub>2</sub> O	Rb	Zn
21	76.60	12.10	0.11	0.90	0.0	0.02	0.12	0.31	2.60	4.89	-	1.10	0.025	-
22	73.60	13.10	0.33	1.20	0.6	0.04	0.40	0.45	2.50	4.05	0.02	1.80	0.019	0.001
25	72.60	14.40	0.35	1.40	0.7	0.04	0.37	0.55	2.60	4.60	0.04	1.90	0.020	-
26	75.40	13.00	0.30	1.40	0.3	0.02	0.36	0.00	2.20	4.92	0.02	1.60	0.019	0.002
27	79.30	10.70	0.14	0.70	0.1	0.10	0.18	0.17	2.00	4.85	-	0.50	0.019	-
28a	75.00	12.10	0.46	1.70	0.6	0.06	0.59	0.27	1.90	3.99	0.03	1.80	0.019	0.001
28b	75.20	12.60	0.23	1.40	0.1	0.03	0.20	0.15	2.10	4.86	-	1.20	0.018	0.001
30b	76.90	11.60	0.15	0.70	0.4	0.01	0.14	0.32	2.30	4.69	0.01	0.90	0.020	-
31a*	75.23	12.29	0.14	1.08		0.04	0.17	0.69	2.93	5.15	-	0.47		
31b*	77.87	12.52	0.13	0.88		0.03	0.18	0.67	2.40	5.30	-	0.39		
31c <sub>1</sub> *	73.10	11.12	0.12	0.90		0.04	0.15	0.65	2.54	4.45	-	0.11		
31c <sub>2</sub>	74.60	12.50	0.36	1.50	0.4	0.03	0.34	0.37	2.70	4.02	0.02	1.80	0.017	-
31d*	75.43	12.11	0.23	1.49		0.03	0.31	0.64	2.34	4.67	-	0.38		
32b	79.10	10.80	0.09	0.70	0.0	0.02	0.14	0.25	2.30	4.83	-	0.40	0.021	-

\* XRF Analysis

B. Pierce Mountain - Major Element Analysis

Sample	SiO <sub>2</sub>	Al <sub>2</sub> O <sub>3</sub>	TiO <sub>2</sub>	Fe <sub>2</sub> O <sub>3</sub>	FeO	MnO	MgO	CaO	Na <sub>2</sub> O	K <sub>2</sub> O	P <sub>2</sub> O <sub>5</sub>	H <sub>2</sub> O	Rb	Zn
Aa	73.80	14.50	0.12	1.30	0.0	0.05	0.13	0.25	2.10	4.38	0.03	2.30	0.034	-
Ab	75.80	13.20	0.10	0.70	-	0.01	0.08	0.02	2.10	4.58	-	1.70	0.033	-
Ac	63.70	22.50	0.21	0.40	-	0.00	0.21	0.00	4.80	2.99	-	3.10	0.023	0.005
Ad <sub>1</sub>	78.30	14.50	0.11	0.30	0	0.00	0.08	0.00	3.00	1.33	-	2.50	0.009	-
Ad <sub>12</sub> *	77.38	14.56	0.12	0.45	0	0.04	0.13	0.22	2.57	1.24	-	2.66		
Ad <sub>2</sub>	77.50	13.90	0.11	0.40	0.0	0.00	0.13	0.00	2.00	2.26	0.01	2.50	0.018	0.000
Ae	76.30	13.10	0.12	0.90	0.0	0.02	0.10	0.01	1.90	4.71	0.01	1.60	0.033	-
Af	75.00	13.00	0.11	1.00	0.0	0.02	0.09	0.12	1.70	5.17	0.02	1.90	0.036	-
Ag*	75.43	13.90	0.16	1.61		0.05	0.30	0.50	2.30	5.40	0.00	1.34		
Ba	71.90	17.00	0.18	0.80	0.3	0.00	0.27	0.00	0.00	4.97	0.00	2.50	0.037	0.002
Bb	77.60	13.70	0.11	0.00	0.4	0.00	0.17	0.00	1.60	2.23	0.00	2.30	0.020	-
Bc*	74.44	13.28	0.12	0.91		0.03	0.16	0.36	2.30	2.30	0.00	1.54		
C*	85.97	9.35	0.10	0.52		0.04	0.21	0.20	0.00	2.44	0.00	1.61		
Da	75.70	13.20	0.12	0.70	0.3	0.01	0.18	0.12	2.20	4.12	0.02	1.80	0.028	
Db	76.20	14.60	0.13	0.80	0.0	0.00	0.20	0.00	2.20	1.49	0.01	3.60	0.013	
Dc*	82.21	12.14	0.11	0.46		0.03	0.16	0.19	0.90	2.30	0.00	2.23		
35*	75.50	12.95	0.10	0.97		0.04	0.00	0.79	2.88	4.67	0.00	0.42		

\* XRF Analysis

## APPENDIX 2

## Cation Percentages

## A. Big Bald Mountain

Sample	Si	Al	Ti	Fe <sup>3</sup>	Fe	Mn	Mg	Ca	Na	K	P
5a*	73.14	13.98	0.11	0.85	-	0.03	0.57	0.68	4.34	6.29	
5b*	74.07	13.52	0.10	0.79	-	0.02	0.45	0.67	4.60	5.77	
5d*	73.43	13.64	0.10	0.79	-	0.03	0.36	0.68	4.92	6.06	
5e <sub>1</sub> *	75.60	12.51	0.06	0.50	-	0.02	0.17	0.55	4.45	6.14	
5e <sub>2</sub>	76.32	12.45	0.05	0.51	-	0.02	0.19	0.28	4.28	5.91	
6b	67.77	17.01	0.51	1.80	1.08	0.05	1.02	0.51	5.91	4.21	0.05
7*	73.92	13.68	0.08	0.68	-	0.03	0.37	0.63	4.21	5.99	
7a*	74.27	13.66	0.09	0.67	-	0.03	0.21	0.60	5.99	6.04	
7c*	74.04	13.59	0.09	0.70	-	0.02	0.16	0.66	6.04	5.81	
8	91.12	4.93	0.04	0.17	-	0.00	0.09	1.03	5.81	2.41	
8a	72.85	14.46	0.11	0.36	0.48	0.02	0.22	0.41	2.41	5.83	0.01
9a	74.16	13.54	0.10	0.29	0.40	0.02	0.09	0.38	5.83	5.94	0.02
9b	71.36	16.33	0.10	-	0.96	0.02	0.23	0.37	5.94	5.55	0.04
12a	78.61	11.17	0.07	0.07	0.08	-	0.01	0.23	5.55	6.01	-
12b	75.02	13.09	0.09	0.44	0.24	0.02	0.16	0.30	6.01	6.16	-
13a*	74.32	13.56	0.10	0.64	-	0.02	0.37	0.60	6.16	6.03	-
13b*	72.83	14.13	0.13	0.88	-	0.03	0.39	0.67	6.03	6.28	
14	73.89	13.98	0.13	0.37	0.57	0.02	0.23	0.39	6.28	5.90	0.01
20a	80.89	10.25	0.17	0.22	0.08	0.01	0.09	0.22	5.90	5.62	
20b	72.32	15.23	0.17	0.67	0.66	0.02	0.53	0.38	5.62	5.78	0.03



## A. Big Bald Mountain/continued

Sample	Si	Al	Ti	Fe <sup>3</sup>	Fe	Mn	Mg	Ca	Na	K	P
20c	72.14	14.82	0.24	1.47	-	0.04	0.39	0.60	5.78	5.36	0.03
20d	73.25	14.05	0.14	0.44	0.41	0.02	0.25	0.54	5.36	6.40	0.01
21	74.06	13.79	0.08	0.65	-	0.02	0.17	0.32	6.40	6.03	-
22	72.28	15.16	0.24	0.89	0.49	0.03	0.59	0.47	6.03	5.07	0.02
25	70.08	16.38	0.25	1.02	0.57	0.03	0.53	0.57	5.07	5.66	0.03
26b	72.59	14.82	0.22	1.02	0.24	0.02	0.52	-	4.13	6.07	0.02
27	76.82	12.22	0.10	0.51	0.08	0.08	0.26	0.18	3.76	5.99	-
28a	73.96	14.06	0.34	1.26	0.49	0.05	0.87	0.29	3.63	5.02	0.03
28b	73.64	14.54	0.17	1.03	0.08	0.02	0.29	0.16	3.99	6.07	-
30b	74.98	13.33	0.11	0.51	0.33	0.01	0.20	0.33	4.35	5.83	0.01
31a*	72.40	13.94	0.10	0.78	-	0.03	0.24	0.71	5.47	6.32	-
31b*	73.59	13.94	0.09	0.63	-	0.02	0.25	0.68	4.40	6.39	-
31c	74.19	13.30	0.09	0.69	-	0.03	0.23	0.71	5.00	5.76	-
31c <sub>2</sub> *	72.87	14.59	0.26	1.10	0.33	0.02	0.50	0.39	5.11	5.01	0.02
31d *	73.47	13.90	0.17	1.39	-	0.02	0.45	0.67	4.42	5.83	-
32b	76.40	12.29	0.07	0.51	-	0.02	0.20	0.26	4.31	5.95	-

## Cation Percentages

## B. Pierce Mountain

Sample	Si	Al	Ti	Fe <sup>3+</sup>	Fe <sup>2+</sup> +Mn <sup>2+</sup>	Mg	Ca	Na	K
Aa	72.35	16.73	0.09	0.96	0.04	0.19	0.26	3.99	5.47
Ab	74.30	15.25	0.07	0.52	0.01	0.12	0.02	3.99	5.73
Ac	61.19	25.47	0.15	0.29	-	0.30	-	8.94	3.66
Ad <sub>1</sub>	75.78	16.54	0.08	0.22	-	0.12	-	5.63	1.64
Ad <sub>12</sub> *	75.87	16.82	0.09	0.33	0.03	0.19	0.23	4.88	1.55
Ad <sub>2</sub>	76.56	16.18	0.08	0.30	-	0.19	-	3.83	2.85
Ae	74.52	15.08	0.09	0.66	0.02	0.15	0.01	3.60	5.87
Af	74.01	15.12	0.08	0.74	0.02	0.13	0.13	3.25	6.51
Ag*	71.49	15.52	0.11	1.15	0.04	0.42	0.51	4.23	6.53
Ba	72.13	20.10	0.14	0.60	0.25	0.40	-	0.02	6.36
Bb	77.32	16.09	0.08	-	0.33	0.25	-	3.09	2.83
Bc*	75.26	15.82	0.09	0.69	0.03	0.24	0.39	4.51	2.97
C*	84.99	10.89	0.07	0.39	0.03	0.31	0.21	0.02	3.08
Da	74.17	15.24	0.09	0.52	0.26	0.26	0.13	4.18	5.15
Db <sup>+</sup>	75.76	17.11	0.10	0.60	-	0.30	-	4.24	1.89
Dc*	80.53	14.01	0.08	0.34	0.02	0.23	0.20	1.71	2.87
35*	72.61	14.68	0.07	0.70	0.03	-	0.81	5.37	5.73

## APPENDIX 3

## A. Big Bald Mountain - Meso Norm Analysis

Sample	Qtz	Cor	Or	Ab	An	Bi	Hm	Mt	Il	Tn	Ap
5a*	39.97	2.19	30.50	21.72	2.89	1.52	0.79	0.10	-	0.32	-
5b*	41.74	2.02	28.09	22.98	2.85	1.21	0.74	0.07	-	0.30	-
5d*	39.24	1.50	29.68	24.61	2.90	0.96	0.72	0.10	-	0.29	-
5e <sub>1</sub> *	42.78	0.92	30.41	22.26	2.48	0.46	0.45	0.07	-	0.17	-
5e <sub>2</sub>	45.23	1.80	29.26	21.40	1.14	0.50	0.47	0.05	-	0.15	-
6	36.76	6.81	19.11	29.91	-	3.14	-	2.70	0.16	1.28	0.14
7*	40.92	1.97	29.35	73.05	2.78	0.99	0.61	0.10	-	0.24	-
7a*	41.75	2.16	29.87	22.14	2.57	0.57	0.61	0.10	-	0.26	-
7c*	40.54	1.68	28.81	24.68	2.89	0.42	0.65	0.07	-	0.26	-
8	80.34	1.34	11.66	5.94	-	0.61	-	-	0.07	0.01	0.05
8a	38.93	2.80	28.24	26.22	1.46	1.45	-	0.55	-	0.33	0.02
9a	40.58	2.04	29.07	25.27	1.27	0.99	-	0.44	-	0.31	0.04
9b	39.03	5.31	25.76	25.24	1.04	3.22	-	-	-	0.31	0.09
12a	48.96	1.09	29.94	18.75	0.81	0.16	-	0.11	-	0.20	-
12b	42.56	2.01	30.46	22.46	1.06	0.53	-	0.65	-	0.26	-
13a*	42.05	2.17	29.55	21.77	2.51	0.98	0.59	0.07	-	0.30	-
13b*	38.79	2.10	30.73	23.33	2.70	1.03	0.82	0.10	-	0.39	-
14	42.00	3.07	28.46	22.62	1.20	1.69	-	0.55	-	0.40	0.02
20a	56.37	2.06	27.95	12.31	0.25	0.23	0.04	0.27	-	0.51	-
20b	41.89	4.94	27.43	21.04	0.77	2.33	-	1.00	-	0.51	0.09

A. Big Bald Mountain - Meso norm analysis/continued

Sample	Qtz	Cor	Or	Ab	An	Bi	Hm	Mt	Il	Tn	Ap
20c	40.48	3.95	26.14	24.57	1.49	1.05	1.38	0.12	-	0.73	0.09
20d	39.61	2.36	31.27	22.54	1.94	1.20	-	0.66	-	0.42	0.02
21	40.79	2.40	29.87	24.37	1.21	0.46	0.62	0.05	-	0.24	-
22	42.13	4.92	24.25	23.80	1.01	1.78	-	1.33	-	0.73	0.04
25	37.72	5.33	27.29	24.33	1.30	1.66	-	1.53	-	0.76	0.09
26	42.35	4.62	29.49	20.63	-	1.38	0.94	0.12	0.44	-	-
27	47.32	2.32	29.53	18.78	0.37	0.69	0.18	0.49	-	0.31	-
28a	47.76	5.41	23.65	18.16	-	2.31	0.37	1.34	0.20	0.73	0.07
28b	43.31	4.48	29.87	19.94	-	0.78	0.84	0.28	0.02	0.47	-
30b	43.91	2.73	28.70	21.74	1.05	0.75	-	0.77	-	0.33	0.02
31a*	35.71	0.93	31.21	27.33	3.05	0.65	0.72	0.10	-	0.30	-
31b*	39.97	1.99	31.52	21.99	2.93	0.68	0.58	0.07	-	0.28	-
31c <sub>1</sub>	40.59	1.31	28.43	24.99	3.08	0.61	0.62	0.10	-	0.28	-
31c <sub>2</sub> *	42.05	4.08	24.22	25.57	0.48	1.32	0.40	1.06	-	0.79	0.04
31d*	41.64	2.68	28.26	22.09	2.50	1.20	1.04	0.07	-	0.51	-
32	45.18	1.65	29.42	21.53	0.97	0.54	0.48	0.05	-	0.20	-

\*XRF analysis

B. Pierce Mountain - Meso Norm Analysis

Sample	Qtz	Cor	Or	Ab	An	Bi	Hm	Mt	Il	Tn	Ap
Aa	43.53	7.01	27.03	19.93	0.66	0.51	0.88	0.12	-	0.27	0.07
Ab	45.13	5.53	28.36	19.95	-	0.36	0.52	-	0.02	0.06	-
Ac	23.38	12.87	17.56	44.69	-	0.95	0.29	-	-	-	-
Ad <sub>1</sub>	53.97	9.27	7.88	28.14	-	0.39	0.22	-	-	-	-
Ad <sub>12</sub> *	56.19	10.10	7.44	24.43	0.71	0.51	0.27	0.10	-	0.27	-
Ad <sub>2</sub>	56.53	9.50	13.78	19.15	-	0.59	0.30	-	-	-	-
Ae	46.13	5.61	28.98	17.99	-	0.46	0.66	-	0.03	-	-
Af	44.61	5.32	32.32	16.26	0.09	0.35	0.71	0.05	-	0.25	0.05
Ag*	38.32	3.98	31.93	21.13	1.97	1.13	1.07	0.12	-	0.34	-
Ba	52.99	13.72	31.13	0.10	-	1.08	0.37	0.35	0.27	-	-
Bb	59.55	10.16	13.33	15.45	-	1.34	-	-	0.17	-	-
Bc*	52.15	7.75	14.43	22.54	1.49	0.64	0.64	0.08	-	0.27	-
C*	75.36	7.52	14.87	0.10	0.69	0.83	0.32	0.10	-	0.22	-
Da	46.08	5.89	25.31	20.89	0.05	0.70	0.01	0.76	-	0.27	0.04
Db†	57.37	10.98	8.79	21.20	0.89	0.60	-	-	-	-	-
Dc*	66.46	9.19	13.98	8.55	0.59	0.62	0.29	0.08	-	0.24	-
35*	37.76	2.10	28.64	26.85	3.71	-	0.64	0.10	-	0.22	-

\* XRF analysis

† Excess P<sub>2</sub>O<sub>5</sub>, F, Si, Cr

## Modal Minerals

<u>Mineral</u>	<u>Abbreviation</u>	<u>Formula Used in Calculation</u>
1. Quartz	Qtz	$\text{SiO}_2$
2. Corundum	Cor	$\text{Al}_2\text{O}_3$
3. Orthoclase	Or	$\text{K}_2\text{O} \cdot \text{Al}_2\text{O}_3 \cdot 6\text{SiO}_2$
4. Albite	Ab	$\text{Na}_2\text{O} \cdot \text{Al}_2\text{O}_3 \cdot 6\text{SiO}_2$
5. Anorthite	An	$\text{CaO} \cdot \text{Al}_2\text{O}_3 \cdot 2\text{SiO}_2$
6. Biotite	Bi	$\text{K}(\text{Mg}+\text{Fe})_3\text{AlSi}_3\text{O}_{10}(\text{OH})_2$
7. Hematite	Hm	$\text{Fe}_2\text{O}_3$
8. Magnetite	Mt	$\text{FeO} \cdot \text{Fe}_2\text{O}_3$
9. Ilmenite	Il	$\text{FeO} \cdot \text{TiO}_2$
10. Sphene	Tn	$\text{CaO} \cdot \text{TiO}_2 \cdot \text{SiO}_2$
11. Apatite	Ap	$3\text{CaO} \cdot \text{P}_2\text{O}_5 \cdot 1/3\text{CaF}_2$

## APPENDIX 4

## Weathered vs. "Fresh" Cation % Ratios

## A. Big Bald Mountain

Sample	Si	Al	Ti	Fe <sup>3+</sup>	Fe <sup>2+</sup> +Mn <sup>2+</sup>	Mg	Ca	Na	K
5a*	0.994	1.003	1.222	1.349	1.5	2.28	1	0.986	0.984
5b*	1.007	0.970	1.111	1.254	1	1.80	0.985	1.045	0.903
5d*	0.998	0.978	1.111	1.254	1.5	1.44	1	1.118	0.948
5e <sub>1</sub> *	1.027	0.897	0.667	0.794	1	0.68	0.809	1.011	0.961
5e <sub>2</sub>	1.037	0.893	0.556	0.810	1	0.76	4.120	0.973	0.925
6	0.921	1.220	5.667	2.857	56.5	4.08	0.750	1.359	0.659
7*	1.004	0.981	0.889	1.079	1.5	1.48	0.926	1.048	0.937
7a*	1.009	0.980	1.000	1.063	1.5	0.84	0.882	1.007	0.945
7c*	1.006	0.975	1.000	1.111	1	0.64	0.971	1.123	0.909
8	1.238	0.354	0.444	0.270	-	0.36	1.515	0.270	0.377
8a	0.990	1.037	1.222	0.571	25	0.88	0.603	1.191	0.912
9a	1.008	0.971	1.111	0.460	21	0.36	0.559	1.480	0.930
9b	0.970	1.171	1.111	0	49	0.92	0.544	1.480	0.869
12a	1.068	0.801	0.778	0.111	4	0.04	0.338	0.852	0.941
12b	1.019	0.939	1.000	0.698	13	0.64	0.441	1.020	0.964
13a*	1.010	0.973	1.111	1.016	1	1.48	0.882	0.989	0.944
13b*	0.990	1.014	1.444	1.398	1.5	1.56	0.985	1.061	0.983
14	1.004	1.003	1.444	0.587	29.5	0.92	0.574	1.027	0.923
20a	1.099	0.735	1.889	0.349	4.5	0.36	0.324	0.559	0.879
20b	0.983	1.092	1.889	1.063	34	2.12	0.559	0.957	0.905

A. Big Bald Mountain Weathered vs. "Fresh" Cation  
Percent Ratios/continued

Sample	Si	Al	Ti	Fe <sup>3+</sup>	Fe <sup>2+</sup> +Mn <sup>2+</sup>	Mg	Ca	Na	K
20c	0.980	1.063	2.667	2.333	2	1.56	0.884	1.116	0.839
20d	0.995	1.008	1.556	0.698	21.5	0.10	0.794	1.025	1.002
21	1.006	0.989	0.889	1.032	1	0.68	0.471	1.107	0.944
21	0.982	1.086	2.667	1.413	26	2.36	0.691	1.081	0.793
25	0.952	1.175	2.778	1.619	30	2.12	0.838	1.107	0.886
26	0.986	1.063	2.445	1.619	13	2.08	very high	0.936	0.950
27	1.044	0.877	1.111	0.810	8	1.04	0.264	0.855	0.937
28a	1.005	1.009	3.778	2.000	27	3.48	0.426	0.825	0.786
28b	1.001	1.043	1.889	1.635	5	1.16	0.235	0.907	0.950
30b	1.019	0.956	1.222	0.811	17	0.80	0.485	0.989	0.912
31a*	0.984	1	1.111	1.238	15	0.96	1.044	1.243	0.989
31b*	1	1	1	1	1	1	1	1	1
31c <sub>1</sub> *	1.008	0.954	1	1.10	1.5	0.92	1.044	1.136	0.901
31c <sub>2</sub>	0.990	1.032	2.889	0.746	17.5	2	0.574	1.161	0.784
31d *	0.998	0.997	1.889	1.730	1	1.80	0.985	1.005	0.908
32b	1.038	0.882	0.778	0.810	1	0.80	0.382	0.980	0.931

\*XRF Analysis

194



## Weathered vs. "Fresh" Cation % Ratios

## B. Pierce Mountain

Sample	Si	Al	Ti	Fe <sup>3+</sup>	Fe <sup>2+</sup> +Mn <sup>2+</sup>	Mg	Ca	Na	K	P
Aa	1.016	1.140	1.286	1.371	1.333	19	0.321	0.743	0.955	2
Ab	1.023	1.039	1	0.793	0.333	12	0.025	0.743	1	0
Ac	0.843	1.735	2.143	0.414	0	30	0	1.665	0.639	0
Ad <sub>1</sub> *	1.044	1.127	1.143	0.314	0	12	0	1.048	0.286	0
Ad <sub>12</sub>	1.045	1.146	1.286	0.471	1	19	0.284	0.909	0.271	0
Ad <sub>2</sub>	1.0541	1.102	1.143	0.210	0	19	0	0.713	0.497	1
Ae	1.026	1.027	1.286	0.943	0.667	15	0.012	0.670	1.024	1
Af	1.019	1.030	1.143	1.057	0.667	13	0.161	0.605	1.136	2
Ag *	0.985	1.057	1.571	1.643	1.333	42	0.630	0.788	1.140	0
Ba	0.993	1.369	2	0.857	11	40	0	0.004	1.110	0
Bb	1.065	1.096	1.143	0	1	25	0	0.575	0.494	0
Bc *	1.036	1.078	1.286	0.986	1	24	0.481	0.840	0.518	0
C *	1.171	0.742	1	0.557	1	31	0.259	0.004	0.538	0
Da	1.022	1.038	1.286	0.743	8.333	26	0.160	0.778	0.899	2
Db	1.043	1.166	1.429	0.857	0	30	0	0.790	0.330	1
Dc*	1.109	0.954	1.143	0.486	0	23	0.247	0.318	0.501	0

## APPENDIX 4

DiscussionA. Big Bald MountainWeathered vs. fresh ratios (cation %)

Fresh sample is represented by sample 3lb, based on weathering index value.

- Si Silica is stable under the conditions present. Variation ranged from 0.921 to 1.238. Note a value of 1 indicates that no change has occurred (i.e. the abundance of the element in question has not changed due to stability of quartz.
- Al Also is generally constant except for leached horizons where values range from 0.354 to 0.735. The general variation is greater than Si. The range is 0.887-1.22
- Ti As would be expected, Ti generally shows an increase in abundance in the weathering profile, except for rock interface and highly leached samples, which have anomalously low values (e.g. 0.44-0.78). However the general range is from 1-5.66.

- $\text{Fe}^{3+}$  On first inspection the ratio is variable. However it seems that leached soil-bedrock samples are depleted in  $\text{Fe}^{3+}$ . Other samples are generally larger than 1. Range is from 0-2.86.
- $\text{Fe}^{2+}$  +  $\text{Mn}^{2+}$  Soil-bedrock interface samples have extremely large values (maximum 56.5). Values always greater than 1 most likely indicating the increase in Mn with weathering.
- $\text{Mg}^{2+}$  Distribution is highly variable but there is a trend for grus and bedrock samples to be greater than 1. Overall range is 0.04-4.08.
- $\text{Ca}^{2+}$  Generally values are less than 1 indicating depletion. However a few leached and soil-rock interflow samples have values greater than 1. Range is 1.52-0.24, but values usually greater than 0.5.
- $\text{Na}^{2+}$  Na is relatively stable in the profile as would be expected, since Na feldspar is not generally deeply altered. Leached horizons show anomalous depletion of Na (i.e. 0.27-0.56). General range is 0.83-1.48.

K      Almost invariably slightly depleted in K, possibly due to the hydrolysis of K feldspars producing kaolinite (?). Again leached zones have strong depletion as well as some bedrock-soil interface samples (eg. 33). The general range for K is 0.784-1.002.

P      P is present only in near surface soil horizons suggesting that source of P may be the decomposition of organic debris.

Thus in terms of sample type leached and soil bedrock interface samples tend to act in the same way, while grus bedrock samples follow the same trends. The depletion of cations can be related to the weathering of feldspars or biotite.

B. Pierce Mountain

Weathered vs. fresh ratios (cation %)

Ratios were taken with respect to sample 35. The purpose of the ratio is to determine the relative gains or losses upon weathering.

Si Si shows a slight increase as would be expected, since quartz is generally resistant to alteration and secondary products take Si into their structure. Clay samples are depleted in Si as well as rock-regolith interface sample (Ag). Si values range from 1.77-0.84.

Al Generally samples show a slight increase in Al, but clay samples show a much larger increase, possibly indicating the dominance of clay minerals which take Al into their structures. Samples C, Dc are anomalously depleted.

Ti All samples have an increase in Ti, but clay samples have generally a much greater concentration in Ti. Range is from 1.14-2.14.

$\text{Fe}^{3+}$  Ferrous iron is generally depleted except for samples beneath colluvium and rock-regolith interface samples. Range of values is 1.64-0. The general depletion of  $\text{Fe}^{3+}$  indicates that  $\text{Fe}_2\text{O}_3$  is being illuviated through the deposit.

$\text{Fe}^{2+}$  + Values are variable. The range is 0-8.33

$\text{Mn}^{2+}$

Mg All values are very high due to fresh samples; anomalously low Mg value. Note however that clay samples have especially high Mg ratios as well as bedrock interface samples. This indicates that Mg is either taken into the "clay" structure or is precipitated as an oxide along joint planes. Average value is 20. Another source of Mg is required therefore. Metasomatic processes must be invoked.

Ca Shows intense depletion generally due to the solution of Ca, associated with the weathering of plagioclase. Values range from 0.63-0.

Na Clay samples show the maximum variability in Na content most likely a function of the clay produced and ground water source which most likely produced the

clay (1.66-0.004). Generally Na is depleted indicating that plagioclase is most likely highly altered to "clay" minerals.

K Samples show large variability as some of the clay and bedrock-grus interface samples have an addition of K. Generally however values are depleted in K, indicating that K feldspar has also been intensely altered.